Vol. 59 • No. 10

October 2016

Microwave Journal
.com

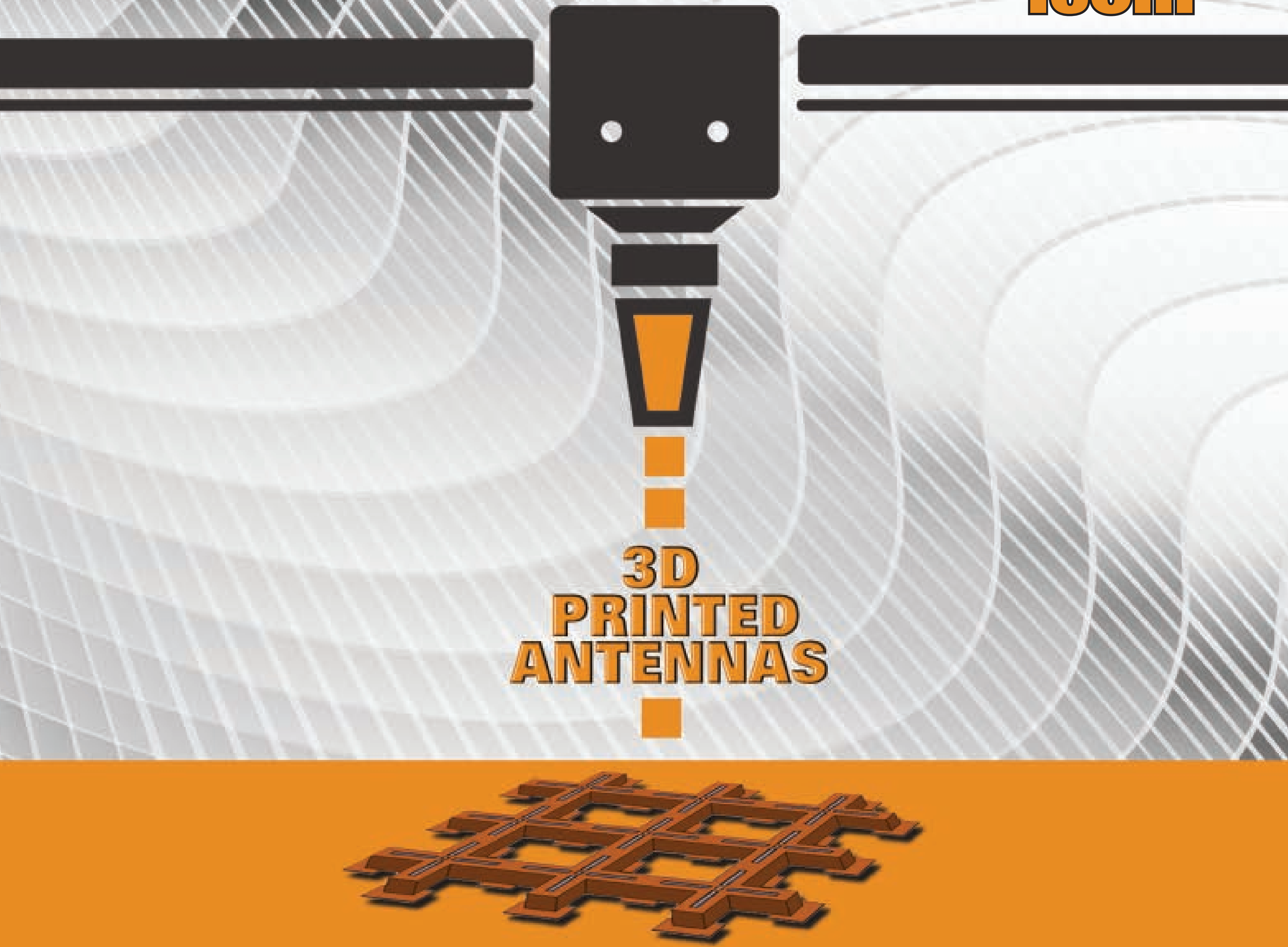

horizon house®
Founded in 1958

BETTER COMMUNICATION SOLUTIONS

Public Safety

Satcom, mmWave & Military

Aeronatutical/Space Transportation

AMER, EMEA, & D.A.S

MECA 5G Products & Equipment

MECA Electronics designs and manufactures an extensive line of RF/Microwave Equipment and Components with industry leading performance including D.A.S. Equipment, Low PIM Products, supports 5G & Millimeter-Wave, Power Dividers & Combiners, Directional & Hybrid Couplers, Fixed & Variable Attenuators, RF Terminations, Circulators/Isolators, DC Blocks & Bias Tees, Adapters & Jumpers. Models available in industry common connector styles: N, SMA, 2.92mm, TNC, BNC, 7/16, 4.1/9.5 & 4.3/10.0 DIN as well as QMA, Reverse Polarity SMA, TNC and various mounting solutions. Since 1961 MECA Electronics (Microwave Equipment & Components of America) has served the RF/Microwave industry with equipment and passive components covering Hz to 40 GHz. MECA is a privately held ISO9001:2008 Certified, global designer and manufacturer for the communications industry with products manufactured in the United States of America We stock products so that you do not need to.

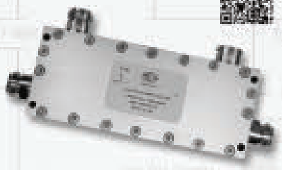

Low PIM Couplers

Low PIM Attenuators

Low PIM Terminations

Power Divider/Combiner

Products in STOCK when you need it!

Low PIM & D.A.S Equipment

Circulators/Isolators

Buy

RFPartsOnDemand.com

Online

Attenuators/Terminations

e-MECA.com
Since 1961

MECA Electronics, Inc.

Microwave Equipment & Components of America

The Professional's Choice for RF/Microwave Passive Components

459 E. Main St., Denville, NJ 07834

Tel: 973-625-0661 • Fax: 973-625-9277 • Sales@e-MECA.com

iBwave

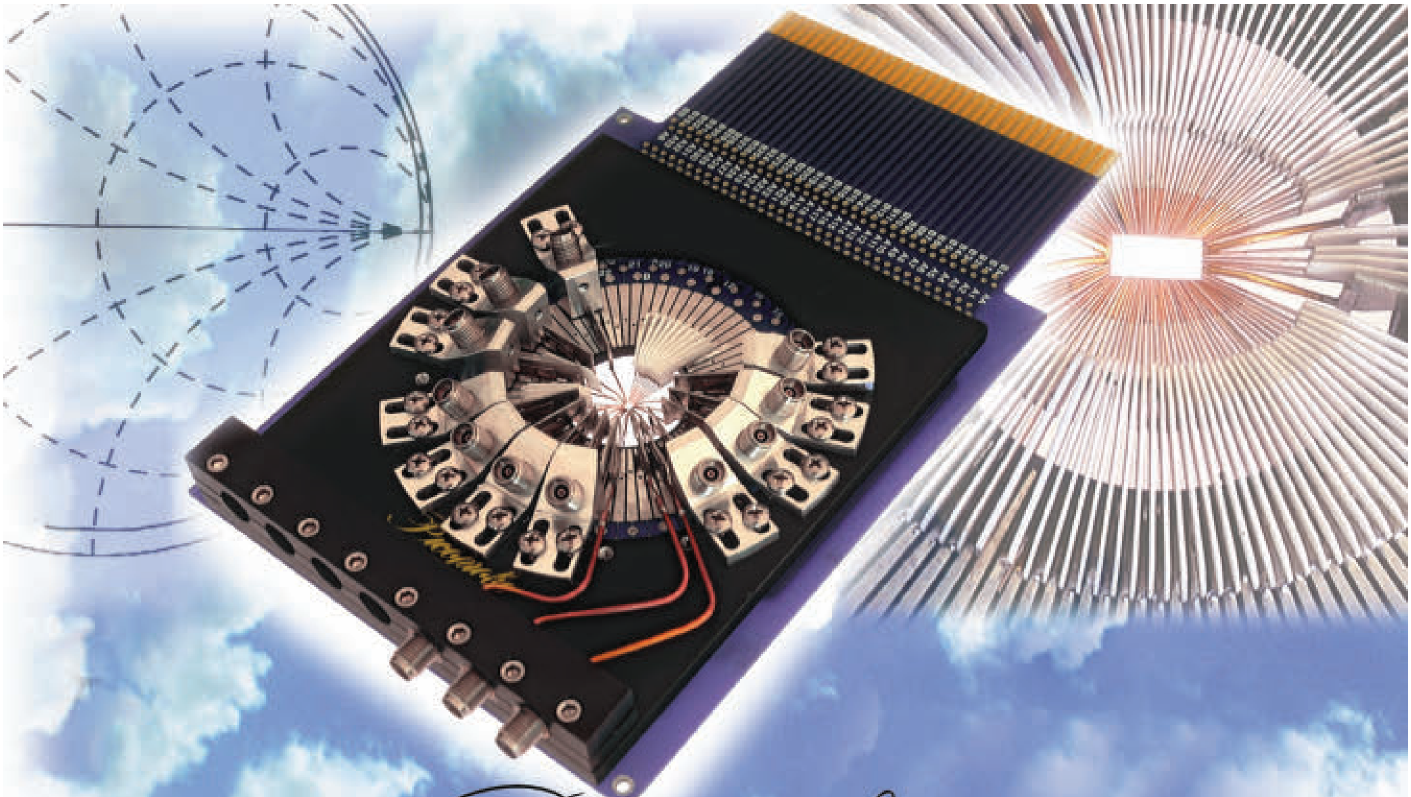

Picoprobe®

Picoprobe elevates probe cards to a higher level…

(…110 GHz to be exact.)

Since 1981, GGB Industries, Inc., has blazed the on-chip measurement trail with innovative designs, quality craftsmanship, and highly reliable products. Our line of custom microwave probe cards continues our tradition of manufacturing exceptional testing instruments.

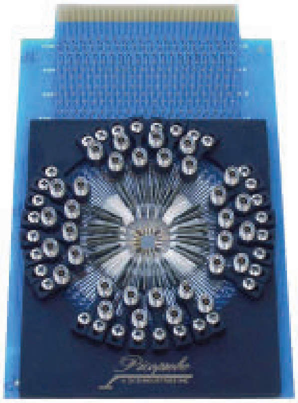

Through unique modular design techniques, hundreds of low frequency probe needles and a variety of microwave probes with operating frequencies from DC to 40, 67, or even 110 GHz can be custom configured to your layout.

Our patented probe structures provide the precision and ruggedness you require for both production and characterization testing. And only Picoprobe® offers the lowest loss, best match, low inductance power supplies, and current sources on a single probe card.

Our proven probe card design technology allows full visibility with inking capability and ensures reliable contacts, even when probing non-planar structures.

Not only do you get all the attractive features mentioned, but you get personal, professional service, rapid response, and continuous product support--all at an affordable price so your project can be completed on time and within budget.

Typical Specs	10GHz	20GHz	40GHz
Insertion Loss	0.6 dB	0.8 dB	1.3 dB
Return Loss	22 dB	18 dB	15 dB

For technical assistance, custom product designs, or off-the-shelf delivery,call GGB Industries, Inc., at (239) 643-4400.

GGB INDUSTRIES, INC. • P.O. BOX 10958 • NAPLES, FL 34101

Telephone (239) 643-4400 • Fax (239) 643-4403 • E-mail email@ggb.com • www.picoprobe.com


MCL B 744
ADP-2-10

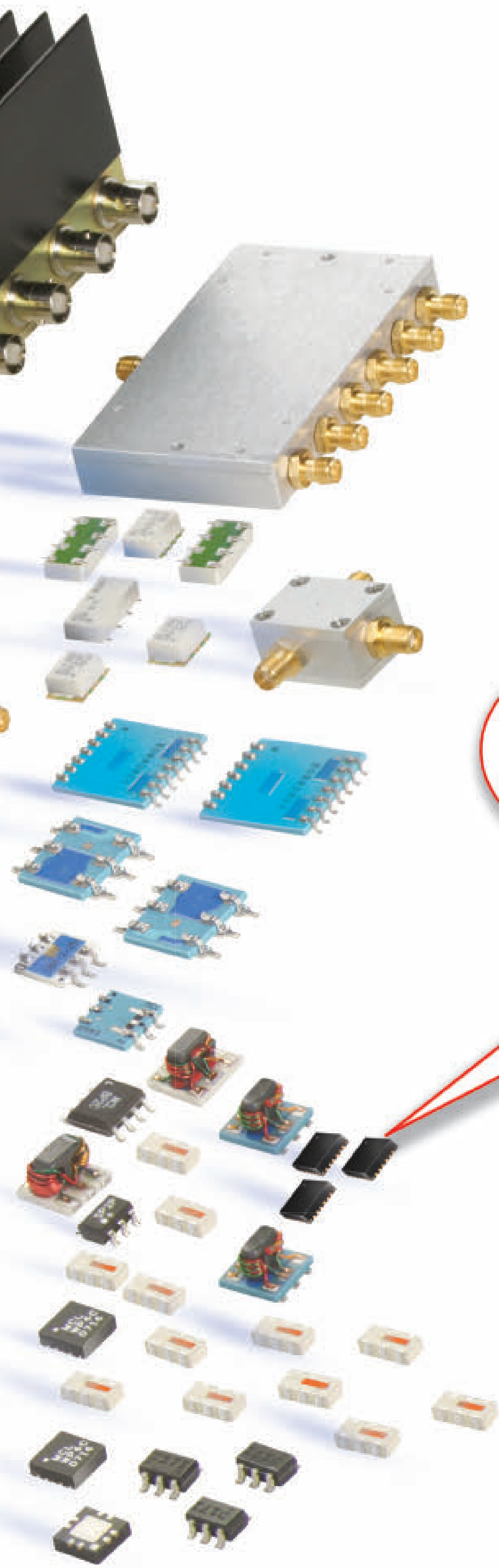

Technology On the Move™

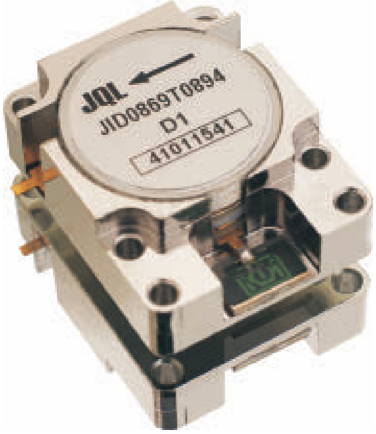

Drop-in Isolators

Cavity Filters

Surface Mount Circulators

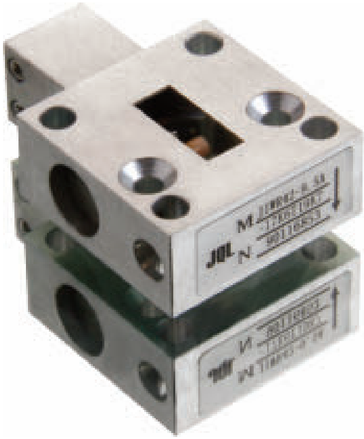

Waveguide Isolators

Power Combiners

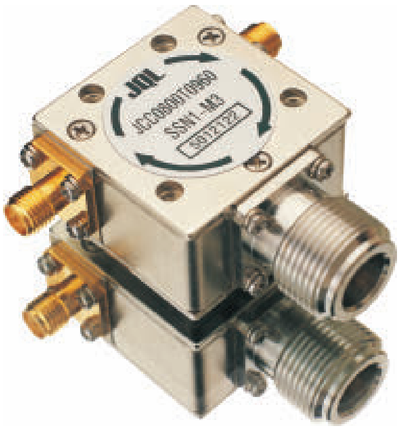

Coaxial Circulators

JQL

Tel:1(888)236-9828(US&Canada)
1(630)930-9917(Worldwide)
www.jqlelectronics.com sales@jqlelectronics.com


Amplifiers
Packaged
Transistors
& MMICs
DIE
Detectors
Diodes
Oscillators
Filters
GaN
Devices
Counterfeit Parts
Frequency Dividers
Attenuators
POWER DIVIDERS
Mixers
Custom Packaged Devices
STANDARD & CUSTOM SCREENING FLOWS
MILITARY SPACE & INDUSTRIAL
MICROCIRCUIT & SEMICONDUCTOR DIE EVALUATION
DIE VISUAL, SORTING, PACKAGING
ON-SITE ENVIRONMENTAL TEST LAB
DIE BANK & STORAGE
BUILD TO PRINT ASSEMBLY


YOUR COMPLETE MILLIMETER WAVE
SOLUTION
new
Low-Cost
VNA Extender
MANY ITEMS IN STOCK
MADE IN USA
www.sagemillimeter.com | 3043 Kashiwa Street, Torrance, CA 90505
T: 424-757-0168 | F: 424-757-0188 | sales@sagemillimeter.com
SAGE
Millimeter, Inc.

Microwave Journal

CONTENTS

October 2016
Vol. 58 • No. 10
Passive & Control Components
mwjournal.com

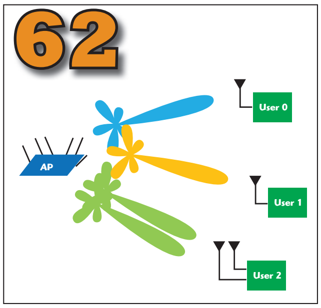

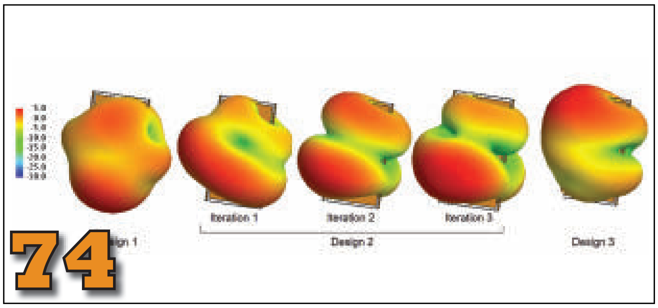

Cover Feature

MWJ Perspective

Technical Features

Application Notes

AUGMENTED REALITY: HOW IT WORKS

STEP 1
Download the free Layar app from the iTunes (iOS) or Google Play (Android) store.

STEP 2
Launch the app to view enhanced content on any page with the layar logo.

STEP 3
Frame the entire page in the screen and tap to experience enhancements (tap screen again for full screen view).

Look for the Layar logo on participating pages.

AR pages may expire after 30 days.

59 YEARS OF PUBLISHING EXCELLENCE

Microwave Journal

CONTENTS

mwjournal.com

Product Features

Tech Briefs

Departments

Microwave Journal (USPS 396-250) (ISSN 0192-6225) is published monthly by Horizon House Publications Inc., 685 Canton St., Norwood, MA 02062. Periodicals postage paid at Norwood, MA 02062 and additional mailing offices.

POSTMASTER: Send address corrections to *Microwave Journal*, PO Box 1143, Skokie, IL 60076 or e-mail mwj@halldata.com. Subscription information: (847) 763-4943. This journal is issued without charge upon written request to qualified persons working in the RF & microwave industry. Other subscriptions are: domestic, $120.00 per year, two-year subscriptions, $185.00; foreign, $200.00 per year, two-year subscriptions, $370.00; back issues (if available) and single copies, $10.00 domestic and $20.00 foreign. Claims for missing issues must be filed within 90 days of date of issue for complimentary replacement.

STAFF

Publisher: Carl Sheffres
Editor: Patrick Hindle
Technical Editor: Gary Lerude
Managing Editor: Jennifer DiMarco
Associate Technical Editor: Cliff Drubin
Multimedia Staff Editor: Leslie Nikou
Multimedia Staff Editor: Barbara Walsh
Contributing Editor: Janine Love
Consulting Editor: Harlan Howe, Jr.
Consulting Editor: Frank Bashore
Consulting Editor: David Vye
Consulting Editor: Raymond Pengelly
Electronic Marketing Manager: Chris Stanfa
Digital Content Production Specialist: Lauren Tully
Audience Development Manager: Carol Spach
Traffic Manager: Edward Kiessling
Director of Production & Distribution: Robert Bass
Art Director: Janice Levenson
Graphic Designer: Sachiko Stiglitz

EUROPE

International Editor: Richard Mumford
Office Manager: Nina Plesu

CORPORATE STAFF

CEO: William M. Bazzy
President: Ivar Bazzy
Vice President: Jared Bazzy

EXECUTIVE EDITORIAL OFFICE
685 Canton Street, Norwood, MA 02062
Tel: (781) 769-9750
FAX: (781) 769-5037
e-mail: mwj@mwjournal.com

EUROPEAN EDITORIAL OFFICE
16 Sussex Street, London SW1V 4RW, England
Tel: Editorial: +44 207 596 8730 Sales: +44 207 596 8740
FAX: +44 207 596 8749

SUBSCRIPTION SERVICES
Send subscription inquiries and address changes to:
Tel: (847) 291-5216
e-mail: mwj@halldata.com

BPA WORLDWIDE

www.mwjournal.com

Printed in the USA

Microwave Journal Online

Scan page using layar app

Visit us @ mwjournal.com

eLEARNING free webinars

Real-Time Recordings and Post-Processing of Wide-Bandwidth EW Signals
Sponsored by: Keysight Technologies 10/11

VCO Fundamentals
Sponsored by: Mini-Circuits 10/12

Innovative Passives and Substrates Enable RF Power Amplifier Designs for Cooking Applications
Sponsored by: Rogers Corp. 10/13

Preparing for the Autonomous Car: Developing a 5G Network and Integrating Sensors
Sponsored by: IDT 10/19

Millimeter Wave PA
Sponsored by: National Instruments/AWR 10/25

Web Survey

Where will 3D printing see the greatest near-term adoption in the RF/microwave industry?

Look for our multiple choice survey online at mwjournal.com

August Survey

Which satellite system will be first to provide global, high-speed internet service?

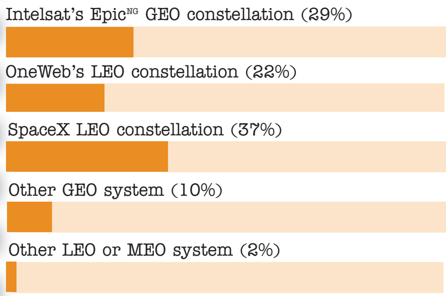

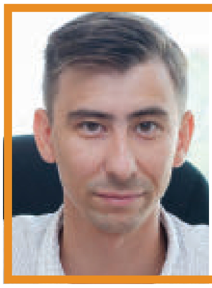

ExecutiveInterview

Egor Ilin, director of marketing and sales, **Micran**, explains the company's evolution and relationship with Tomsk State University, Russia, its portfolio of microwave electronics products and activity in the global marketplace.

WHITE PAPERS

Altair · Keysight Technologies · Innovative Integration (a molex company) · National Instruments

Join Us Online

Follow us @Pathindle

Become a fan at facebook.com/microwavejournal

Catch *Frequency Matters*, the industry update from *Microwave Journal*,
www.microwavejournal.com/FrequencyMatters

COM

Has Amplifier Performance or Delivery Stalled Your Program?

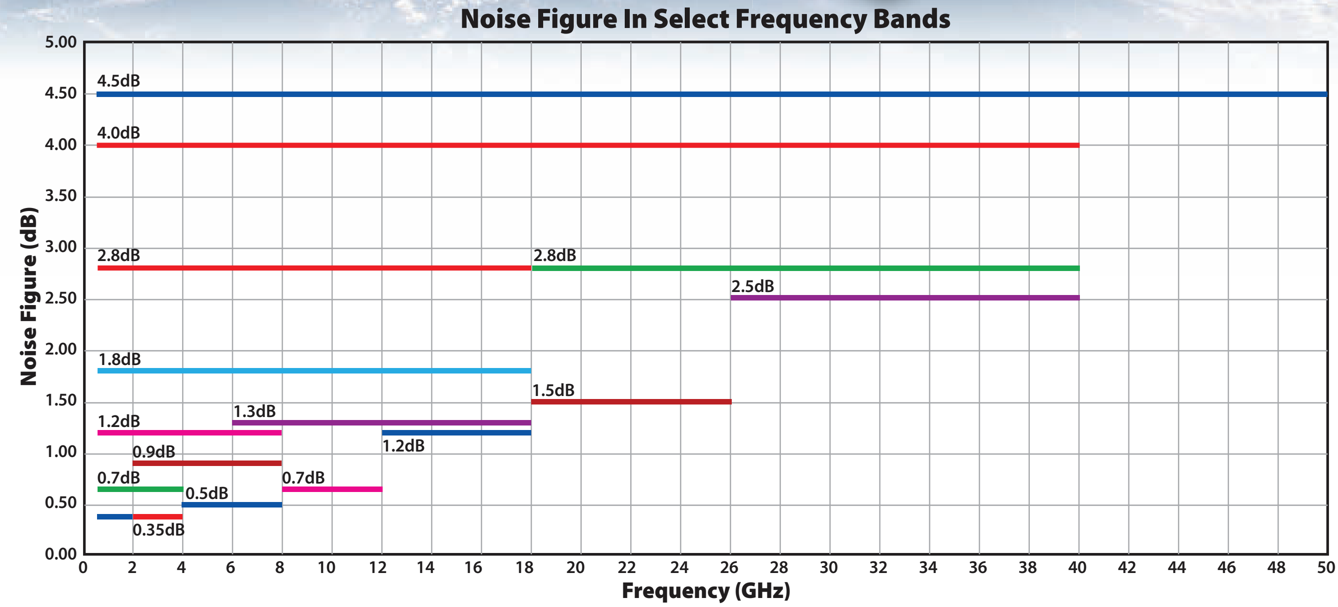

B&Z TECHNOLOGIES

Innovating to Excel

www.bnztech.com

NOVEMBER MARK YOUR CALENDAR

1
WEBINAR Sponsored by: Anritsu envision : ensure

7-10
ITC/USA International Telemetering Conference • Plan To Attend •

Glendale, Ariz.

The International Telemetering Conference/ USA (ITC/USA) is the premier annual forum and technical exhibition providing telemetry specific short courses, technical papers from professionals and students, and exhibits from industry-leading companies.
www.telemetry.org

10
WEBINAR **Passive Components**
Sponsored by: Mini-Circuits

15
WEBINAR *Sponsored by:* RfMW It's who we are It's what we do

16
WEBINAR *Sponsored by:* National Instruments

17
WEBINAR **Ampleon Revolutionizes RF Energy**
Sponsored by: AMPLEON

29
NIDays

London, UK

This one-day, multi-track conference on Graphical System Design features keynote presentations, interactive sessions taught by NI experts as well as domain experts from the industry, hands-on workshops and an exhibition.
uk.ni.com/nidays

1-3
MILCOM2016

Baltimore, Md.

Leaders from around the world will address the critical role communications plays in military readiness and operations at MILCOM 2016. Topics include the spectrum of command, control, communications, computers, intelligence, surveillance and reconnaissance (C4ISR) technologies and capabilities that address 21st century communications challenges related to national defense, homeland security, disaster response and interoperability.
www.milcom.org

10/30-11/4
AMTA 2016 October 30 - November 4

Austin, Texas

The Antenna Measurement Techniques Association (AMTA) is a non-profit, international organization dedicated to the development and dissemination of theory, best practices and applications of antenna, radar signature and other electromagnetic measurement technologies.
www.amta2016.org

FOR DETAILS, VISIT MWJOURNAL.COM/EVENTS

Coming**Events**

CALL FOR PAPERS

CS ManTech 2017
October 31, 2016

ICMIM 2017
November 4, 2016

RFIC 2017
January 9, 2017

mwjournal.com

NOVEMBER

MILCOM 2016
November 1–3, 2016 • Baltimore, Md.
www.milcom.org

ITC/USA
November 7–10, 2016 • Glendale, Ariz.
www.telemetry.org

NIDays London
November 29, 2016 • London, UK
uk.ni.com/nidays

DECEMBER

IEEE International Electron Devices Meeting (IEDM)
December 3–7, 2016 • San Francisco, Calif.
www.ieee-iedm.org

APMC 2016 and IMaRC 2016
December 5–9, 2016 • New Delhi, India
www.apmc2016.org, www.imarc-ieee.org

88th ARFTG Microwave Measurement Conference
December 6–9, 2016 • Austin, Texas
www.arftg.org

IEEE MTT-S Latin America Microwave Conference (LAMC 2016)
December 12–14, 2016 • Puerto Vallarta, Mexico
www.lamc-ieee.org

JANUARY

RWW2017
January 15–18, 2017 • Phoenix, Ariz.
www.radiowirelessweek.org

DesignCon 2017
January 31–February 2, 2017
Santa Clara, Calif.
www.designcon.com

FEBRUARY

Mobile World Congress 2017
February 27–March 2, 2017 • Barcelona, Spain
www.mobileworldcongress.com

MARCH

Satellite 2017
March 6–9, 2017 • Washington, DC
www.satshow.com

ICMIM 2017
March 19–21, 2017 • Nagoya, Aichi, Japan
http://icmim-ieee.org

GOMACTech 2017
March 20–23, 2017 • Reno, Nev.
www.gomactech.net

Microwave & RF 2017
March 22–23, 2017 • Paris, France
www.microwave-rf.com

APRIL

WAMICON 2017
April 24–27, 2017 • Cocoa Beach, Fla.
www.wamicon.org

EDI CON China 2017
April 25–27, 2017 • Shanghai, China
www.ediconchina.com

MAY

CS ManTech 2017
May 22–25, 2017 • Indian Wells, Calif.
http://csmantech.org

JUNE

RFIC 2017
June 4–6, 2017 • Honolulu, Hawaii
http://rfic-ieee.org

IMS2017
June 4–7, 2017 • Honolulu, Hawaii
http://ims2017.org

EW Europe
June 6–8, 2017 • Olympia, London
www.eweurope.com

89th ARFTG Conference
June 9, 2017 • Honolulu, Hawaii
www.arftg.org

Universal Footprint RF Duplexers

Universal-footprint series of RF filters from CTS provide better communications in small cells, active antenna arrays, distributed antenna systems (DAS), repeaters and remote radio heads. This new breed of ceramic monoblock filters is offered for all the major 3GPP FDD frequency bands, sharing a common footprint for ease of system design. Our high-reliability, surface-mounted, ceramic filters support 20-year operating lifetimes and as much as 200 W peak input power handling capability. Universal footprint filters provide industry-leading insertion loss and rejection. For more information on our ceramic universal duplexers and bandpass filters go to **richardsonrfpd.com/ Universal-Footprint**

CTS

Filters with Industry-leading insertion loss and rejection.

	UMD DUPLEXER For Metro Cell	USD DUPLEXER For Small Cell	UPD DUPLEXER For Pico Cell
Input Power Rating	20W Avg 200W Pk	6W Avg 60W Pk	1.5W Avg 15W Pk
Insertion Loss (5MHz AVG)	2.2dB	2.6dB	3.0dB
Rx Band Isolation*	80dB	72dB	63dB
Tx Band Isolation	74dB	66dB	57dB
Universal Footprint Size (mm)	62 x 44	63 x 18	44 x 18
Operating Temp Range	-40 to +85°C	-40 to +85°C	-40 to +85°C

* Note: "Difficult" bands may have 2dB lower worst case Rx band isolation.

RichardsonRFPD
An Arrow Company

Scan me to **LEARN MORE**

www.richardsonrfpd.com/Universal-Footprint

Your Global Source for RF, Wireless, Energy & Power Technologies
www.richardsonrfpd.com | 800.737.6937 | 630.262.6800

COVER FEATURE
INVITED PAPER

3D Printed Material Characterization for Complex Phased Arrays and Metamaterials

M. Wajih Elsallal, Jamie Hood and Ian McMichael
The MITRE Corporation, Bedford, Mass.
Travis Busbee
Voxel8, Somerville, Mass.

The MITRE Corporation is investigating the potential of a new generation of additive manufacturing (AM), commonly known as 3D printing, to realize complex geometries of wideband phased array and metamaterial designs using low-cost, compact, desktop printers. Samples of the 3D printed plastic and conductive ink printed at room temperature were characterized over frequency. The polylactic acid (PLA) dielectric constant and loss tangent are found to be stable up to 18 GHz. The PLA internal architecture was varied to achieve lower effective dissipation factors, which extends usefulness to high frequency applications. Microstrip line samples were fabricated with simulated and measured insertion loss data validating the high conductivity through millimeter wave frequencies. A 3D printed monopole Wi-Fi antenna was built and tested. The measured gain patterns showed excellent agreement with the computational electromagnetic model. The next step is to build and test a complex, electrically-functional phased array and a complex metamaterial structure, and verify simulation through measurement.

There has been increasing demand from the defense and intelligence communities to come up with creative ways to put urgently needed capabilities into the hands of warfighters in a very short time with a combination of lower cost, smaller form factor and covertness in mind. To meet these challenges with agility, the ability to achieve both metallic patterning and polymer deposition in a single, automated process from a low-cost 3D printer has opened the door for the next-generation of rapid prototyping systems. The MITRE Corporation, with the help of 3D printer manufacturer Voxel8, is investigating the applicability of multi-material additive manufacturing, or 3D printed electronics, for high-performance antennas and RF devices. ***Figure 1*** shows the Voxel8 3D printer used for these experiments.

MATERIAL CHARACTERIZATION

In order to design antennas and RF circuits, well defined electrical properties within the frequency band of operation are needed. The dielectric material was characterized by measuring a 3D printed dielectric sleeve in a 7 mm coaxial airline standard.[2] A variety of samples were tested to investigate effects of different pigments, print orientations and in fill density (see ***Figure 2***).

First a solid cube was 3D printed from four different colors of PLA filament. Then solid cylinders from different orientations were cut out to test print orientations. Solid cylinders were also printed using rectilinear and concentric rings to test effects of infill patterns. Next, all cylinders were machined to have specific inner diameter, outer diameter and sample length to fit inside the coaxial airline test fixture shown in ***Figure 3***. ***Table 1*** shows the construction and dimensions of each sample.

The permittivity and loss tangent were measured using a Keysight network analyzer loaded with a material characterization software.[3] The reflection/transmission permeability and permittivity polynomial fit technique was used. This technique best fits material properties to an iterative polynomial model until the difference between S-parameters calculated from the polynomial and the measured S-parameters is very small. For brevity, only the results from grey samples are discussed here. The results from characterizing other colored PLA ma-

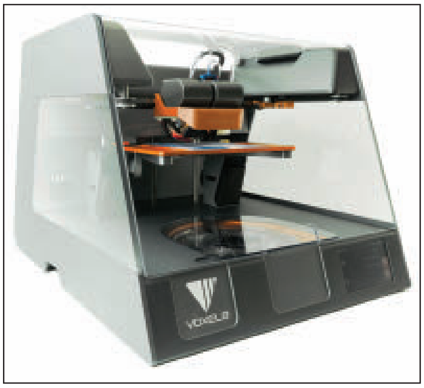

Fig. 1 Low-cost Voxel8 Developers Kit 3D printer. Picture is taken from the Voxel8 website.[1]

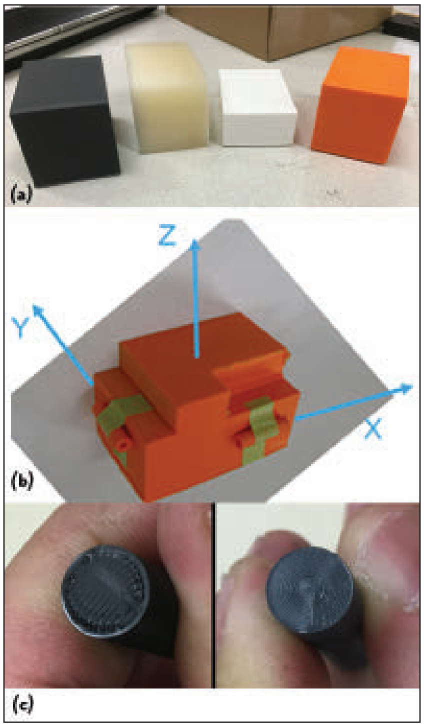

Fig. 2 3D printed cubes, realized from four different colored PLA spools (a), machined dielectric sleeves cut out from different side of the cube: XZ and YZ planes (b), and cylinders printed in the XY plane with rectilinear infill (left) and concentric infill (right)(c).

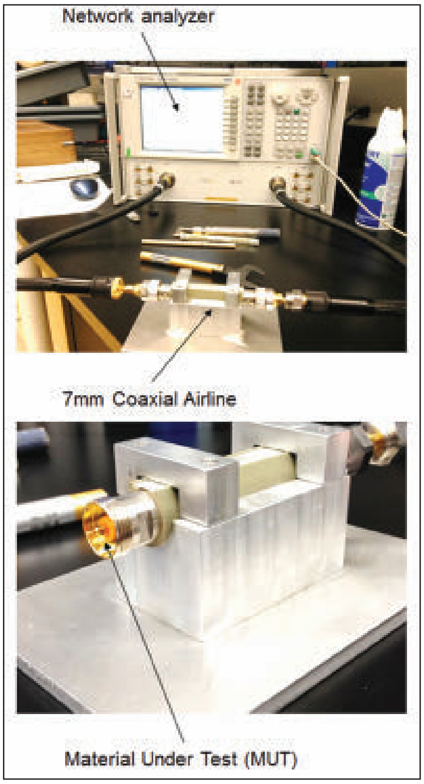

Fig. 3 The solid cylinders are machined as sleeves to specific dimensions that fit inside the 7 mm coaxial airline standard and measured in the test setup.

TABLE 1

CONSTRUCTION AND DIMENSIONS OF MATERIALS SAMPLES TESTED

Sample Name	Construction	Outside Diameter, OD (mm)	Inside Diameter, ID (mm)	Length, L (mm)
Sample #1	Concentric rings	6.97	3.02	25.46
Sample #2	Rectilinear	6.95	2.98	25.43
Sample #3	3D Cube XZ cut out	6.97	3.06	25.48
Sample #4	3D Cube YZ cut out	6.97	3.00	25.43

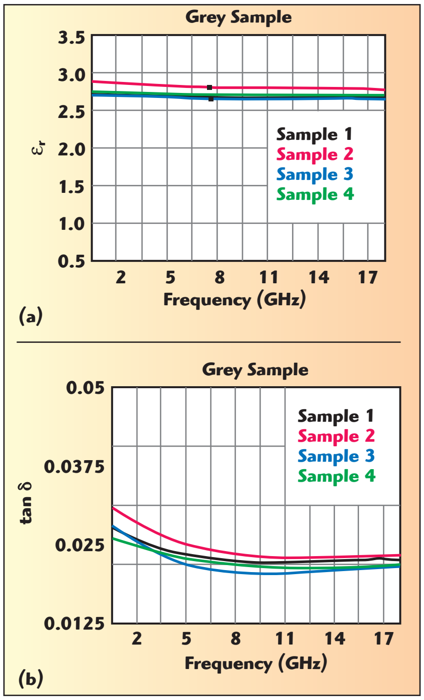

▲ *Fig. 4 Electrical properties for one of the extruded PLA samples using Voxel8 printer - grey colored sample.*

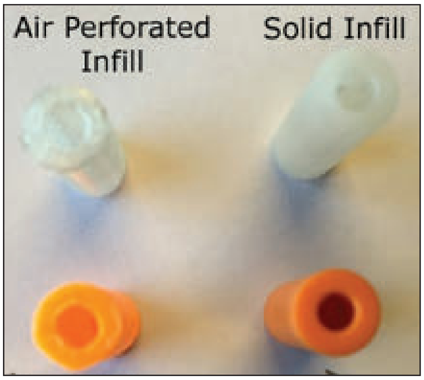

▲ *Fig. 5 Comparison of test samples made by adding air perforation to the material and normal samples.*

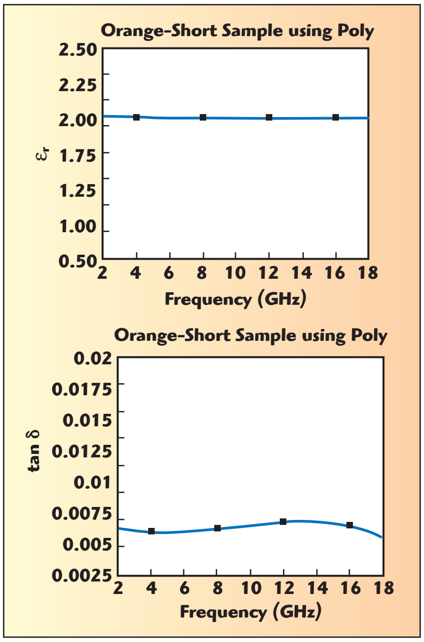

▲ *Fig. 6 The measured material properties of the partially infilled PLA.*

terial are available on Voxel8's website.[4] ***Figure 4*** shows the extruded PLA has electrical properties that are stable from DC to 18 GHz with minor variations with respect to print orientation. The measurement suggests that Voxel8's Developer Kit PLA grey material, for example, has an average dielectric constant of 2.75 and an average loss tangent equals to 0.015.

In some applications, lower dielectric constant and loss tangent are desired. Polymers with low intrinsic dielectric constant, like PTFE for example, generally do not have ideal thermal processing properties for 3D printing. To mitigate this problem, Voxel8 printed dielectric cylinders that include concentric rings of air gaps instead of solid infill as shown in ***Figure 5***. The air perforated infill samples were 0.61 g for the natural color and 0.59 g for the orange. The solid infill samples were 0.92 g for the natural color and 0.94 for the orange. These air perforated infill samples have an effective dielectric constant that is in the middle range between free-space air (ε_r=1, tanδ=0) and the PLA (ε_r=2.75, tanδ=0.015) as shown in ***Figure 6***. The

air pockets in dielectric substrate are impractical for many applications due to structural and environmental concerns, but this experiment shows the potential to achieve these parameters with custom materials.

Voxel8 specifies their proprietary silver ink with a volume resistivity below 5.0×10^{-7} Ω-m. Even lower values have been verified by printing traces, letting them dry for eight hours, and measuring their cross sectional area with a laser profilometer, and their resistance with a 4-point probe. To verify these direct conductivity measurements using a printed RF part, a 50 Ω microstrip line was modeled using CST's computational electromagnetic tool using the measured dielectric constant for the substrate material.

Voxel8 printed two 4" microstrip circuit (plastic, substrate and conductive trace) samples and MITRE added coaxial connectors and an aluminum plate to hold the connectors. Voxel8's silver ink was dispensed from a syringe as an electrically conductive adhesive to attach the connector to the microstrip trace instead of using conventional solder. ***Figure 7*** shows that the measured results are in good agreement with simulation.

In the 4" sample, the 3D printed microstrip has approximately 1 dB more loss at 12 GHz than that in a similar microstrip line model using a traditional PCB substrate with a ½ oz. electrodeposited (ED) copper trace (see Figure 7). The additional loss is believed to be due to the surface roughness (19 microns) of the 3D printed silver trace, which is much higher than typical ED copper (0.5 micron). After re-simulating the 3D printed microstrip line using a lower surface roughness (0.5 micron) and same measured resistivity of Voxel8's silver ink, the difference in the simulated losses was reduced to less than 0.5 dB at 12 GHz.

Wi-Fi ANTENNA MEASUREMENT

A simple printed monopole Wi-Fi antenna was manufactured and measured. Three different samples were made using three different 3D printers, at three different times in order to test the repeatability of the process. Again, the connection to the coaxial cable was made by a dot of Voxel8's silver ink dispensed from a syringe. The measured VSWRs are found to be consistent with simulation and the results are repeatable

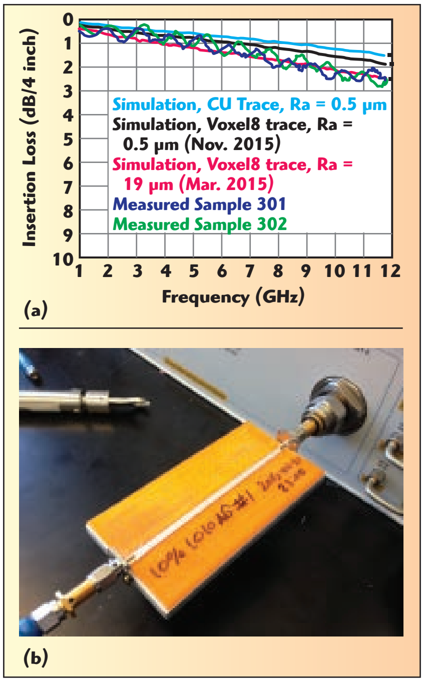

▲ *Fig. 7 Validating Voxel8's conductivity by comparing the measured insertion loss to simulation using the electrical properties of Voxel8 materials.*

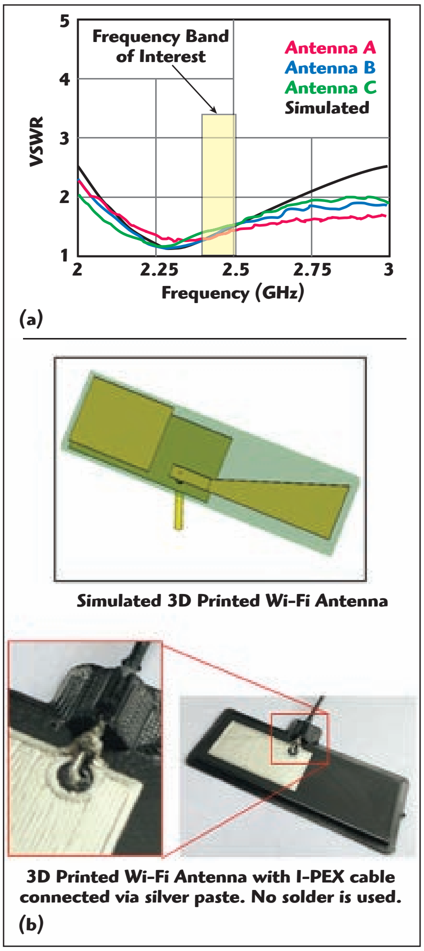

▲ *Fig. 8 VSWRs of three Wi-Fi antennas made using three different 3D printers, at three different times including photos.*

as shown in ***Figure 8***. The radiation patterns were also measured at MITRE's antenna chamber. A symmetric omnidirectional beam was seen in the measurements, which agrees with the simulation as shown in ***Figure 9***. Lastly, the antenna was cycled through temperature extremes from -40° to 60°C, and didn't show significant impact on measured patterns or VSWR after thermal cycling.

After subjecting the antenna to extreme external temperatures, the effects of electrically induced temperature from high power transmission were measured. MITRE powered a 3D printed antenna with 30 W for five minutes without adverse effect on electrical performance or structural integrity.

3D PRINTING – COMPLICATED STRUCTURE

Additive manufacturing has opened the design space to realize increased design sophistication and manufacturing agility that leads to increased access and operational effectiveness. MITRE is currently exploring the potential for a high performance 3D printed metamaterial structure and a 3D printed wideband phased array design.

3D PRINTED METAMATERIAL STRUCTURE

Metamaterials are composed of an assembly of subwavelength structures that exhibit bulk properties not found in nature. One such property is negative index of refraction. Many of the metamaterial designs in the literature require the incident electric field to be polarized in a particular direction in order for the extraordinary metamaterial properties to exist.[5,6] MITRE is working on a biaxial metamaterial that supports fields with

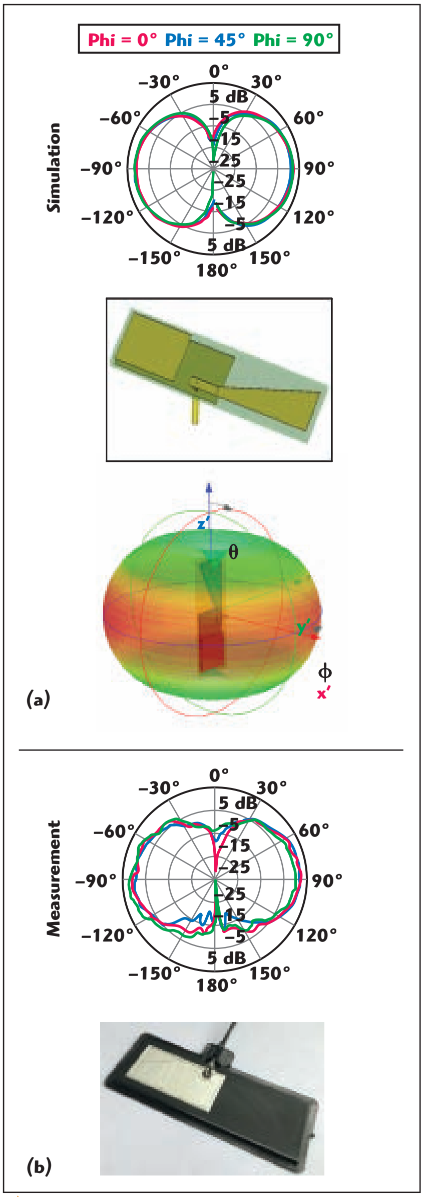

▲ *Fig. 9 Radiation patterns at 2.45 GHz showing good agreement between simulation (a) and measurement (b).*

multiple incident polarizations.

An early negative index of refraction metamaterial was composed of a lattice of split ring resonators (SRR) combined with rods.[5] The split ring resonators create a negative permeability and the rods created a negative permittivity. When the structures were combined, a negative index of refraction was achieved. However, this property only exists if the incident electric field is aligned with the rods and the magnetic field goes through the split ring resonators as shown in ***Figure 10a***. An alternative structure called the S-shaped split ring resonator (S-SRR), shown in ***Figure 10b***, was proposed in reference 6 and exhibits similar properties to the combined SRR and rods. Again, the electric field must be aligned in a particular direction, i.e., along the longer axis of the S-SRR, and the magnetic field must go through the loops.

MITRE's biaxial metamaterial is based on the S-SRR. The interesting feature in this design is an orthogonal and intersecting copy of the unit cell. This metamaterial is composed of intersecting three dimensional lattices that are relatively easy to 3D print, but would be very difficult, if not impossible, to make with conventional methods. The orthogonal structures allow the metamaterial to keep its properties, like negative index of refraction, for multiple electric field polarizations, whereas the original structure only works when the electric field is aligned in a particular direction. When using a metamaterial on a mobile platform where the direction or polarization of the incident fields is not known, it is easy to see the advantages of this modified metamaterial. ***Figure 11*** shows a model of the biaxial S-SRR unit cell structure. The metamaterial properties are the same when the incident electric field is vertically or horizontally polarized.

The biaxial S-SRR was simulated using periodic boundary conditions and Floquet ports in HFSS. The passband occurs from approximately 5 to 5.5 GHz, as seen from the simulated S-parameters in ***Figure 12a***. The reflection and transmission coefficients were used to calculate the effective index of refraction using the Nicolson-Ross-Weir method.[7] ***Figure 12b*** shows that the index of refraction is negative in the passband of the metamaterial, with a value of approximately -0.3 at 5 GHz. The passband and the value of the index of refraction can be controlled by varying the metamaterial dimensions.

Figure 13 shows a small test coupon of the biaxial metamaterial created using a Voxel8 multi-material 3D printer. Several coupons will be manufactured to measure the reflection coefficients when they are mounted inside a waveguide fixture.

3D PRINTED PHASED ARRAY

MITRE developed a wideband phased array concept that has a complex design. It is based on a printed circuit board (PCB) design that was not physically realizable. The design resembles an egg-crate construction with contiguous electrical connection (interdigitiated fingers) that is embedded within the orthogonal board interface as illustrated in ***Figure 14***.

Multi-material additive manufacturing is thought to be the only practi-

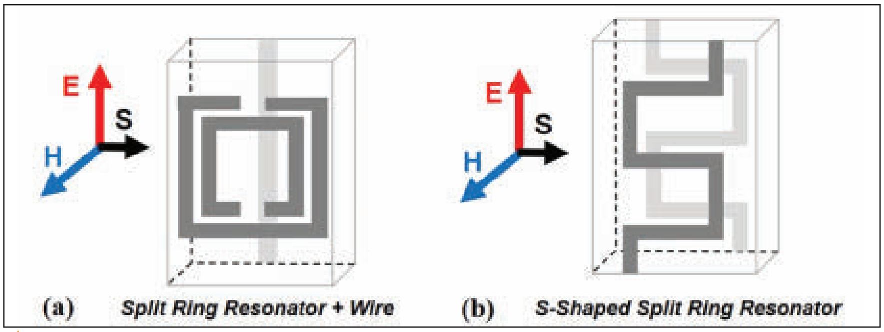

Fig. 10 A negative index of refraction metamaterial unit cell composed of a split ring resonator combined with a rod (a) and an S-shaped split ring resonator unit cell (b).

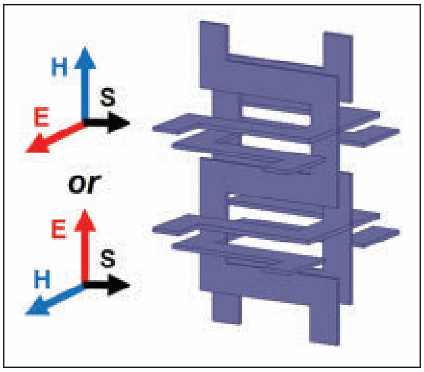

Fig. 11 MITRE's biaxial metamaterial unit cell with intersections that can be easily 3D printed, but would be difficult to manufacture otherwise.

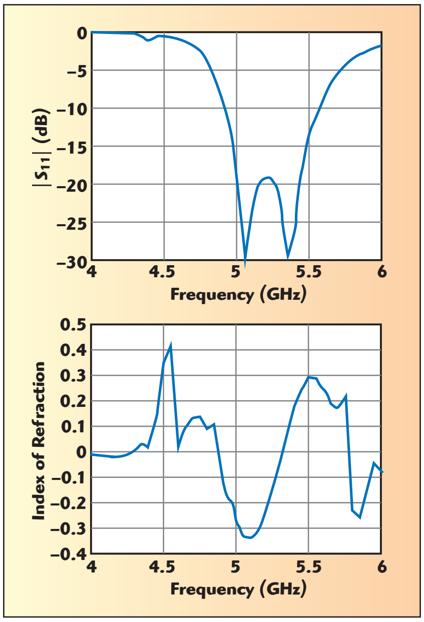

Fig. 12 Simulated reflection coefficient of the biaxial metamaterial (a) and calculated index of refraction of the metamaterial with a negative value within the passband (b).

cal way to realize this design. Voxel8 printed a sample of the cross in the middle of the array. The CT-scan shows the details of all of the fingers. The details of the design will be discussed in a future publication. Currently we are building a finite size array to be measured at MITRE.

CONCLUSION

Recent advances in multi-material additive manufacturing have enabled complex RF structures to be realized. The characterization of the materials used in additive manufacturing processes has been shown to be of utmost importance in designing and accurately predicting performance of these structures. Understanding the RF properties of the materials through rigorous characterization has

NI PXI, LabVIEW, and TestStand

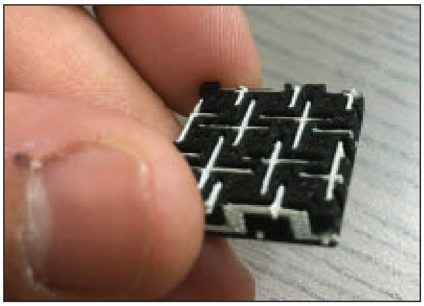

▲ *Fig. 13. A small test coupon of MITRE's biaxial metamaterial created with a Voxel8 multi-material 3D printer.*

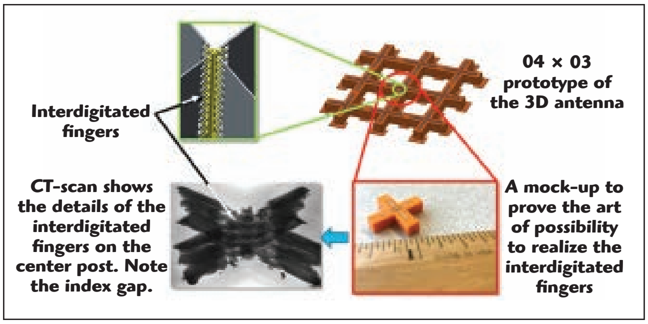

▲ *Fig. 14. 3D printed phased array design with complex features.*

led to the development of novel prototype structures, like the biaxial metamaterial and phased array antenna with interdigitated fingers. Future efforts will focus on utilizing advanced additive manufacturing methods to realize even smaller RF structures for higher frequency applications. As the materials and methods of multi-material additive manufacturing improve, RF structures that could previously only be imagined will be easily built for low cost implementation of advanced technologies.■

ACKNOWLEDGMENTS

The authors would like to thank Prof. Jennifer Lewis, Karl Willis, Jack Minardi, Kyle Dumont and Daniel Thompson from Voxel8 for their technical discussions and collaboration in this project. They would also like to thank Cecelia Franzini and Erin Jaffke of the MITRE Corporation for their contributions to the effort.

DISCLAIMER

In support of our government sponsors, The MITRE Corporation evaluates technology and collaborates with industry and academia as appropriate. The article reflects the results of such testing and/or collaboration and is not intended to be an endorsement of any technology or product.

References

1. Voxel8 website, www.voxel8.co/.
2. Keysight Technologies 85051B 7 mm Verification Kit, www.keysight.com/.
3. Keysight 85071E Materials Measurement Software, www.keysight.com/.
4. Voxel8's materials, www.voxel8.co/materials/.
5. D.R. Smith, W.J. Padilla, D.C. Vier, S.C. Nemat-Nasser and S. Schultz, "Composite Medium with Simultaneously Negative Permeability and Permittivity," *Phys. Rev. Lett.*, Vol. 84, No. 18, May 2000.
6. H. Chen, L. Ran, J. Huangfu, X. Zhang and K. Chen, "Left-Handed Materials Composed of Only S-Shaped Resonators," *Phys. Rev. E*, Vol. 70, 2004.
7. A.M. Nicolson and G.F. Ross, "Measurement of the Intrinsic Properties of Materials by Time Domain Techniques," *IEEE Trans. Intrum. Meas.*, Vol. IM-19, pp. 377–382, Nov. 1970.

Industry Visionary Q&A

Professor Theodore Rappaport, Founding Director, NYU WIRELESS

On July 14, 2016 the FCC adopted new rules for wireless broadband operations above 24 GHz, making the U.S. the first country to make this spectrum available and leapfrogging other nations in the race for 5G mmWave technology. We thought this was a perfect time to talk with Theodore (Ted) Rappaport, Professor at NYU and the Founding Director of NYU Wireless, who was the first to prove that mmWave technologies were viable for cellular communications.

What exactly did the FCC adopt in the way of frequency allocations and rules in July?

In its July 14, 2016 Report and Order and Further Notice of Proposed Rulemaking (based on the FCC's original request for comments in GN Docket No. 14-177), the FCC agreed to open up a vast amount of mmWave spectrum for use in a wide range of flexible wireless uses. This is unprecedented, as many of the authorized frequencies were either not available at all for wireless/mobile use, or were previously defined for only certain uses. The Report and Order (FCC 16-89) is 289 pages long, and offers extensive rulemaking for a wide range of new flexible uses that will include mobility, internet access, point to point, as well as satellite use.

To give just a few examples, the new rules will enable new wideband allocations for mobility (for 5G) and a vast range of unlicensed access spectrum with channel bandwidths much wider than ever before used in wireless communications. For example, the new rules provide access to 7 GHz of spectrum for use by unlicensed devices, from 64 to 71 GHz. This turns the current 60 GHz band where WiGig devices operate (57 to 64 GHz) into a contiguous 14 GHz block of spectrum for unlicensed Wi-Fi devices under Part 15 rules. And, for the first time, spectrum in the 28 GHz and 37 to 40 GHz bands becomes available for terrestrial mobile use with flexible rules (turning the old LMDS spectrum bands into a much broader type of licensing for mobile, fixed, portable, etc.). As an example, for the 27.5 to 28.35 GHz and 38.6 to 40 GHz bands, the FCC has allowed incumbent license holders to use their existing spectrum under the expanded new rules and under geographic area licensing rules for new acquirers of spectrum. For the 27.5 to 28.35 GHz band (28 GHz band), the FCC will use channel bandwidths up to 425 MHz and will issue licenses based on county-sized geographic areas, and in the 38.6 to 40 GHz band (39 GHz band), the FCC shall authorize channel bandwidths up to 200 MHz and Partial Economic Area (PEA) licenses. In the 39.5 to 40 GHz band, the FCC will maintain the military co-primary fixed and mobile satellite service allocations.

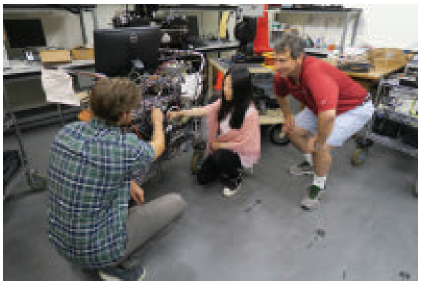

For the 37 to 38.6 GHz band, the FCC instates a band plan that allows for continuity of commercial operations between the 37 and 39 GHz bands, while protecting the spectrum use of a limited number of Federal military sites across the full 37 GHz band, in addition to protecting military satellite use and existing Federal fixed and mobile allocations throughout the band. In the 37 to 37.6 GHz band, new rules will allow coordinated co-primary shared access between Federal and non-Federal users. Through this new shared licensed structure, the FCC hopes to spawn proposals and collaboration between industry and government to determine new spectrum sharing procedures.

In its historic rulemaking, the FCC also proposes and invites comments on new 40 MHz channel bandwidths for 24 GHz spectrum, and seeks comment on new rules for 24, 32, 42, 47.2 to 50 GHz, and for the 71 to 76 GHz and 81 to 86 GHz bands which are proposed for spectrum sharing as implemented in the Citizens Broadband Radio Service at 3.5 GHz. Fortunately for amateur radio operators, the FCC safeguarded the amateur radio service spectrum at 47 to 47.2 GHz (a good thing for the future of America).

Why did they take this approach of just allocating spectrum and not implementing regulations?

Actually, the FCC did institute very detailed regulations, but they allowed the spectrum usage to be flexible, since commercial 5G and future massively broadband applications and services do not yet exist. By specifying channel bandwidths (license block sizes), and allowing for flexible use, the FCC is allowing new business models, carriers and applications to arise in a natural manner, well before the 3GPP 5G wireless air interfaces are developed. This will enable rapid early adoption of new technologies

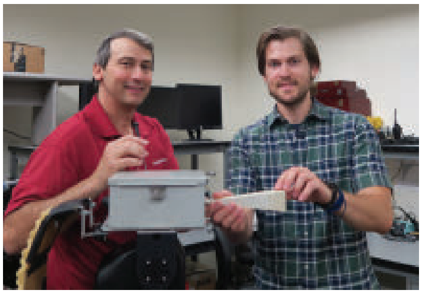

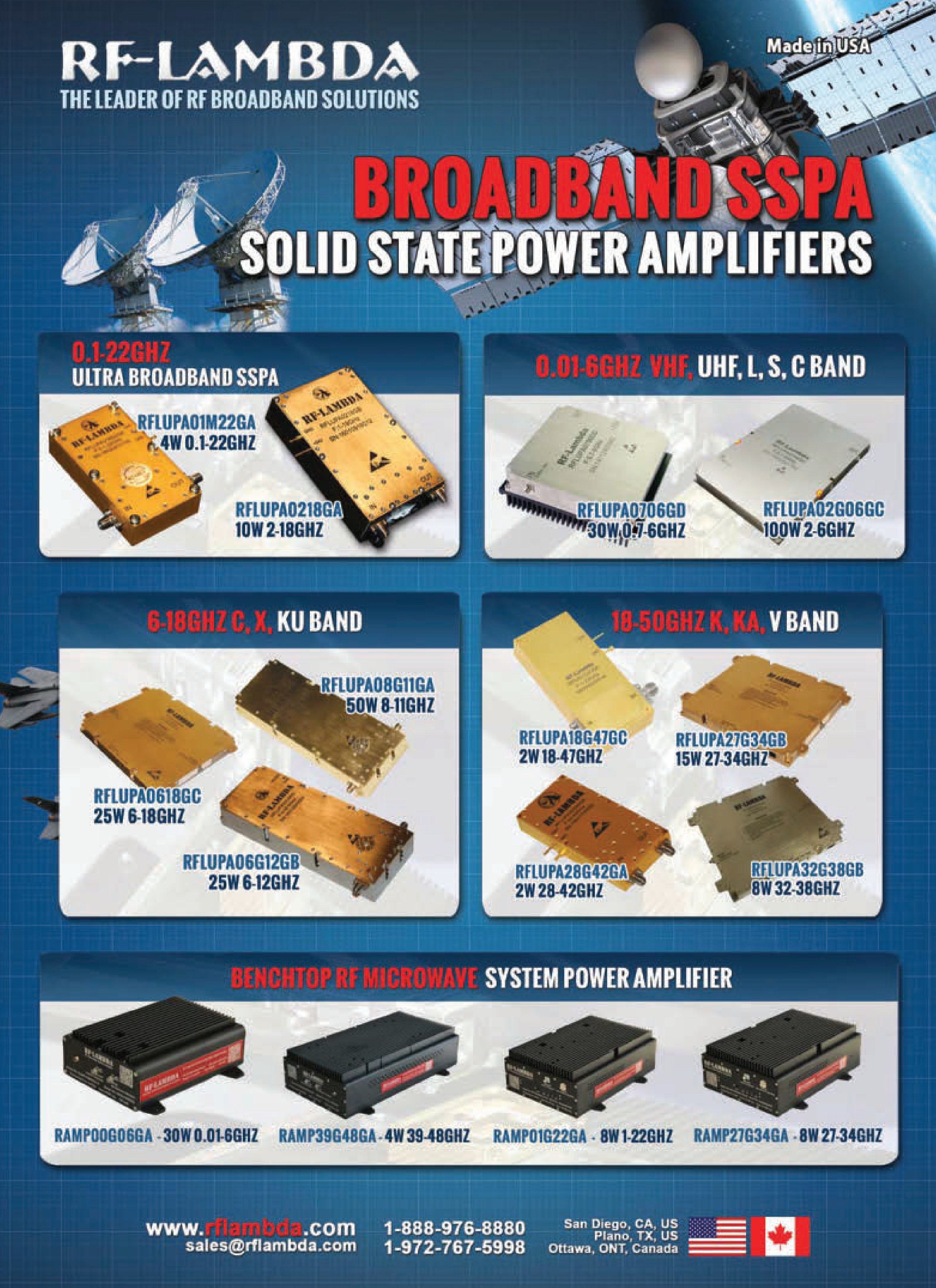
RF-LAMBDA
THE LEADER OF RF BROADBAND SOLUTIONS
Made in USA
BROADBAND SSPA
SOLID STATE POWER AMPLIFIERS
0.1-22GHZ
ULTRA BROADBAND SSPA
RFLUPA01M22GA
4W 0.1-22GHZ
RFLUPA0218GA
10W 2-18GHZ
0.01-6GHZ VHF, UHF, L, S, C BAND
RFLUPA0706GD
30W 0.7-6GHZ
RFLUPA02G06GC
100W 2-6GHZ
6-18GHZ C, X, KU BAND
RFLUPA08G11GA
50W 8-11GHZ
RFLUPA0618GC
25W 6-18GHZ
RFLUPA06G12GB
25W 6-12GHZ
18-50GHZ K, KA, V BAND
RFLUPA18G47GC
2W 18-47GHZ
RFLUPA27G34GB
15W 27-34GHZ
RFLUPA28G42GA
2W 28-42GHZ
RFLUPA32G38GB
8W 32-38GHZ
BENCHTOP RF MICROWAVE SYSTEM POWER AMPLIFIER
RAMP00G06GA - 30W 0.01-6GHZ
RAMP39G48GA - 4W 39-48GHZ
RAMP01G22GA - 8W 1-22GHZ
RAMP27G34GA - 8W 27-34GHZ
www.rflambda.com
sales@rflambda.com
1-888-976-8880
1-972-767-5998
San Diego, CA, US
Plano, TX, US
Ottawa, ONT, Canada

Q&A

while allowing the U.S. to be the de facto standard in the very early days of 5G adoption. The FCC is still seeking further comments in the coming months to help them solidify the rules and make further refinements.

What impact will these historic regulations have on the industry and race toward 5G communications?

These regulations will enable incumbent wireless carriers with mmWave spectrum to immediately partner with major carriers and equipment makers, and will make America the first place in the world where new equipment, business models and applications can be tested in a real-world, revenue-generating scenario. Basically, the ruling opens up the U.S. spectrum to the future of wireless, whatever that will look like, by offering unprecedented bandwidths and frequencies. As the race to 5G unfolds, America will be the most important race track because of these FCC regulations that will permit rapid deployment.

The day after the FCC action, the White House announced an Advanced Wireless Research Initiative including significant funding for broadband initiatives lead by the NSF—How does this work with the FCC announcement for 5G research and development activities?

The NSF has traditionally done a good job funding academics who are pursuing new ideas for the future of wireless communications, but it was not always this way. As a young professor, I was concerned about the U.S. research complex developing knowledge for the wireless industry, and in 1991, I wrote a paper called "The Wireless Revolution"— it was a call for the NSF and the U.S. research community to realize that wireless would be foundational to the future of the U.S., while Europe was way ahead on that vision at the time. Since then, NSF and DARPA have realized the importance of wireless communications. The four test beds (Platforms for Advanced Wireless Research—PAWRs) announced by NSF on July 15 will enable academics to work with industry to test new concepts and ideas that are perhaps too immature or bold to be deployed on commercial networks. It was a nice announcement to ensure that U.S. research could play a role in the wireless future.

What are some of the expected initiatives that you think will be funded first?

Two of the four announced PAWRs will likely be funded first by NSF, and I suspect the winning test beds will require close coordination with several academic institutions that want to run national research platforms, along with a strong industrial backing and a strong connection with local government. Also, NSF will continue to fund individual principal investigators, as well as collaborative teams in new initiatives such as Information-Centric Networking and Wireless Edge Networking.

What are some of the leading applications you expect to be enabled by mmWave 5G technologies?

Massively broadband wireless applications, such as wireless displays, memory transfer/backup, 3D/virtual reality, gaming solutions and personal radar/sensing applications will emerge first. Wireless replacement of all kinds will evolve, including triple play offerings to rural customers and new business applications using the wide bandwidths now available. New types of repeater devices (to extend wideband coverage due to the power versus bandwidth trade-off), networking protocols to enhance caching and security, and new spectrum sharing technologies that enable real time sensing and service provisioning will evolve (based on the FCC's July 14 rulemaking). The Internet of Things (IoT) is already evolving, and new products and services will emerge that exploit both the vast new bands available for unlicensed devices as well as 5G services.

How is mmWave technology going to work with all of the other new technologies expected to be part of 5G systems?

As has occurred in all past cellular generations, the newest generation is first deployed with a carefully planned dovetail into the existing network, and over time, the networks, infrastructure and consumer devices are upgraded and morphed into the latest generation. I suspect you will see 5G mmWave deployments in urban cores and rural settings first, as an up-banded option for legacy 4G LTE (that continues to be improved). The directionality of mmWave channels will require new antenna technology and will especially exploit small cell architecture in urban/indoor deployments, as well as highly directional phased array antennas for rural deployments. Over the next decade, the sheer bandwidth available at mmWave will bring all of the networks and devices up these higher frequency bands.

All of these developments come only a few years after you and your students proved that millimeter wave technologies were practical for cellular communications—How are you feeling about all of these developments coming in such a short time after your research results and what do you think is next for the world?

It is very gratifying to know that our research at NYU WIRELESS, and my involvement in millimeter wave research over the past 20 years, has made an impact on humanity. There are a great many students who worked tirelessly to show that millimeter waves will work in mobile settings, when most of the world did not think that could ever work. This is our job in academia and why I continue to work at the University—to pursue knowledge that benefits industry while offering educational opportunities to bright, hungry students who are destined to change the world. I often tell students that our job as researchers is to "put ourselves out of business"—to let everyone know what we have learned, so that we are forced to go out and learn something new again, and to then again tell the world what we know to put ourselves out of business, and on and on, as we continue to push the envelope forward. I am very blessed to have the job I do, to be engaged with wonderful young people who will do great things, to work with industrial sponsors that have an interest in our work and students, and to be able to interact regularly with industry and start-up companies.■

RF Amplifiers and Sub-Assemblies for Every Application

Delivery from Stock to 2 Weeks ARO from the catalog or built to your specifications!

- Competitive Pricing & Fast Delivery
- Military Reliability & Qualification
- Various Options: Temperature Compensation, Input Limiter Protection, Detectors/TTL & More
- Unconditionally Stable (100% tested)

ISO 9001:2000 and AS9100B CERTIFIED

OCTAVE BAND LOW NOISE AMPLIFIERS

Model No.	Freq (GHz)	Gain (dB) MIN	Noise Figure (dB)	Power-out @ P1-dB	3rd Order ICP	VSWR
CA01-2110	0.5-1.0	28	1.0 MAX, 0.7 TYP	+10 MIN	+20 dBm	2.0:1
CA12-2110	1.0-2.0	30	1.0 MAX, 0.7 TYP	+10 MIN	+20 dBm	2.0:1
CA24-2111	2.0-4.0	29	1.1 MAX, 0.95 TYP	+10 MIN	+20 dBm	2.0:1
CA48-2111	4.0-8.0	29	1.3 MAX, 1.0 TYP	+10 MIN	+20 dBm	2.0:1
CA812-3111	8.0-12.0	27	1.6 MAX, 1.4 TYP	+10 MIN	+20 dBm	2.0:1
CA1218-4111	12.0-18.0	25	1.9 MAX, 1.7 TYP	+10 MIN	+20 dBm	2.0:1
CA1826-2110	18.0-26.5	32	3.0 MAX, 2.5 TYP	+10 MIN	+20 dBm	2.0:1

NARROW BAND LOW NOISE AND MEDIUM POWER AMPLIFIERS

Model No.	Freq (GHz)	Gain (dB) MIN	Noise Figure (dB)	Power-out @ P1-dB	3rd Order ICP	VSWR
CA01-2111	0.4 - 0.5	28	0.6 MAX, 0.4 TYP	+10 MIN	+20 dBm	2.0:1
CA01-2113	0.8 - 1.0	28	0.6 MAX, 0.4 TYP	+10 MIN	+20 dBm	2.0:1
CA12-3117	1.2 - 1.6	25	0.6 MAX, 0.4 TYP	+10 MIN	+20 dBm	2.0:1
CA23-3111	2.2 - 2.4	30	0.6 MAX, 0.45 TYP	+10 MIN	+20 dBm	2.0:1
CA23-3116	2.7 - 2.9	29	0.7 MAX, 0.5 TYP	+10 MIN	+20 dBm	2.0:1
CA34-2110	3.7 - 4.2	28	1.0 MAX, 0.5 TYP	+10 MIN	+20 dBm	2.0:1
CA56-3110	5.4 - 5.9	40	1.0 MAX, 0.5 TYP	+10 MIN	+20 dBm	2.0:1
CA78-4110	7.25 - 7.75	32	1.2 MAX, 1.0 TYP	+10 MIN	+20 dBm	2.0:1
CA910-3110	9.0 - 10.6	25	1.4 MAX, 1.2 TYP	+10 MIN	+20 dBm	2.0:1
CA1315-3110	13.75 - 15.4	25	1.6 MAX, 1.4 TYP	+10 MIN	+20 dBm	2.0:1
CA12-3114	1.35 - 1.85	30	4.0 MAX, 3.0 TYP	+33 MIN	+41 dBm	2.0:1
CA34-6116	3.1 - 3.5	40	4.5 MAX, 3.5 TYP	+35 MIN	+43 dBm	2.0:1
CA56-5114	5.9 - 6.4	30	5.0 MAX, 4.0 TYP	+30 MIN	+40 dBm	2.0:1
CA812-6115	8.0 - 12.0	30	4.5 MAX, 3.5 TYP	+30 MIN	+40 dBm	2.0:1
CA812-6116	8.0 - 12.0	30	5.0 MAX, 4.0 TYP	+33 MIN	+41 dBm	2.0:1
CA1213-7110	12.2 - 13.25	28	6.0 MAX, 5.5 TYP	+33 MIN	+42 dBm	2.0:1
CA1415-7110	14.0 - 15.0	30	5.0 MAX, 4.0 TYP	+30 MIN	+40 dBm	2.0:1
CA1722-4110	17.0 - 22.0	25	3.5 MAX, 2.8 TYP	+21 MIN	+31 dBm	2.0:1

ULTRA-BROADBAND & MULTI-OCTAVE BAND AMPLIFIERS

Model No.	Freq (GHz)	Gain (dB) MIN	Noise Figure (dB)	Power-out @ P1-dB	3rd Order ICP	VSWR
CA0102-3111	0.1-2.0	28	1.6 Max, 1.2 TYP	+10 MIN	+20 dBm	2.0:1
CA0106-3111	0.1-6.0	28	1.9 Max, 1.5 TYP	+10 MIN	+20 dBm	2.0:1
CA0108-3110	0.1-8.0	26	2.2 Max, 1.8 TYP	+10 MIN	+20 dBm	2.0:1
CA0108-4112	0.1-8.0	32	3.0 MAX, 1.8 TYP	+22 MIN	+32 dBm	2.0:1
CA02-3112	0.5-2.0	36	4.5 MAX, 2.5 TYP	+30 MIN	+40 dBm	2.0:1
CA26-3110	2.0-6.0	26	2.0 MAX, 1.5 TYP	+10 MIN	+20 dBm	2.0:1
CA26-4114	2.0-6.0	22	5.0 MAX, 3.5 TYP	+30 MIN	+40 dBm	2.0:1
CA618-4112	6.0-18.0	25	5.0 MAX, 3.5 TYP	+23 MIN	+33 dBm	2.0:1
CA618-6114	6.0-18.0	35	5.0 MAX, 3.5 TYP	+30 MIN	+40 dBm	2.0:1
CA218-4116	2.0-18.0	30	3.5 MAX, 2.8 TYP	+10 MIN	+20 dBm	2.0:1
CA218-4110	2.0-18.0	30	5.0 MAX, 3.5 TYP	+20 MIN	+30 dBm	2.0:1
CA218-4112	2.0-18.0	29	5.0 MAX, 3.5 TYP	+24 MIN	+34 dBm	2.0:1

LIMITING AMPLIFIERS

Model No.	Freq (GHz)	Input Dynamic Range	Output Power Range Psat	Power Flatness dB	VSWR
CLA24-4001	2.0 - 4.0	-28 to +10 dBm	+7 to +11 dBm	+/- 1.5 MAX	2.0:1
CLA26-8001	2.0 - 6.0	-50 to +20 dBm	+14 to +18 dBm	+/- 1.5 MAX	2.0:1
CLA712-5001	7.0 - 12.4	-21 to +10 dBm	+14 to +19 dBm	+/- 1.5 MAX	2.0:1
CLA618-1201	6.0 - 18.0	-50 to +20 dBm	+14 to +19 dBm	+/- 1.5 MAX	2.0:1

AMPLIFIERS WITH INTEGRATED GAIN ATTENUATION

Model No.	Freq (GHz)	Gain (dB) MIN	Noise Figure (dB)	Power-out @ P1-dB	Gain Attenuation Range	VSWR
CA001-2511A	0.025-0.150	21	5.0 MAX, 3.5 TYP	+12 MIN	30 dB MIN	2.0:1
CA05-3110A	0.5-5.5	23	2.5 MAX, 1.5 TYP	+18 MIN	20 dB MIN	2.0:1
CA56-3110A	5.85-6.425	28	2.5 MAX, 1.5 TYP	+16 MIN	22 dB MIN	1.8:1
CA612-4110A	6.0-12.0	24	2.5 MAX, 1.5 TYP	+12 MIN	15 dB MIN	1.9:1
CA1315-4110A	13.75-15.4	25	2.2 MAX, 1.6 TYP	+16 MIN	20 dB MIN	1.8:1
CA1518-4110A	15.0-18.0	30	3.0 MAX, 2.0 TYP	+18 MIN	20 dB MIN	1.85:1

LOW FREQUENCY AMPLIFIERS

Model No.	Freq (GHz)	Gain (dB) MIN	Noise Figure dB	Power-out @ P1-dB	3rd Order ICP	VSWR
CA001-2110	0.01-0.10	18	4.0 MAX, 2.2 TYP	+10 MIN	+20 dBm	2.0:1
CA001-2211	0.04-0.15	24	3.5 MAX, 2.2 TYP	+13 MIN	+23 dBm	2.0:1
CA001-2215	0.04-0.15	23	4.0 MAX, 2.2 TYP	+23 MIN	+33 dBm	2.0:1
CA001-3113	0.01-1.0	28	4.0 MAX, 2.8 TYP	+17 MIN	+27 dBm	2.0:1
CA002-3114	0.01-2.0	27	4.0 MAX, 2.8 TYP	+20 MIN	+30 dBm	2.0:1
CA003-3116	0.01-3.0	18	4.0 MAX, 2.8 TYP	+25 MIN	+35 dBm	2.0:1
CA004-3112	0.01-4.0	32	4.0 MAX, 2.8 TYP	+15 MIN	+25 dBm	2.0:1

CIAO Wireless can easily modify any of its standard models to meet your "exact" requirements at the Catalog Pricing.

Visit our web site at **www.ciaowireless.com** for our complete product offering.

Ciao wireless

Ciao Wireless, Inc. 4000 Via Pescador, Camarillo, CA 93012

Tel (805) 389-3224 Fax (805) 389-3629 sales@ciaowireless.com

DefenseNews
Cliff Drubin, Associate Technical Editor

Raytheon Unveils Battle Management Tool for U.S. Army

Raytheon Co. showcased Cyber and Electromagnetic Battle Management, a new battle management tool, at Cyber Quest, a U.S. Army event that informs cybersecurity requirements and priorities. CEMBM integrates cyber and electromagnetic spectrum awareness capabilities into the Electronic Warfare Program Management Tool, an Army program of record since 2014.

"CEMBM was one tool we experimented with, and each tool showed us a different level of the 'art of the possible' regarding the convergence of EW and cyber," said Major Steve Roberts, Cyber Branch chief, Cyber Battle Lab, Cyber Center of Excellence.

Raytheon's EWPMT focuses on the ability to see and understand events in the electromagnetic spectrum. CEMBM provides a shared situational understanding of electronic warfare, EMS and cyber, and management and control of organic assets.

> Shared awareness across cyber domain and electromagnetic spectrum.

Using CEMBM, EW officers can determine the best path forward without being jammed or discovered; jam the enemy's communication ability; and if there are cyber emitters, disrupt the ability to use them.

"The challenge lies in operating in the EMS while managing it in a way that minimizes negative impacts to other players and parts of the mission," said Frank Pietryka, director, Airborne Information Operations at Raytheon Space and Airborne Systems. "With CEMBM, teams now have a common operational picture where they can move back and forth, at will, between cyber, EMS and physical terrains. It is a true game changer."

This latest cyber and EW tool provides significant operational and life-cycle cost benefits, including increased mission effectiveness, reduced planning cycles, coordination of effects, collaboration with other elements of mission command, EW and cyber effectiveness analysis and reduced training costs.

Air Force, Lockheed Martin and Northrop Grumman Celebrate 100 Years of Protected Satellite Communications

VIEW VIDEO

When it comes to transmitting sensitive information in highly contested areas, the Advanced Extremely High Frequency (AEHF) system and Milstar satellites are proving their value, achieving 100 years of combined successful operations.

Designed as a protected, global network, the first Milstar was launched in 1994 aboard a Titan IV rocket. Since then, the constellation has served as a critical resource for troops and national leaders in delivering secure and reliable communications. In 2010, the first AEHF launched as the follow-on to Milstar, providing expansive coverage and five times faster connections.

AEHF Satellite - Courtesy Lockheed Martin

The Military Satellite Communications Directorate at the U.S. Air Force Space and Missile Systems Center leads the team, with Lockheed Martin as the prime contractor and Northrop Grumman Aerospace Systems as the payload provider.

"Protected communications means more than encryption and authentication—these systems must be the communications channel that stands when all others fail," said Iris Bombelyn, vice president of Lockheed Martin's Protected Communications mission area. "This is an important milestone in our support of that mission, and we continue to remain focused on anticipating changing needs and innovating new capabilities long into the future."

The nuclear-hardened communications satellites are resistant to high-tech jammers, eavesdropping and cyber attack. The system is also designed to insulate communications from vulnerability by eliminating the need for ground relay stations. Instead, the system uses on-board signal processing and radio frequency crosslinks, allowing communication between on-orbit satellites.

In July 2015, the AEHF system achieved initial operational capability and is being operated by the U.S. Air Force's 4th Space Operations Squadron. The next AEHF satellite, AEHF-4, is scheduled to launch in 2017. AEHF-5 and 6 are in production at Lockheed Martin in Sunnyvale, Calif., before they undergo final assembly, integration and test operations prior to launch.

Drone Payload Market

The global drone payload market is estimated to be $3.63 billion in 2016 and is projected to reach $7.72 billion by 2021, registering a CAGR of 16.25 percent during the forecast period.

On the basis of type, the synthetic aperture segment is estimated to lead the drone payload market, and is expected to continue its dominance during the forecast period. The market for SAR is primarily driven by the need for economical surveillance solutions with enhanced performance abilities for defense applications, in terms of identifying potential threats. The market for commercial is expected to register significant growth owing to increasing use of UAVs in civil applications, and relaxing of various regulatory norms.

For More Information — **Visit mwjournal.com for more defense news**

North America is expected to lead the market due to increasing focus of the U.S. Department of Defense (DOD) on using unmanned aerial vehicles for surveillance, and battle assessment and target acquisition-related tasks. This is due to the low cost of operations as compared to manned aircraft, which are expensive to procure and entail higher risks.

Major players are SZ DJI Technologies (China), Lockheed Martin, Northrop Grumman Corp., 3D Robotics (U.S.), Elbit Systems (Israel) and Thales Group (France) among others.

Predator B Detects and Tracks Ballistic Missile in Pacific Dragon Exercise

General Atomics Aeronautical Systems Inc., a manufacturer of remotely piloted aircraft (RPA) systems, radars, electro-optic and related mission systems solutions recently announced that through a contract with the Missile Defense Agency (MDA), it executed a missile tracking test as part of the Pacific Dragon (PD) exercise off the coast of the Pacific Missile Range Facility (PMRF) in Kauai, Hawaii.

Pacific Dragon is a trilateral Ballistic Missile Defense (BMD) tracking event between the U.S. Navy, Japan Maritime Self Defense Force, and Republic of Korea Navy. The biennial exercise focuses on improving tactical and technical coordination among its participants, including the detection, tracking and reporting of ballistic targets Two Predator® B RPA equipped with Raytheon Multi-spectral Targeting Systems-B (MTS-B) Electro-optical Infrared (EO/IR) turrets were used to detect and track a Ballistic Missile (BM) target as part of an ongoing program with MDA. The Predator B aircraft also participated in exercises with U.S. Navy vessels.

Predator - U.S. Air Force Photo

"The test provided valuable data in our ongoing effort to develop an effective airborne missile defense capability," said Linden Blue, CEO, GA-ASI.

A technologically advanced derivative of the combat-proven Predator, the multi-mission Predator B/MQ-9 Reaper® is a long-endurance, medium- to high-altitude RPA that can be used for surveillance, military reconnaissance, and targeting missions. The current aircraft configuration features an extensive payload capacity and is powered by a Honeywell turboprop engine with an altitude of over 45,000 feet. It is currently operational with the U.S. Air Force, U.S. Department of Homeland Security, NASA and a number of NATO countries.

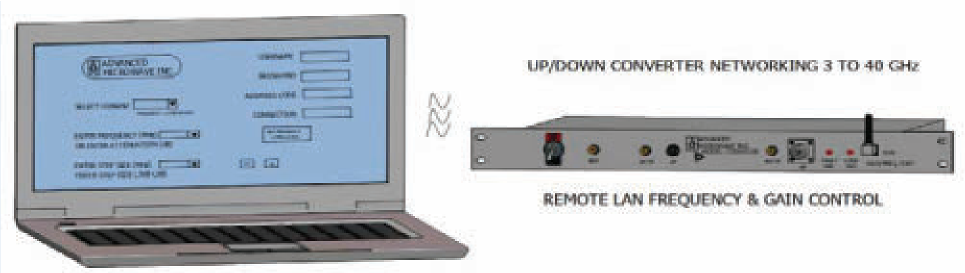

EU Project Takes Connected Driving to New HIGHTS

Connected driving technologies will enable vehicles to connect and share information with one another, as well as with infrastructure and other parts of the transport network. The high precision positioning for the cooperative ITS applications (HIGHTS) project, which is supported by the European Union under the Horizon 2020 funding scheme, aims to combine traditional satellite systems with on-board sensing and infrastructure-based wireless communication technologies such as Wi-Fi, Bluetooth, Zigbee and LTE to produce advanced, highly-accurate positioning technologies for C-ITS.

Today's satellite-based positioning systems such as GPS and Galileo are unable to provide sufficiently accurate position information for many important applications and in certain challenging but common environments including urban canyons and tunnels.

> ...an enhanced European-wide positioning service platform...

The HIGHTS project is expected to produce advanced, highly accurate positioning technologies that could be used for connected driving as well as other applications. The system could contribute to Cooperative Adaptive Cruise Control (C-ACC) on the road, leading to smoother driving conditions as vehicles, arranged in platoons, would maintain their distance and speed in relation to one another. Lane detection technologies would also provide more efficient guidance in towns and on motorways.

The results of the project will be integrated into the facilities layer of ETSI C-ITS architecture and will thereby become available for all C-ITS applications. The project will go beyond ego-structure-based and infrastructure-based positioning by incorporating them as building blocks to develop an enhanced European-wide positioning service platform based on enhanced Local Dynamic Maps and built on open European standards.

© vectorfusionart – fotolia.com

LTE Connects 1 in 5 Mobile Subscribers Worldwide

The Global mobile Suppliers Association (GSA) has confirmed that LTE is growing faster than any other mobile communications system technology with 19.5 percent of the global mobile base connected to LTE systems by June 30, 2016. LTE subscriptions reached 1.453 billion in Q2 2016 with 160.3 million net connections coming in that quarter. The rate of connections is about four times faster than 3G/HSPA systems, which grew by 40.5 million while GSM subscriptions fell 101.6 million in the same quarter.

> ...LTE is growing faster than any other mobile communications system technology...

The Asia region, with over 838 million LTE subscriptions, further grew its share of global LTE subscriptions quarter-on-quarter to reach 57.7 percent and by June 2016 China had passed 591 million LTE subscriptions, adding 80.3 million in the quarter. North America is the second largest LTE market with 268.4 million and 18.5 percent of the global total. After APAC the European region gained the most LTE subscriptions during Q2 by adding 20.5 million and slightly growing its global share of the total to 14.1 percent.

The Latin America and Caribbean region added 13.3 million to reach 81.9 million 4G/LTE subscriptions, representing 19.4 percent growth. The Middle East has over 50 million LTE subscriptions following a 10 percent rise in Q2 while Russia has 19.6 million LTE subscriptions. Africa, now with over 10 million LTE subscriptions, is the fastest growing region by percentage, following a 22.4 percent increase in Q2 and India has 5.5 million LTE subscriptions.

QinetiQ to Integrate Unmanned Air, Sea and Subsea Vehicles

QinetiQ will provide the UK component of a multinational demonstration of unmanned and autonomous systems under a new contract with the Defence Science and Technology Laboratory (Dstl).

The demonstration, dubbed Hell Bay 4, will see a variety of unmanned underwater, surface and air vehicles working co-operatively within a number of squads, autonomously undertaking mine countermeasures missions. QinetiQ will lead a team that includes Seebyte, Blue Bear Systems Research and ASV in the exercise, which involves participants from the U.S., Canada and Australia.

Hell Bay 4 will be delivered under the Maritime Autonomy Framework (MAF), a Dstl-led initiative and development programme that has enabled the UK to participate in a number of regular multinational demonstrations and trials. Phase one of the Framework established software and

For More Information — **Visit mwjournal.com for more international news**

> ...multinational demonstration of unmanned and autonomous systems...

architecture to test Unmanned Underwater Vehicles (UUV), with Phase Two seeing the integration of an Unmanned Surface Vehicle (USV) into a cooperative squad.

QinetiQ is contracted to deliver the third phase of the MAF, in which an Unmanned Aerial Vehicle (UAV) will be introduced into the squad to provide situational awareness and communications relay to vehicles on and under the water.

The contract win is the fifth in a year for the QinetiQ Maritime Autonomy Centre (QMAC), established in 2013 to accelerate the UK's adoption of autonomous systems by facilitating their design, development, testing and evaluation.

World's Largest Nanomaterial Production Plant Opens

The SHYMAN project aims to establish continuous hydrothermal synthesis as the most flexible and sustainable process to create nanomaterials on an industrial scale. After demonstrating this potential in the lab, the project has now announced the opening of its first facility in Nottingham,UK.

This spin-out of the University of Nottingham is in charge of operating the new plant, which is expected to produce over 1000 tonnes of nanomaterials every year. The production cost is lower than that of other facilities and the chosen production method—continuous hydrothermal synthesis—is expected to impact even markets for which sale prices had so far been an obstacle.

> ...the potential to benefit both industry and society...

Professor Ed Lester, Technical Coordinator of Promethean Particles commented, "We have already had a lot of interest from companies in a diverse range of sectors. From healthcare, where nano-particles can be used in coatings on medical devices, to enhanced fabrics, where nano-materials can add strength and flexibility to textiles, and in printed electronics, as we are able to print materials such as copper."

"These are very exciting times for Promethean Particles," said Dr Susan Huxtable, Director of Intellectual Property and Commercialisation at the University of Nottingham. "The new facility opens up a myriad of opportunities for them to sell their services into new markets right across the world. It is a great example of how many of the technologies developed by academics here at the University of Nottingham have the potential to benefit both industry and society."

Directional/Bi-Directional

COUPLERS

5 kHz to 18 GHz up to 250 W *from* 95¢ *ea. (qty. 1000)*

Now! 475 ~~326~~ models in stock, and we're adding even more! Looking for couplers or power taps? Mini-Circuits has 475 models in stock, and we're adding even more! Our versatile, low-cost solutions include surface-mount models down to 1 MHz, and highly evolved LTCC designs as small as 0.12 x 0.06", with minimal insertion loss and high directivity. Other SMT models are designed for up to 100W RF power, and selected core-and-wire models feature our exclusive Top Hat™ for faster, more accurate pick-and-place.

At the other end of the scale, our new connectorized air-line couplers can handle up to 250W RF input power, with low insertion loss and exceptional coupling flatness! All of our couplers are RoHS compliant. So if you need a 50 or 75Ω, directional or bi-directional, DC pass or DC block coupler, for military, industrial, or commercial applications, you can probably find it at minicircuits.com, and have it shipped today!

Mini-Circuits®

www.minicircuits.com P.O. Box 350166, Brooklyn, NY 11235-0003 (718) 934-4500 sales@minicircuits.com

495 rev E

Hand Flex Cables conform to any shape required.

from $9.75 ea. (qty.1-9) DC to 18 GHz

Get the performance of semi-rigid cable, <u>and</u> the versatility of a flexible assembly. Mini-Circuits Hand Flex cables offer the mechanical and electrical stability of semi-rigid cables, but they're easily shaped by hand to quickly form any configuration needed for your assembly, system, or test rack. Wherever they're used, the savings in time and materials really adds up!

Excellent return loss, low insertion loss, DC-18 GHz. Hand Flex cables deliver excellent return loss (33 dB typ. at 9 GHz for a 3-inch cable) and low insertion loss (0.2 dB typ. at 9 GHz for a 3-inch cable). Why waste time measuring and bending semi-rigid cables when you can easily install a Hand Flex interconnect?

Two popular diameters to fit your needs. Hand Flex cables are available in 0.086" and 0.141" diameters, with a tight turn radius of 6 or 8 mm, respectively. Choose from SMA, SMA Right-Angle, SMA Bulkhead, SMP Right-Angle Snap-On and N-Type connectors to support a wide variety of system configurations.

Standard lengths in stock, custom models available. Standard lengths from 3 to 50" are in stock for same-day shipping. You can even get a Designer's Kit, so you always have a few on hand. Custom lengths and right-angle models are also available by preorder. Check out our website for details, and simplify your high-frequency connections with Hand Flex! *RoHS compliant*

SMA | SMA Right Angle | SMA Bulkhead | SMP Right Angle Snap-On | N-Type | N-Type Bulkhead

Mini-Circuits®

www.minicircuits.com P.O. Box 350166, Brooklyn, NY 11235-0003 (718) 934-4500 sales@minicircuits.com

Scan page using layar app

Cliff Drubin, Associate Technical Editor

Mobile Operators Reach for Unlicensed Spectrum

With operators struggling to maintain cost-effective operations in the face of exponentially growing data demand, many are now turning to unlicensed spectrum technologies. ABI Research predicts that the support for unlicensed spectrum technologies, including LTE-LAA and Wi-Fi, will be one of the main drivers for the indoor small cell market, resulting in overall revenue hitting $1.8 billion in 2021.

"Unlicensed LTE had a rough start, meeting negative and skeptic reactions to its possible conflict with Wi-Fi operations in the 5 GHz bands," says Ahmed Ali, senior analyst at ABI Research. "But the ongoing standardization and coexistence efforts increased the support in the technology ecosystem."

> Support for LTE-based and Wi-Fi unlicensed spectrum technologies within small cell equipment will grow to 51% of total annual shipments by 2021 at a CAGR of 47%.

For the LAA standard, the 3GPP adopted a Listen-Before-Talk channel access mechanism to share the spectrum fairly. The IEEE and Wi-Fi Alliance are also developing a coexistence testing process to help stakeholders deliver a harmonized, multi-technology environment in the unlicensed spectrum.

In harmony with the adoption of unlicensed LTE solutions, Wi-Fi remains an essential and well-established element of indoor connectivity. The availability of multiple access technologies aligns well with the different enterprise requirements and will drive further convergence among these technologies in the years ahead.

"The dynamic and diverse nature of indoor venues calls for an all-inclusive small cell network that intelligently adapts to different user requirements," concludes Ali. "Support for multi-operation features like 3G/4G and Wi-Fi/LAA access is necessary for the enterprise market."

Next-Gen BLE and Ultra-Wideband Technologies Threaten Growth of RTLS Solutions

VIEW VIDEO

A host of next-generation BLE beacon and Ultra-Wideband (UWB) technologies threaten to dramatically disrupt the real-time location system (RTLS) and asset tracking markets. ABI Research forecasts that new solutions by innovators like Bluvision, DecaWave and UWINLOC, along with the arrival of Industrial IoT, will result in a combined RTLS and asset tracking market that more than triples from its current standpoint to reach $15 billion in 2021.

"For the first time, enterprises don't have to choose between high accuracy, low cost and ease of deployment," says Patrick Connolly, principal analyst at ABI Research. "Emerging startups like SINTRA, Quuppa, Quantitec and MIST can offer all three using proprietary BLE and UWB. This poses a serious threat to current market holders, as traditional technologies, like active-RFiD, Wi-Fi and legacy UWB, remain restricted due to its inability to meet the aforementioned criteria."

These traditional technologies will still have a place, but it will be increasingly marginalized, particularly as smartphones and wearables become more predominant in industrial spaces. ABI Research forecasts a 5:1 ratio on new RTLS technology tags versus traditional RTLS technologies by 2021, with significant growth into new greenfield applications like pallet tracking, condition monitoring and inventory management. Companies like Zebra that offer a mixture of traditional and new technologies that can be implemented and managed together under one platform will do well in the new market dynamic.

And the divide between active RTLS and passive asset tracking is blurring. Retailers' growing need for accurate, real-time in-store inventory data led to Impinj and View Technologies developing passive radio frequency identification (RFiD) RTLS solutions, with ABI Research expecting many more to follow given the huge potential of this market. Similarly, UWINLOC's passive UWB technology offers high accuracy at passive RFID level costs, with near real-time location updates. However, it is important to point out that passive ultra-high frequency (UHF) RFiD remains the dominant technology in terms of volumes and revenues throughout the forecast period.

> "For the first time, enterprises don't have to choose between high accuracy, low cost and ease of deployment."

Moving forward, companies like Avery Dennison, which recently partnered with EVRYTHING, will develop solutions that can track items beyond the point-of-sale (POS) and throughout their lifetimes. This brings benefits like authenticity verification, customer engagement, re-orders, loyalty programs, and post-sale services via a BLE beacon community.

"The increasing demand for instant gratification from customers will drive new competitive business models, including on-demand load matching and the uberization of delivery, from companies like Cargomatic and Confreight," concludes Connolly. "Longer term, wearables and robotics will lead to an even greater need for accurate, real-time location data to improve performance."

For More Information

Visit mwjournal.com for more commercial market news

Mobile Biometrics Market Outlook

According to Aerospace and Defense News, the growing penetration of mobile devices and the increasing number of mobile transactions are driving the growth of the mobile biometrics market. Over the last few years, the number of online transactions and e-commerce has gradually gone up and has created a huge opportunity for the companies to invest in the biometric industry to secure these transactions. A shift from traditional commerce to smart commerce using biometric-enabled mobile devices would save time and provide high security for transactions.

The market in the healthcare industry is expected to grow at the highest rate. The proliferation of electronic health records (EHR) and the transition of data across health information exchanges (HIE) has created a huge demand for mobile biometrics as it is essential to secure and protect these digital records. Healthcare providers are using biometric patient identification systems to ensure patient safety by ensuring that patients are accurately identified prior to treatment.

The fingerprint recognition technology is the most prominent biometrics technology in use at present. Most of the smartphone manufacturers such as Apple and Samsung use fingerprint recognition technology in their offerings. This strategy is being followed by emerging companies across the world. As fingerprint recognition is the most convenient technology in terms of investment and market acceptance, it is expected to lead the market during the forecast period.

> The market is expected to grow at a CAGR of 22%, reaching $49 billion by 2022.

The adoption of mobile biometric technologies in passports & visas, banking & finance, large-scale funded programs and employee access monitoring in buildings is driving the growth of the mobile biometrics market in North America.

The market in APAC is expected to grow at the highest CAGR. Many countries in the Asia-Pacific region have started adopting mobile biometric technologies in national IDs and e-passports, and their governments are actively promoting and adopting them. India has introduced biometric-based unique identification (UID) which is likely to cover 1.25 billion Indians. In 2012, China introduced the new China Resident Identity Card Law which requires Chinese citizens to have their fingerprints scanned and recorded. Large-scale township projects in Japan have also started adopting biometrics as a standard security device.

The major companies in the mobile biometrics market include Apple Inc., Nuance Communications Inc., M2SYS Technology, 3M Cogent Inc., Crossmatch, BIO-key, Aware Inc., EyeVerify Inc. and Fulcrum Biometrics LLC (U.S.); Safran SA (France); Precise Biometric (Sweden) and Applied Recognition Inc. (Canada).

Around the **Circuit**

Barbara Walsh, Multimedia Staff Editor

MERGERS & ACQUISITIONS

Analog Devices Inc. announced the acquisition of the **Cyber Security Solutions (CSS) business of Sypris Electronics LLC.** This acquisition represents a significant leap forward in ADI's ability to deliver secure high-performance analog solutions demanded by current and future market needs. The CSS business of Sypris Electronics LLC is well-known as a leader in secure system and software products and technology. For more than 50 years, Sypris has built a proven track record of delivering high-assurance information security services to the world's most demanding customers, including military and government organizations needing to protect against sophisticated nation-state level threats and attacks.

AMBER Wireless GmbH, manufacturer of wireless connectivity solutions, is now part of **Würth Elektronik eiSos GmbH & Co. KG**. With the merger the owner-run wireless specialist founded in 1998 lays the foundation for further growth and the globalization of its activities. Through the acquisition, Würth Elektronik eiSos considerably expands its range in growth fields, such as Internet of Things, Industry 4.0 and Smart Metering. AMBER Wireless is a manufacturer of low power ISM/SRD solutions in Europe and offers highly efficient wireless products in the 169 MHz, 433 MHz, 868 MHz, 915 MHz and 2.4 GHz frequency bands.

COLLABORATIONS

Aemulus, a leader in automated test equipment (ATE) solutions, and **Peregrine Semiconductor Corp.**, founder of RF SOI and pioneer of advanced RF solutions, announced their strategic partnership in the development of a new microwave frequency tester. Building on the success of Aemulus's Amoeba™ AMB7600 RF tester, this next-generation test solution will extend its support into microwave frequency bands and enable more complex testing. The Aemulus Amoeba AMB7600 will be upgraded with key peripheral modules to expand into microwave bands X, Ku and Ka. The AMB7600 is the world's first true multi-site, multi-instance RF tester, and it supports RF, digital and analog testing.

Modelithics Inc. announced the availability of new Microwave Global Models™ for Passive Plus 0505C and 1111C surface mount chip capacitor families. Modelithics and Passive Plus recently collaborated through the Modelithics Vendor Partner (MVP) Program to extend the 0505C model through 1000 pF (originally 0.1 pF through 150 pF), and the 1111C model through 10,000 pF (originally 0.1 through 150 pF). The models have also been upgraded to include orientation selectability, which defines the mounting orientation of the capacitor (horizontal or vertical) on the PCB fixture.

Akoustis Technologies Inc. has signed non-exclusive agreements with a Chinese, tier one, RF front-end (RFFE) module manufacturer to develop and supply RF filter products. Under the terms of the joint development agreement (JDA), the companies will work together to develop high band BAW filters for front-end modules for 4G, 4.5G, 5G and Wi-Fi applications. A statement of work accompanying the JDA defines the design, specifications and productization of high band, single crystal BAW filters. Akoustis expects to begin producing initial prototype filters by the end of 2016, with production purchase orders in 2017.

Ericsson and **China Mobile** have partnered to conduct the world's first 5G-enabled drone prototype field trial on operator's network. The trial represents a major milestone on the road to 5G. In the trial, held in Wuxi in China's Jiangsu province, a drone was flown using operator's cellular network with 5G-enabled technologies and with handovers across multiple sites. In order to demonstrate the concept's validity in a real-world setting, the handovers were performed between sites that were simultaneously in use by commercial mobile phone users.

NEW STARTS

Advanced Switch Technology announced the launch of a new company logo that reflects the evolution of their brand. Proud of their 24-year history serving the Telecom industry, the company says the new logo harnesses their past and symbolizes their current growth and dynamic future. You can view the new logo by visiting www.astswitch.com.

ACHIEVEMENTS

Custom MMIC is celebrating its 10-year anniversary in 2016. Custom MMIC is proud to celebrate a decade of innovation, and its commitment to their clients, their products and the RF/microwave industry. Custom MMIC's success stems from the desire to deliver every step of the way. Those celebrating with Custom MMIC at IMS2016 praised the company for their leading edge technology, superior delivery and phenomenal customer support.

Richardson RFPD Inc. announced that it has received an award from DAIHEN Corp., a company based in Osaka, Japan that specializes in the manufacturing, sales and service of electric power transmission and distribution products, dispersed power system, welding machines, industrial robots and power supply for plasma applications, and clean transfer robots used in the manufacture of semiconductor, LCD and solar panel.

Raytheon Co. showcased Cyber and Electromagnetic Battle Management (CEMBM), a new battle management tool, at Cyber Quest, a U.S. Army event that informs cyber-security requirements and priorities. CEMBM integrates cyber and electromagnetic spectrum awareness capabilities into the Electronic Warfare Program Management Tool, an Army program of record since 2014. Raytheon's EWPMT focuses on the ability to see and understand events in the electromagnetic spectrum. CEMBM provides a shared

For More Information For up-to-date news briefs, visit mwjournal.com

situational understanding of electronic warfare, EMS and cyber, and management and control of organic assets.

Start-up SAW filter designer **Resonant** has signed another licensing agreement with an existing "tier one" customer, this design an integrated module that combines a duplexer and quadplexer. The quadplexer separates four different frequency bands with only a single antenna connection, which eliminates the need for antenna switching. The module design will combine chip scale packaging (CSP) and wafer level packaging (WLP) to reduce the footprint on the PCB. These two designs are on the heels of three with this same customer that were announced in August, bringing the total to seven.

Nano Dimension Ltd., a leader in the field of 3D printed electronics, announced that its wholly owned subsidiary, Nano Dimension Technologies, has supplied the first DragonFly 2020 system designated for 3D circuitry and PCBs. The supply was made to a leading defense company in Israel for evaluation purposes and is expected to be installed at the partner's site in the coming days. To date, Nano Dimension has proven its capabilities of printing multilayer electric circuits in lab conditions. With the first supply of the DragonFly 2020 system for testing, Nano Dimension marks yet another breakthrough for the company.

MPI announced the successful completion of third-party conformity assessments (testing and certification) based on IEC 61010, EN ISO 12100 and SEMI S2 for all Advanced Semiconductor Tests (AST) automated probe systems. MPI has demonstrated clear leadership in recent years developing numerous and very significant innovations while serving customers within the engineering probe systems market. MPI continues its leadership position with efforts to increase transparency associated with compliance to industry specifications and standards. MPI's receipt of the third-party certification for all of the automated probe stations reflects a commitment to increasingly important standards for end users and corporations requiring vendors to comply with industry specifications.

CONTRACTS

The National Guard Bureau (NGB) has awarded a $28 million modernization and engineering support contract for the Air National Guard Air Force Reserve Command Test Center (AATC) to **Modern Technology Solutions Inc.** (MTSI), an engineering services and technology solutions provider for the defense industry, intelligence community, and commercial markets. Prior to the award of this OASIS Task Order, MTSI had successfully performed this work under a five year task order for NGB. The contract term is for one base year with four option years.

With a combined value of approximately AUD32.5 million, **Saab** has signed a contract with the **Australian Defence Force** to upgrade the Army's RBS 70 ground-based air defence weapon system and Giraffe AMB radar. Delivered under the AIR 90 programme, the existing Identification Friend or Foe (IFF) capability of the RBS 70 and Giraffe AMB systems will be upgraded to include Mode 5 func-

tionality. The Mode 5 waveform uses modern modulation, coding, and cryptographic techniques to overcome performance and security limitations in the current Mode 4 waveform. Additionally, Mode 5 systems provide expanded data handling capabilities to securely pass GPS position and other extended data.

PAR Technology Corp. announced that its indirect wholly-owned subsidiary, **Rome Research Corp.** (RRC), has been awarded a five-year, $13.6 million contract from the **U.S. Navy** to provide Teleport Commercial Satellite Terminal services at the Global Information Grid (GIG) facility in Lago Patria, Italy and other remote locations. The GIG is the global network of information capabilities, processes and personnel for collecting, processing, storing, disseminating and managing information on demand for use by military commanders, policy makers and support personnel.

Orbital ATK Inc., a global leader in aerospace and defense technologies, has received an $11 million contract for the continuation of Contractor Logistic Support (CLS) for the **Iraqi Air Force's Armed Caravan** program. The contract provides funding to provide sustained CLS services including all maintenance and support training for the modified aircraft fleet currently used by the Iraqi Air Force in their security mission. The contract will also include spare parts, component repair, publication updates, maintenance training and logistics. Additional options, if exercised, would bring the cumulative value of the contract to $118 million and extend the period of performance through 2020.

Comtech Telecommunications Corp. announced that during its fourth quarter of fiscal 2016, its Government Solutions segment received a $7.6 million funded order for its Secret Internet Protocol Router and Non-Secure Internet Protocol Router Access Point (SNAP) Very Small Aperture Terminal (VSAT) satellite systems. To-date, Comtech has received $49.5 million of funded orders against the $91 million contract ceiling. The U.S. Army Project Manager for the Warfighter Information Network - Tactical (PM WIN-T) Commercial Satellite Terminal Program is funding this procurement through the Army's GTACS contract vehicle.

Rohde & Schwarz was awarded a contract by the **Procurement Office of the German Federal Ministry of the Interior** for the latest generation of R&S QPS200 security scanners. The three-year framework agreement encompasses 300 systems plus accessories and service. This makes the R&S QPS200 the security scanner of choice for security checks based on millimeter-wave technology within German federal facilities. The instruments will be the preferred selection for the Federal Police for security checks at airports throughout Germany. The scanners can also be used for security access control in other places, such as in ministries, for example.

The Florida-Israel Business Accelerator (FIBA) announced that they have entered into an agreement with the **United States Special Operations Command**


ONE PLATFORM, ZERO BARRIERS
SIMPLY SMARTER
NI AWR DESIGN ENVIRONMENT
NI AWR Design Environment is one platform — integrating system, circuit, and electromagnetic analysis — for the design of today's advanced wireless products from base stations to cellphones to satellite communications. Its intuitive use model, proven simulation technologies, and open architecture supporting third-party solutions translates to zero barriers for your design success. Simply smarter design.
Learn more at ni.com/awr
AWR
NATIONAL INSTRUMENTS™
Microwave Office | Visual System Simulator™ | Analog Office | AXIEM | Analyst™

Around the **Circuit**

(SOCOM) to collaborate on the production of innovative technologies. The Cooperative Research & Development Agreement (CRADA) establishes a partnership between the two organizations in which FIBA cohorts will produce products or services that will fill technology capability shortfalls for SOCOM. SOCOM spends over $3 billion a year on procurement, including an R&D budget of $538 million in 2016. SOCOM's small size and independent budgetary authority (headquartered in Tampa, Fla.) gives the agency both flexibility and an advantage over the rest of the U.S. armed service branches in technology acquisition.

L-3 Communications announced that its **Integrated Sensor Systems** (ISS) sector within its Electronic Systems segment has been selected under a **U.S. Foreign Military Sales** (FMS) contract to provide eight WESCAM MX™-10D electro-optical and infrared (EO/IR) designating turrets to a Middle Eastern nation's Ministry of Defense. L-3's MX-10Ds will be used by the customer in support of counterterrorism operations from its newly acquired UH-60 Black Hawk helicopters. Turret deliveries to Sikorsky, the integrator for the program, began in June 2016 and will continue through February 2017.

PEOPLE

▲ *Alex Davern*

NI, the provider of platform-based systems that enable engineers and scientists to solve the world's greatest engineering challenges, announced that its board of directors has elected **Alex Davern**, to serve as chief executive officer and president of National Instruments, effective January 1, 2017. Davern will succeed Dr. James Truchard, who has served as the chief executive officer of NI since the company's founding in 1976. Dr. Truchard will remain as chairman of the board. This transition is being undertaken as part of the board's succession planning process.

▲ *John Procacci*

Integrated Microwave Technologies (IMT) announced the appointment of **John Procacci** as vice president of sales. Procacci will be responsible for leading the entire sales team at IMT and commercial sales at xG Technology. He will also work in conjunction with cross-functional teams from marketing, product development, operations and support to the design department. Procacci is tasked with delivering superior communications solutions to IMT's range of clients for increased customer support.

▲ *Alan Chang*

Anokiwave Inc., an innovative company providing highly integrated core IC solutions for mmW markets and AESA based solutions, announced the latest addition to its leadership team and the expansion into the Asia-Pacific region with the appointment of **Alan Chang** to the position of director of Asia-Pacific sales. Chang joined Anokiwave in June

Around the **Circuit**

2016 and brings over 18 years of sales and engineering experience to the team. He has a proven track record of establishing new markets, building distributor relations, and leading sales growth in Asia-Pacific.

▲ *John Clinton*

Maury Microwave Corp. announced that **John Clinton** has joined the company as director of sales, Interconnect. With more than 30 years of industry experience, Clinton will champion the company's cable and connector business, building upon the year-over-year growth the company has realized since entering this market space. Clinton brings to Maury his award-winning sales and coaching skills from his time with HP, then Agilent (now Keysight) and Microlease.

Laser Services Inc., an ISO and AS-9100 registered precision laser cutting, drilling, scribing, etching and welding job shop, recently added two new hires in operations and sales. **Mark Flahive** joined Laser Services as a production manager bringing over 30 years of technical, sales and management experience. His extensive background in the medical device, defense, aerospace and microwave industries, makes him a strong asset to the team. Laser Services also welcomed **Michael Rios** to their technical sales team. Rios brings six years of laser mechanical and programming operations experience to the team. He is also a certified ISO auditor.

REP APPOINTMENTS

Richardson RFPD Inc. announced a global agreement with **Power Integrations Inc.** Under the terms of the agreement, Richardson RFPD will distribute Power Integrations' SCALE™ IGBT drivers for the high-power market, as well as its new SCALE-iDriver™ integrated circuits, on a worldwide basis. Power Integrations' family of SCALE gate drivers reduce component count, enhance efficiency and improve reliability.

IN MEMORIAM

Richard T. "Dick" DiBona, 83, formerly of Wayland, Mass. passed away on August 1, 2016. He received his B.S. in engineering management from M.I.T. in 1955. He went on to work for the Ford Motor Co. in Detroit before returning to Massachusetts after the sudden death of his father in 1957. DiBona started his career at M/A-COM, then Microwave Associates, in 1958 as a sales engineering manager and attended the M.I.T. Sloan School Executive Management Program in 1979. He quickly moved up the management ranks and was promoted to president, chairman and chief executive officer of M/A-COM in 1983. After suffering a debilitating stroke in 1986, DiBona retired from M/A-COM, however continued consulting in the microwave semiconductor field and was on the board of Theta-J, CP-Clair and MDT.

ULTRA·REL™ CERAMIC MMIC AMPLIFIERS

10 MHz to 7 GHz

LTCC Construction
Outstanding Thermal Stability

Hermetically Sealed Nitrogen Filled
100% Tested*

Highly Repeatable
Electrical Performance

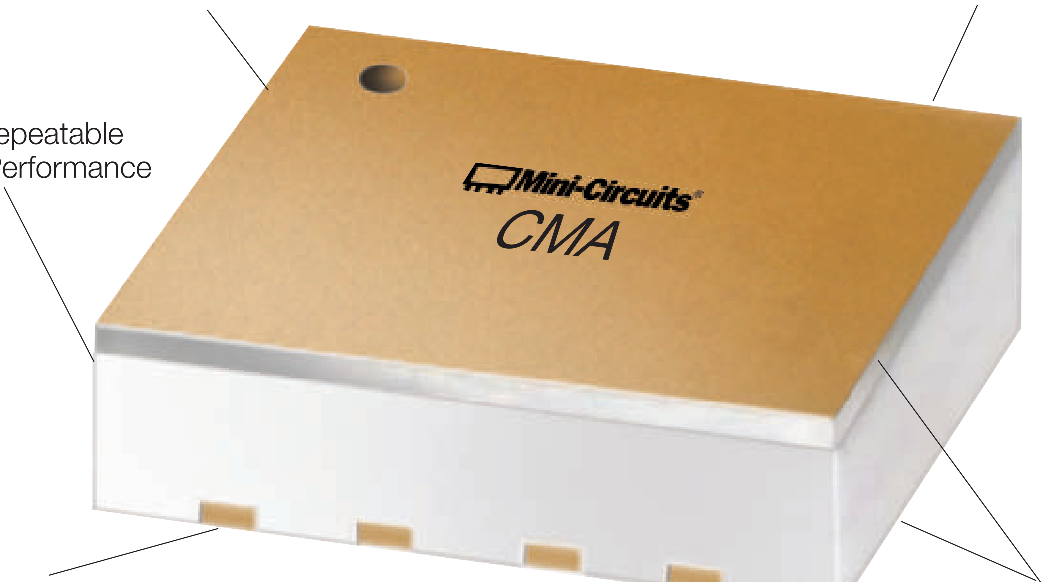

Exposed Terminals for
Easy Solder Inspection

Tiny Size
3 x 3 x 1.14 mm high

Low NF from 0.5 dB *High IP3 up to +42 dBm* *Low DC current 65 mA* from $7[45] ea. (qty 20)

When failure is not an option! Our CMA family of ceramic MMIC amplifiers is expanding to meet your needs for more critical applications. Designed into a nitrogen-filled, hermetic LTCC package just 0.045" high, these rugged models have been qualified and are capable of meeting MIL standards for a whole battery of harsh environmental conditions:

Qualified for: *(see website for complete list and details)*

Gross and Fine Leak	*HTOL (1700 hours @ +105°C)*
Mechanical Shock	*Steam Aging*
Vibration	*Solder Heat Resistance*
Acceleration	*Autoclave*
PIND	*And More!*

**Gross leak only*

Robust performance across wide bandwidths makes them ideal for military and defense applications, hi-rel instrumentation, and anywhere long-term reliability adds bottom-line value. Go to minicircuits.com for all the details today, and have them in your hands as soon as tomorrow!

Electrical Specifications *(-55 to +105°C)*

3 x 3 x 1.14 mm

Model	Freq. (GHz)	Gain (dB)	P_{OUT} (dBm)	IP3 (dBm)	NF (dB)	DC (V)	Price $ ea. (qty 20)
CMA-81+	DC-6	10	19.5	38	7.5	5	8.95
CMA-82+	DC-7	15	20	42	6.8	5	8.95
CMA-84+	DC-7	24	21	38	5.5	5	8.95
CMA-62+	0.01-6	15	19	33	5	5	7.45
CMA-63+	0.01-6	20	18	32	4	5	7.45
CMA-545+	0.05-6	15	20	37	1	3	7.45
CMA-5043+	0.05-4	18	20	33	0.8	5	7.45
CMA-545G1+	0.4-2.2	32	23	36	0.9	5	7.95
CMA-162LN+	0.7-1.6	23	19	30	0.5	4	7.45
CMA-252LN+	1.5-2.5	17	18	30	1	4	7.45

RoHS compliant

Mini-Circuits®

www.minicircuits.com P.O. Box 350166, Brooklyn, NY 11235-0003 (718) 934-4500 sales@minicircuits.com

INVITED PAPER

802.11ax – High Efficiency Wireless

Alejandro Buritica
National Instruments, Austin, Texas

Mobile users have continued to demand more data and greater availability of wireless connectivity networks since the early days of the first Wi-Fi devices. Subsequently, the IEEE 802.11 wireless networking standard has consistently evolved and adapted to meet this growing need.

Around 1999, the 802.11b implementation provided wireless links at about 11 Mbps using direct sequence spread spectrum (DSSS). In 2003 the 802.11a/g revision increased the link speed and wireless performance by adopting orthogonal frequency division multiplexing (OFDM). This implementation offered users data rates of up to 54 Mbps, a big improvement that spurred wider market adoption. The next performance jump came with 802.11n (2009), presenting users with single stream links up to 150 Mbps. The 802.11ac revision (2013), brought with it the possibility of link speeds around 866 Mbps on a single spatial stream (SS) with wider channels (80 and 160 MHz) and higher modulation orders (256-QAM). Using the specified maximum number of eight spatial streams, 802.11ac users would, in theory, benefit from link speeds of 6.97 Gbps, surpassing the data rates of wired Ethernet connections.

If that technology is already in place, then why do users commonly experience frustratingly slow data traffic when connected to a public Wi-Fi network at a busy train station or sports arena? Although there are several factors that affect signal quality and data rates, the way current access points (AP) and stations (STA) deal with overcrowded networks commonly cause the data flow to slow to a crawl.

A new revision of the IEEE 802.11 wireless LAN standard—802.11ax—seeks to remedy this situation. 802.11ax, also called high efficiency wireless (HEW), seeks to improve the average throughput per user by a factor of at least 4× in dense user environments. Looking beyond the raw link speeds of 802.11ac, this new standard implements several mechanisms to serve a consistent and reliable data throughput to more users in crowded places. This includes mixed-environment locations with many access points and a high concentration of users with different kinds of connectivity devices.

CHALLENGES IN DENSE ENVIRONMENTS

The 802.11 protocol uses a carrier sense multiple access (CSMA) method, where STAs first sense the channel and attempt to avoid collisions by transmitting only when they do not detect any 802.11 signals. When an STA hears another one, it waits for a random amount of time for the other STA to stop transmitting before listening again for the channel to be free.

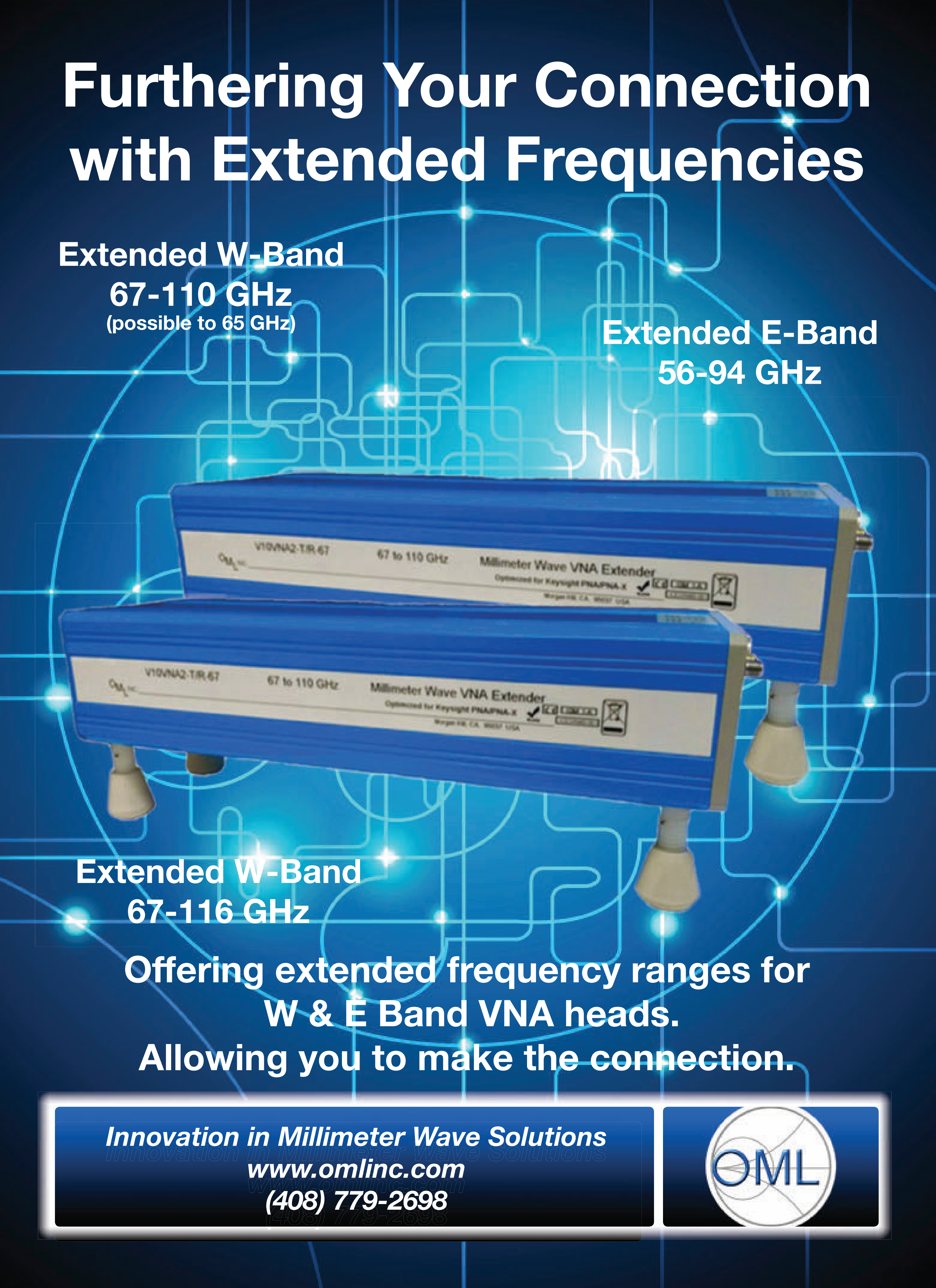

Furthering Your Connection with Extended Frequencies
Extended W-Band
67-110 GHz
(possible to 65 GHz)
Extended E-Band
56-94 GHz
Millimeter Wave VNA Extender
67 to 110 GHz
Extended W-Band
67-116 GHz
Offering extended frequency ranges for W & E Band VNA heads.
Allowing you to make the connection.
Innovation in Millimeter Wave Solutions
www.omlinc.com
(408) 779-2698
OML

When able to transmit, STAs transmit their whole packet data.

Wi-Fi STAs may use "request to send" (RTS) or "clear to send" (CTS) packets to mediate access to the shared medium. The AP only issues a CTS packet to one STA at a time, which, in turn, sends its entire frame to the AP (see ***Figure 1***). The STA then waits for an acknowledgment packet (ACK) from the AP, indicating that it received the packet correctly. If the STA does not get the ACK in time, it assumes the packet collided with some other transmission, moving the STA into a back off period. It will then try to access the medium and retransmit its packet after the backoff counter expires.

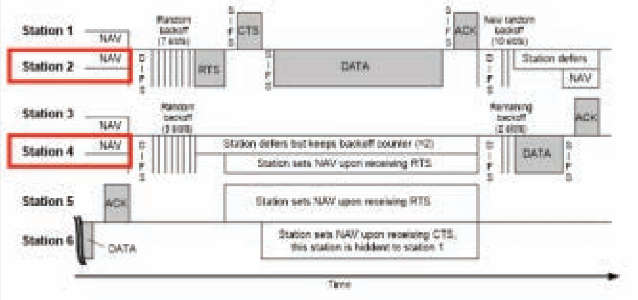

Fig. 1 Clear channel assessment protocol.

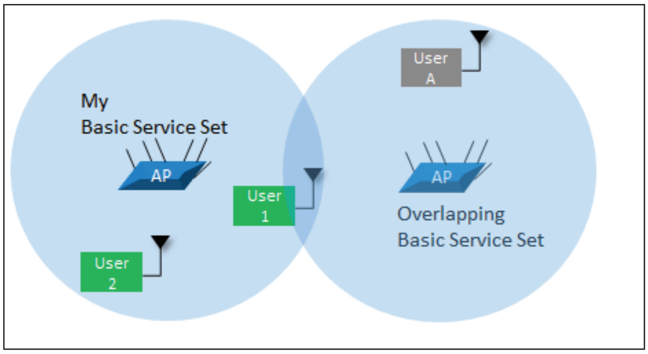

Fig. 2 Medium access inefficiency from users with overlapping APs.

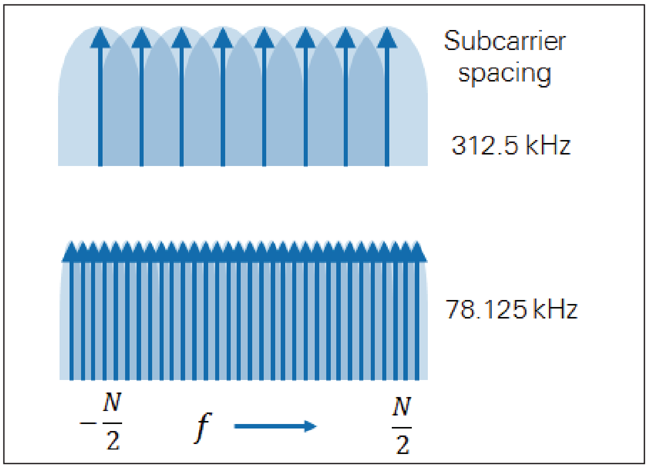

Fig. 3 802.11ax reduces subcarrier spacing to preserve channel bandwidths.

Although this clear channel assessment and collision avoidance protocol serves well to divide the channel somewhat equally among all participants within the collision domain, its efficiency decreases when the number of participants grows very large. Another factor that contributes to network inefficiency is having many APs with overlapping areas of service. ***Figure 2*** depicts a user (user 1) that belongs to the basic service set (BSS), a set of wireless clients associated with an AP, on the left. User 1 contends for access to the medium with other users in its own BSS (e.g., user 2) and then exchanges data with its AP. However, this user hears traffic from the overlapping BSS on the right. In this case, traffic from the overlapping BSS triggers user 1's backoff procedure. This results in users waiting longer for their turns to transmit, effectively lowering their average data throughput.

PHY MECHANISMS FOR HIGH EFFICIENCY

The 802.11ax 0.1 draft specification[1] introduces significant changes to the physical layer of the standard. However, it maintains backward compatibility with 802.11a/b/g/n/ac devices, such that an 802.11ax STA can send and receive data to legacy STAs. These legacy clients will also be able to demodulate and decode 802.11ax packet headers, although not entire 802.11ax packets, and back off when an 802.11ax STA is transmitting. ***Table 1*** highlights the most important

TABLE 1

802.11ax VS. 802.11ac PHY

	802.11ac	802.11ax
Frequency Bands (GHz)	5	2.4 and 5
Channel Bandwidth (MHz)	20, 40, 80, 80+80, 160	20, 40, 80, 80+80, 160
FFT Sizes	64, 128, 256, 512	256, 512, 1024, 2048
Subcarrier Spacing (kHz)	312.5	78.125
OFDM Symbol Duration (µs)	3.2 + 0.8/0.4 CP	12.8 + 0.8/1.6/3.2 CP
Highest Modulation	256-QAM	1024-QAM
Data Rates (Mbps)	433 (80 MHz Channel, 1 SS) 6933 (160 MHz Channel, 8 SS)	600.4 (80 MHz Channel, 1 SS) 9607.8 (160 MHz Channel, 8 SS)

parameters compared to the current 802.11ac implementation. Notice that the 802.11ax standard will operate in both the 2.4 and 5 GHz bands. The specification defines a 4× larger FFT, multiplying the number of subcarriers. However, one critical change with 802.11ax is reducing the subcarrier spacing to one fourth the spacing of previous 802.11 revisions, preserving the existing channel bandwidths (see ***Figure 3***). The OFDM symbol duration and cyclic prefix (CP) also increased 4×, keeping the raw link data rate the same as 802.11ac while improving efficiency and robustness in indoor, outdoor and mixed environments. Nevertheless, the standard does specify 1024-QAM and smaller CP ratios for indoor environments, which will increase the maximum data rate.

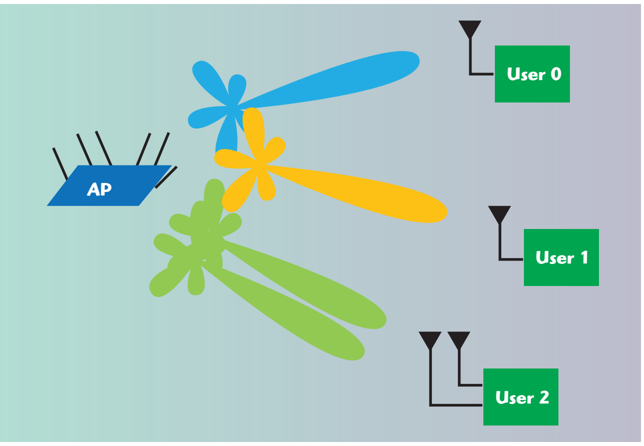

▲ *Fig. 4 AP using MU-MIMO beam forming to serve multiple users located in spatially diverse positions.*

To increase the ability to serve more users at the same time, the 802.11ax standard specifies two modes of operation: single user, a sequential mode where the wireless STAs send and receive data one at a time, and multi-user, a mode that allows for simultaneous communication with multiple STAs. The standard further divides this mode into downlink and uplink multi-user. Downlink multi-user refers to data that the AP serves to multiple associated STAs at the same time, which the existing 802.11ac standard already specifies. Uplink multi-user involves simultaneous transmission of data from multiple STAs to the AP, a new feature that the 802.11ax standard proposes, which did not exist in any of the previous 802.11 versions. Under the multi-user mode of operation, the standard also specifies two different ways of multiplexing more users within a certain area: multi-user MIMO and orthogonal frequency division multiple access (OFDMA). For both of these methods, the AP acts as the central controller of all aspects of multi-user operation. The 802.11ax designers have specified that 802.11ax support downlink and uplink MU-MIMO, MU-OFDMA or both to handle an even larger number of simultaneous users.

Borrowing from the 802.11ac implementation, 802.11ax devices will use beamforming techniques to direct packets simultaneously to spatially diverse users (see ***Figure 4***). That is, the AP will calculate a channel matrix for each user and steer simultaneous beams to different users, each beam containing specific packets for its target user. 802.11ax supports sending up to eight multi-user MIMO transmissions at a time, and up to four of

Switched Filter Banks

NIC NETWORKS INTERNATIONAL CORPORATION

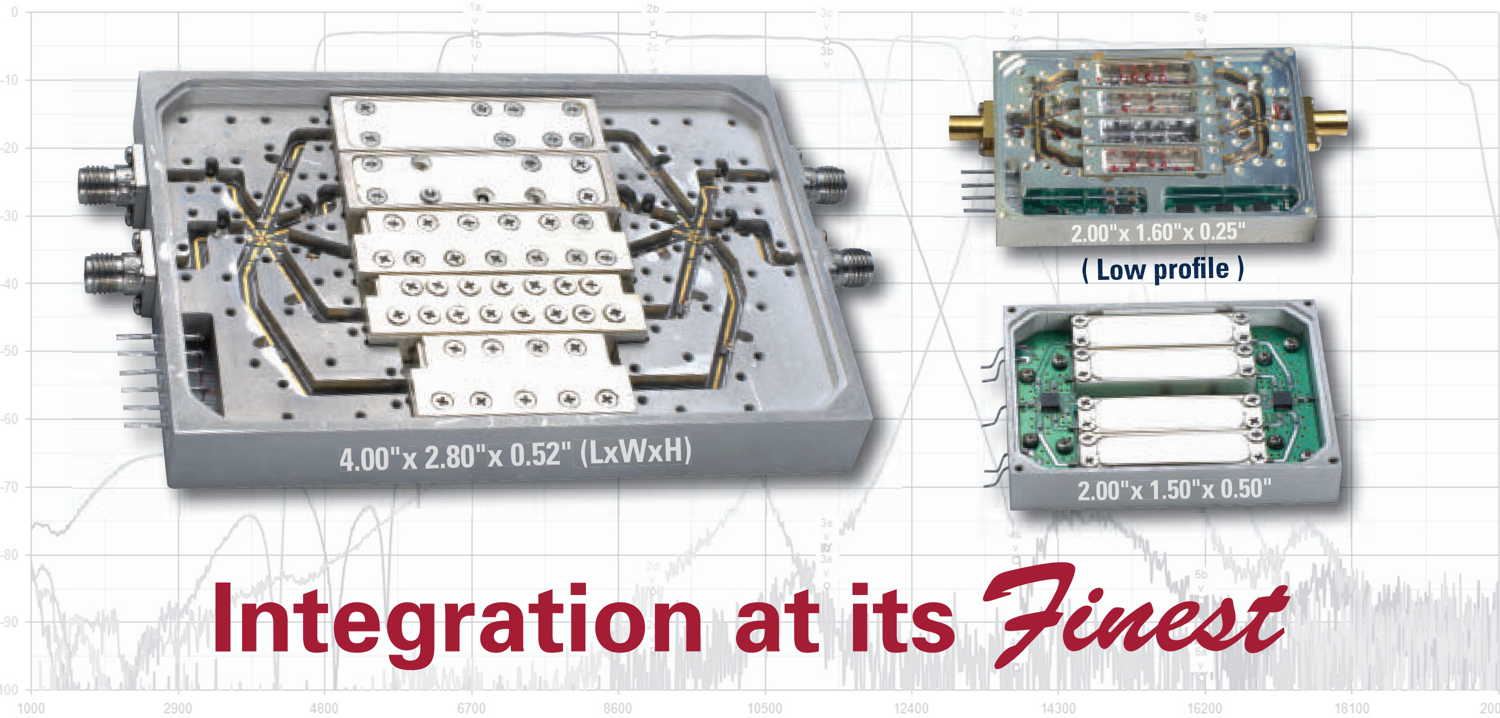

Integration at its *Finest*

- Frequency range: 10 MHz - 18000 MHz
- Customizable channels: 2 to 8
- Multi-octave and sub-octave designs
- Pin-diode, GaAsFET, high power switch technologies
- Compact package size
- Low Insertion loss and high isolation
- Fast switching speeds
- Ruggedized package for hi-rel environments

Radar | UAV | EW | Guidance & Navigation | Communications | GPS & Satellite

ISO 9001:2008
AS9100C
CERTIFIED

NIC

www.nickc.com

913.685.3400
15237 Broadmoor
Overland Park, KS
e-mail: sales@nickc.com

these streams to a single user. Also, each MU-MIMO transmission may have its own modulation and coding set (MCS) and a different number of spatial streams.

For MU-MIMO uplink, the AP will initiate a simultaneous transmission from each of the STAs to the AP by means of a trigger frame. When the multiple users respond in unison with their own packets, the AP applies the channel matrix to the received beams to separate the information from each uplink beam. The AP may also initiate uplink multi-user transmissions to receive beam forming feedback information from all participating STAs (see ***Figure 5***).

The 802.11ax standard also uses OFDMA to multiplex more users in the same channel bandwidth. Building on the existing OFDM digital modulation scheme that 802.11ac already uses, the 802.11ax standard further assigns specific sets of subcarriers to individual users. That is, it divides the existing 802.11 channels (20, 40, 80 and 160 MHz wide) into smaller subchannels with a predefined number of subcarriers. The 802.11ax standard calls the smallest subchannel a resource unit (RU), with a minimum size of 26 subcarriers. Aware of multi-user traffic needs, the AP decides how to allocate the channel, always assigning all available RUs on the downlink. It may allocate the whole channel to only one user at a time, just as 802.11ac currently does, or it may partition the channel to serve multiple users simultaneously (see ***Figure 6***). In dense user environments, where many users would normally contend inefficiently for a turn to use the channel, this OFDMA mechanism serves them simultaneously, with smaller, dedicated subchannels that improve the average throughput per user. ***Figure 7*** illustrates how an 802.11ax system may multiplex the channel using different RU sizes. Note that the smallest division of the channel accommodates up to nine users for every 20 MHz of bandwidth.[2] ***Table 2*** shows the number of users able to get frequency-multiplexed access when the 802.11ax AP and STAs coordinate for MU-OFDMA operation.

To coordinate uplink MU-MIMO or uplink OFDMA transmissions, the AP sends a trigger frame to all users. This frame indicates the number of spatial streams and/or the OFDMA allocations (frequency and RU sizes) of each

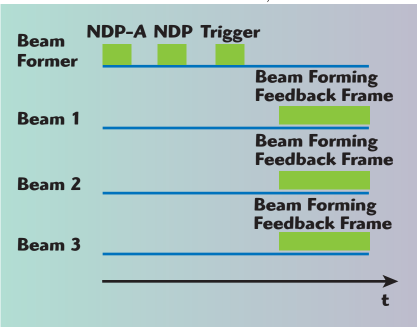

Fig. 5 A beam forming AP requesting channel information for MU-MIMO operation.

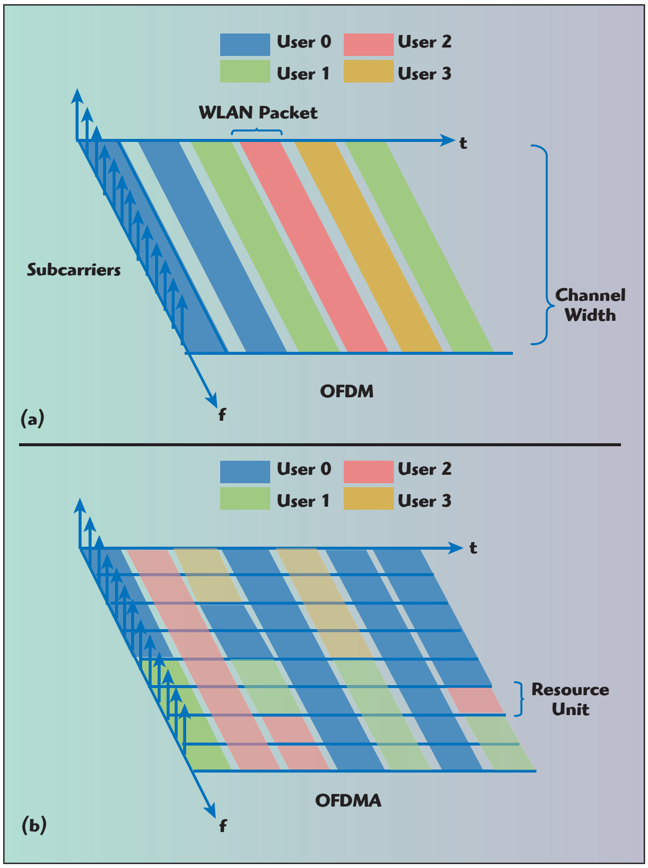

Fig. 6 A single user accessing the channel (a) vs. multiplexing multiple users in the same channel using OFDMA (b).

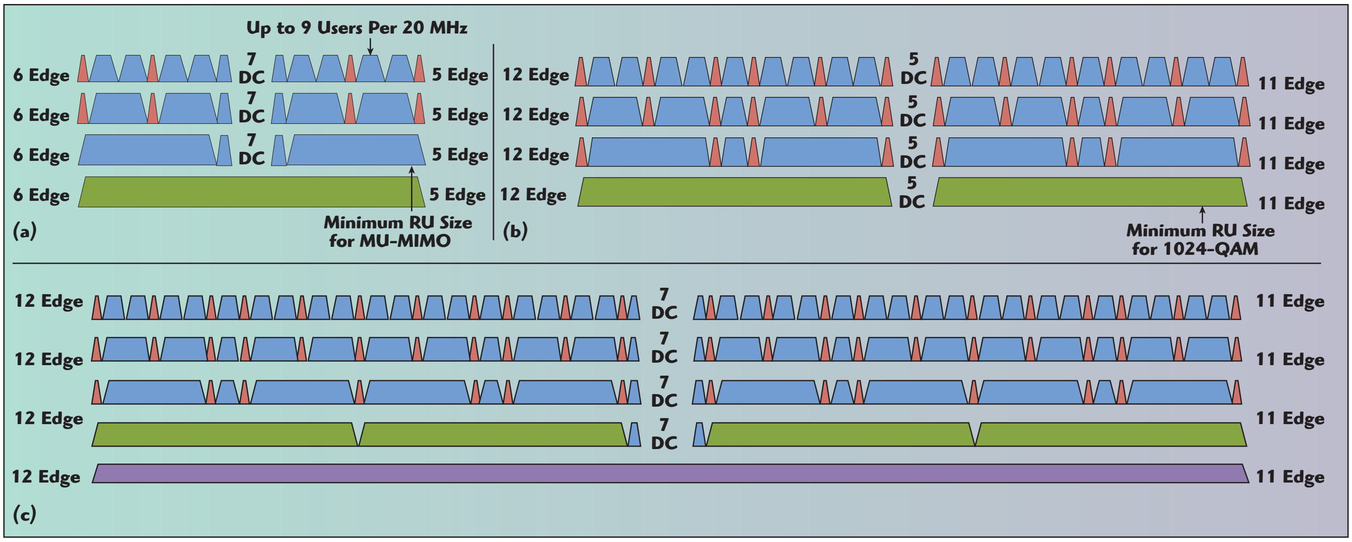

Fig. 7 Subdividing 20 MHz (a), 40 MHz (b) and 80 MHz (c) channels into various RUs.

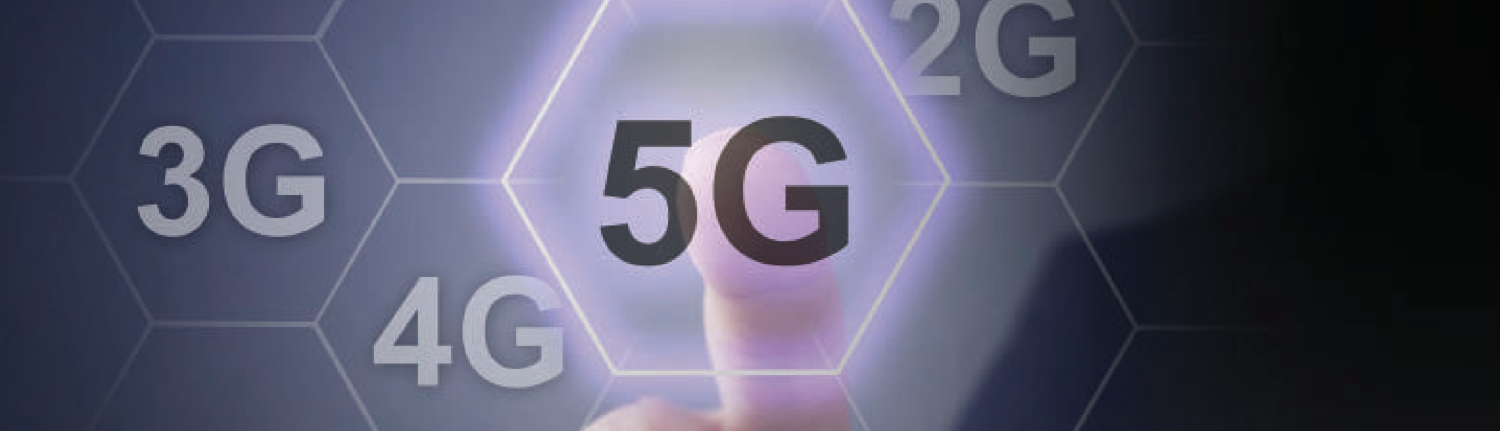

Forward Thinking

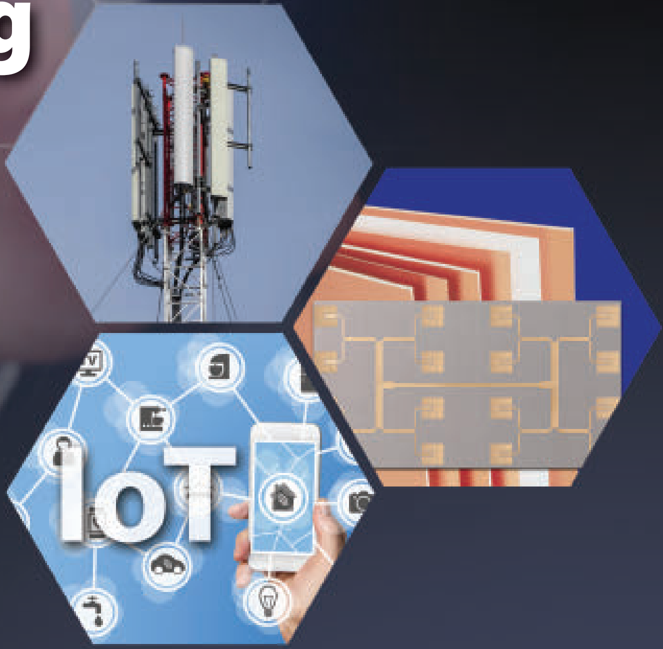

Introducing RO4730G3™ 94 V-0 Laminates: For Tomorrow's Wireless PCB Antennas

Rogers RO4730G3™ circuit laminates have been engineered for next-generation wireless PCB antennas, including in 4G and 5G cellular base stations and IoT networks.

These low-loss, cost-effective circuit materials are lead-free process compatible and flame retardant. RO4730G3 laminates support broadband antenna designs with excellent PIM performance, outstanding dimensional stability and multilayer board design capability.

Built on the proven technology used in Rogers RO4000® thermoset resin/ceramic/woven glass materials, RO4730G3 94 V-0 laminates expand Rogers antenna grade product family, already the most popular for base station antennas.

For tomorrow's PCB antennas today — RO4730G3 Laminates

MATERIAL	Dk	PIM*
RO4730G3 Ceramic Hydrocarbon	**3.0**	**<-160 dBc**
RO4700JXR™ Series Ceramic Hydrocarbon	2.55 to 3.0	<-160 dBc
RO4500™ Series Ceramic Hydrocarbon	3.3 to 3.5	<-157 dBc
AD Series™ PTFE	2.5 to 3.2	<-157 dBc

** On 0.060" (1.524mm) laminate*

Download the **PIM and PCB Antennas Brochure**

Visit us at booth #204

ROGERS CORPORATION

Advanced Connectivity Solutions

USA - AZ, tel. +1 480-961-1382

EUROPE - BELGIUM, tel. +32 9 235 3611

www.rogerscorp.com

TABLE 2

NUMBER OF RUs VS. CHANNEL BANDWIDTH

RU Subcarriers	Channel Bandwidth (MHz)			
	20	40	80	160 and 80+80
26	9	18	37	74
52	4	8	16	32
106	2	4	8	16
242	1-SU/MU-MIMO	2	4	8
484	N/A	1-SU/MU-MIMO	2	4
996	N/A	N/A	1-SU/MU-MIMO	2
2 × 996	N/A	N/A	N/A	1-SU/MU-MIMO

user. It also contains power control information, such that individual users can increase or reduce their transmitted power. This helps to equalize the power that the AP receives from all uplink users and improve reception of frames from users that are farther away. The AP also instructs all users when to start and stop transmitting. As ***Figure 8*** depicts, the AP sends a multi-user uplink trigger frame that tells all users the exact moment at which they are to start transmitting and the duration of their frame, to ensure that they all finish transmitting simultaneously. Once the AP receives the frames from all users, it sends back a block ACK to finish the operation.

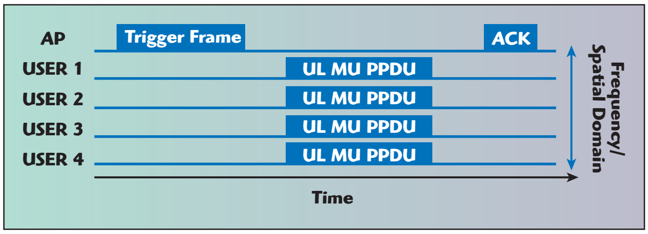

▲ *Fig. 8 The AP coordinates the timing of uplink multi-user transmission.*

802.11ax TEST CHALLENGES

The 802.11ax standard specifies support for higher modulation orders (1024-QAM), in which more information is carried in ever-smaller differences in signal amplitude and phase. Considering that the subcarriers stand only 78.125 kHz apart, 802.11ax devices need cleaner oscillators with improved phase noise and RF front-ends with better linearity, to minimize spectral leakage, reduce bit error rates and achieve the high link speeds that the standard demands. The error vector magnitude (EVM) test provides designers with valuable information about the quality of the modulated signal. One of the biggest test challenges is to measure the EVM of new 802.11ax devices. The EVM noise floor of the test instruments must be significantly lower than the DUT's, pushing current instrument designs to new levels of linearity and noise performance. ***Table 3*** shows the EVM levels that 802.11ax-compliant devices will likely have to meet.

A second challenge is that OFDMA systems have very high susceptibility to frequency and clock offsets. Consequently, 802.11ax MU-OFDMA performance demands tight frequency synchronization and clock offset correction to ensure that all STAs operate exactly within their allocated subchannels. Additionally, the strict timing requirements guarantee that all STAs will transmit simultaneously in response to the AP's multi-user trigger frames. 802.11ax APs will have to maintain system synchronization using their own built-in oscil-

TABLE 3

802.11AX EVM REQUIREMENTS

16-QAM	64-QAM	256-QAM	1024-QAM
-19 dB	-27 dB	-32 dB	-35 dB

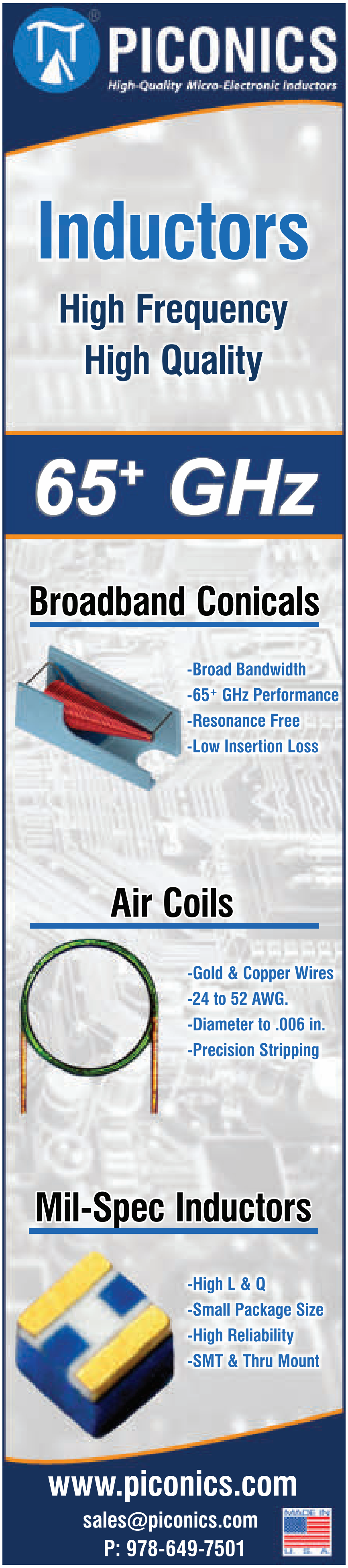

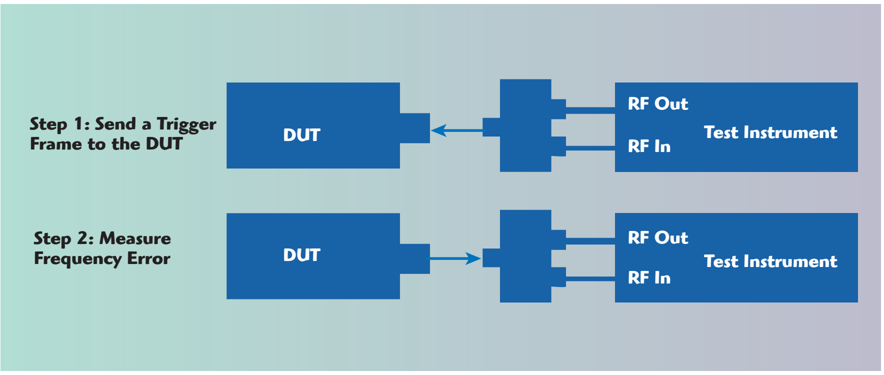

▲ *Fig. 9 Relative frequency error measurement.*

lators as the reference. Associated STAs will then adjust their internal clock and frequency references by extracting clock information from the trigger frames transmitted from the AP. Frequency and clock offset testing of 802.11ax devices will involve both absolute and relative frequency error tests. For the latter, the goal is to determine the ability of a non-AP STA participating in uplink multi-user transmission to correct its oscillator based on the frequency and clock information it derives from the AP's trigger frame. The test methodology includes two steps: first, the test instrument acting as a reference (as the AP would be) sends trigger frames to the DUT. The DUT adjusts its clock to the reference and replies to the test instrument. As a second step, the test instrument measures the adjusted frequency of the DUT (see ***Figure 9***).

Testing the receiver sensitivity of 802.11ax APs presents an additional challenge, considering that the AP acts as the clock and frequency reference. The AP (the DUT) initiates the test by sending a trigger frame. The test instrument adjusts its frequency and clock to match the DUT's and then responds with a predetermined number of stimulus packets. The challenge here is with the strict relative frequency error limits of 802.11ax. The test instrument must derive very precise frequency and clock information from the trigger frames that the AP DUT sends, and it may be necessary to perform the calculation over multiple trigger frames to ensure proper frequency and clock synchronization. As a result, this method can add a significant delay to the test. One possible solution to speed the test is for the AP to export its clock reference, allowing the test equipment to lock its clock to it. This setup avoids the initial synchronization procedure based on trigger frames, leading to faster AP receiver sensitivity tests.

Another consideration arises when testing 802.11ax devices with up to eight antennas in MIMO operation. In this case, a DUT can produce very different results than when testing each signal chain individually and sequentially. For example, the signals from each antenna may interfere destructively with each other and affect power and EVM performance, with negative and potentially noticeable effects on the throughput. The test instrumentation must support sub-nanosecond synchronization of the local oscillators for each signal chain to ensure proper phase alignment and MIMO performance over many channels.

CONCLUSION

802.11ax aims to improve the average per-user data throughput by 4× in crowded environments. This new revision of the standard seeks to implement significant improvements to the physical and medium access layers to enable higher network efficiency. Thanks to multi-user technology, both in the form of MU-MIMO and MU-OFDMA, 802.11ax will have the ability to serve data simultaneously and consistently to multiple users in crowded environments. However, implementing this functionality will present a whole new set of challenges for the scientists, engineers and technologists developing and testing the 802.11ax multi-user ecosystem.■

References

1. IEEE 802.11-16/0024r1, Proposed TGax draft specification.
2. IEEE 802.11-15/0132r16, Specification Framework Document.

INVITED PAPER

Changing Design with Characteristic Mode Analysis

Peter Futter
Altair Engineering Inc., Troy, Mich.

Automated optimization algorithms, like the generic algorithm (GA), offer many advantages for design purposes. However, one of the drawbacks is that the methods typically do not bring much understanding about the design interactions and dependencies. This might be particularly important when design goals are not all achieved, requiring a trade-off analysis and a compromise in performance. Characteristic mode analysis (CMA) can be an extremely useful design tool in such situations. In addition, it is instrumental in answering much broader design questions like: which is the most suitable antenna for a particular application?

CMA enables a systematic design approach that is based on insight into the fundamental resonance behavior of the structure. This makes it well suited to solving challenging antenna design and antenna placement problems. The modal current and modal significance can aid in the choice of the antenna type and placement locations on the structure. CMA is also well suited to MIMO applications, where the fact that the modes are inherently orthogonal can be exploited to improve decoupling between antenna elements. This article will briefly review CMA parameters and typical workflows before presenting a smartphone antenna design example.

CMA OVERVIEW

Characteristic modes are defined as a set of orthogonal current modes that are supported on a conducting surface. The eigenvalue equation is derived from the Method of Moments impedance matrix.[1] One of the major advantages of CMA is that the analysis can be performed before any decisions are taken about the placement of any sources. The following offers a brief review of calculated CMA parameters.

MODAL RESONANCE

The eigenvalue (λ), modal significance (MS) and the characteristic angle (CA) are measures of how resonant a mode is. A mode is resonant when $\lambda = 0$, MS = 1, CA = 180°. These three quantities essentially express the same thing in different ways; which one is used depends on personal preference. If a mode is resonant on a structure, it means that it is more likely to be excited at that frequency. Conversely, a mode with a large eigenvalue will be more difficult to excite than a mode with a smaller eigenvalue. Note that it is not necessary to include an excitation in the CMA simulation in order to calculate these parameters, they are determined purely by the geometry and frequency of the analysis, and are independent of the excitation.

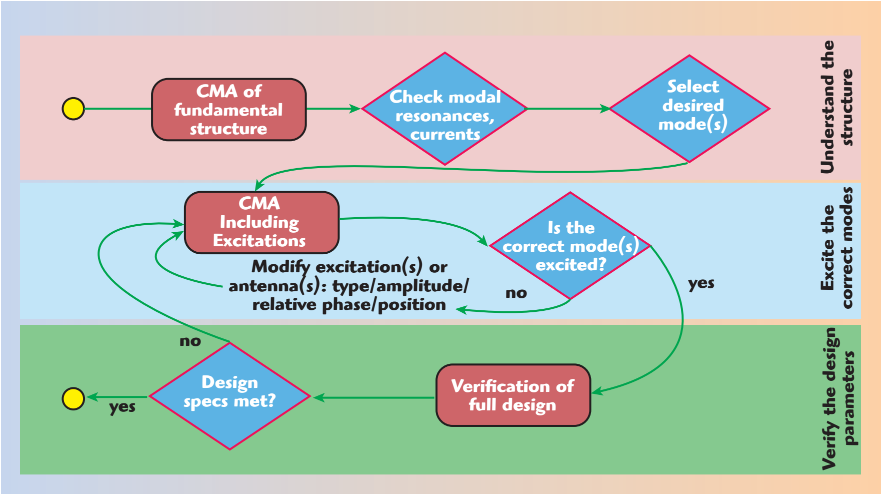

▲ *Fig. 1 A typical workflow for a CMA design study.*

MODAL CURRENT AND FIELDS

Modal currents and fields are calculated for each mode, which is used to calculate the near field and radiation pattern of each mode. The current distribution, near field and radiation patterns of each mode can be extremely useful. From a design perspective, during a CMA study, geometry can be modified to bring a specific mode into resonance because it has desirable modal current/field/pattern attributes. Furthermore, when multiple modes are resonant, a synthesis of these parameters can be applied to predict the total current/fields/pattern.

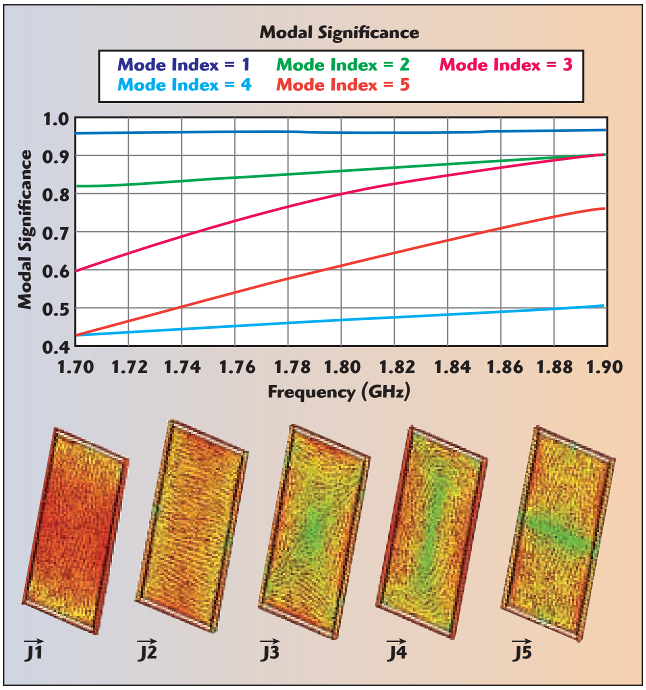

▲ *Fig. 2 Initial CMA analysis of the smartphone PCB and frame showing modal significance and the modal current distributions at 1.8 GHz.*

MODAL EXCITATION AND WEIGHTING COEFFICIENT

When a coefficients excitation is included in the CMA, two additional parameters are available. The modal excitation coefficient is a measure of how well the excitation can excite a specific mode, while the modal weighting coefficient is a measure of the overall modal presence generated by the excitation. These parameters offer a useful measure of how well a design is able to excite a specific mode or combination of modes.

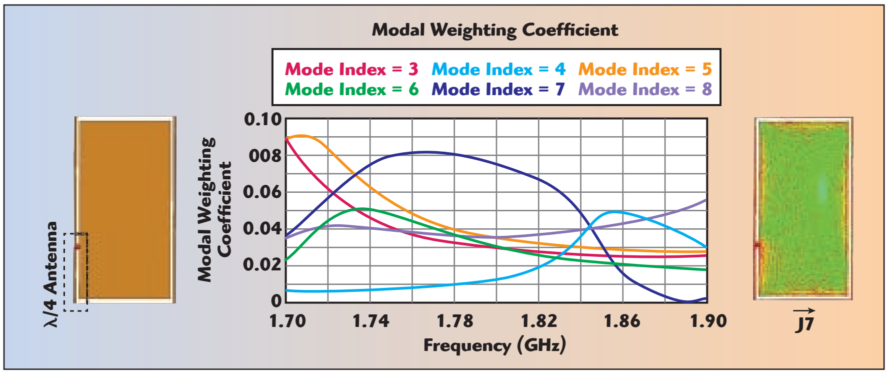

▲ *Fig. 3 Quarter-wavelength design with a capacitive element to excite the dominant mode 7.*

TYPICAL CMA WORKFLOWS

Figure 1 shows an idea of typical workflow associated with a CMA design study and the steps are described in more detail below.

Understand the structure – the first step involves the initial investigation to understand the behavior of the structure. A simplified but representative structure can be used and the excitation and antenna geometry can be excluded at this stage. The CMA analysis will determine which modes are naturally in or near resonance within the frequency range of interest and whether or not the attributes of a single mode or a combination of modes are suitable for the application at hand.

Excite the correct mode – once a mode or a combination of modes have been selected, an excitation must be designed that couples to these modes. Detailed CMA analysis of the structure and antenna(s) is performed and can determine: choice of appropriate antenna type and location, type and location of antenna feed, and in the case of multiple antennas, the amplitude and phase of the excitations. Through evaluation of the modal weighting coefficient the analysis will determine how well the design was able to achieve the selected modal behavior.

Verify the design – the final step involves a verification stage where for example a different solver is used to calculate performance parameters, e.g., S-parameters, gain, etc.

The case study that is presented in the following section will highlight how these steps can be applied by considering a practical design example.

SMARTPHONE ANTENNA DESIGN

In this example, a CMA solver[2] is used to design an antenna for a modern smartphone with a 70 mm × 130 mm PCB. The antenna will be designed to operate in the DCS1800 band, where more resonant modes are present than in the lower GSM900 band[3], and will be integrated directly into the outer metallic frame of the device. Several design scenarios were investigated, three of which are presented here to highlight specific aspects of how CMA can be applied.

A single antenna element is used in this example, which makes it more challenging to excite and control modes.[4] In order to control the modal behavior without adding additional antenna elements, a combination of ground connections, slots and passive resonators are used in the designs.

It is worth noting that automated optimization was not used on any of these designs. All results were obtained by interpreting the CMA results, and where necessary, further design iterations were made to tweak performance. Herein lies the strength of CMA: insight that leads to informative design decisions.

Understanding the Structure – An initial CMA analysis of the PCB and frame is carried out over the frequency band of interest (1.7 to 1.9 GHz) to assess the resonant modes and the associated modal current distributions (see ***Figure 2***). Modes 1 and 2 exhibit dipole-like characteristics with the modal current flowing along the length/width of the PCB and the frame, while modes 3 to 5 have more complex modal current distributions.

The goal is to develop an antenna which naturally couples to specific modes (with appropriate radiation patterns) on the PCB, thus improving the overall performance by incorporating the PCB as part of the antenna. Dipole-like mode 1 is near-resonance throughout the whole frequency band, and also has a suitable modal far-field pattern, making it a good candidate for this application.

Excite the Desired Modes – In the next step, the antenna geometry is included in the CMA. In addition to the modal currents and modal significance, the modal weighting coefficients are now used to measure how well each of the designs excited the desired modes. Three different designs are presented: Design 1 uses a capacitive excitation element, Design 2 clearly shows how CMA can be applied to improve a design, and Design 3 illustrates the relationship between

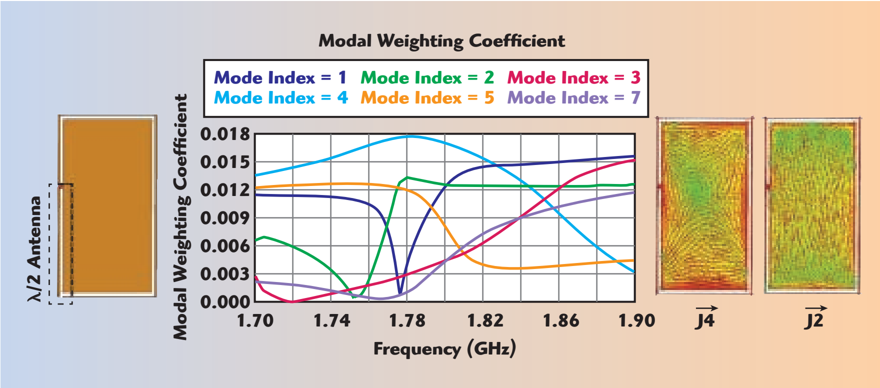

Fig. 4 *Half-wavelength design iteration 1.*

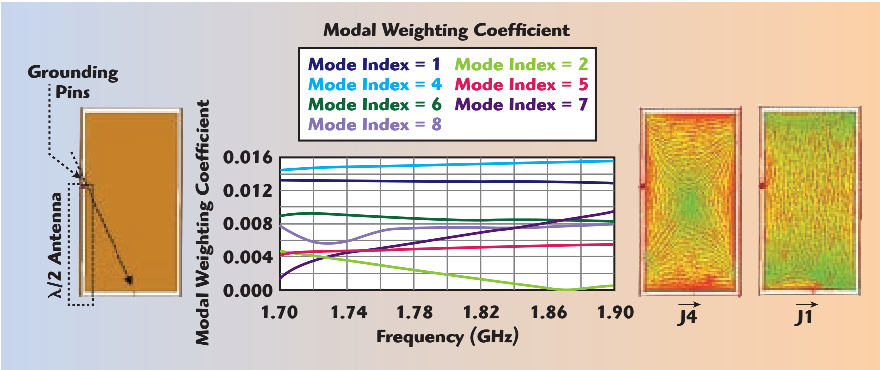

Fig. 5 *Half-wavelength design iteration 2, with grounding pins used to suppress the anti-resonance in the dipole-like mode.*

the modal and actual bandwidth.

Design 1: Quarter-Wavelength Resonator – The CMA design approach[4] shows how antenna elements can be designed to excite specific modes. This approach is used to design a capacitive quarter-wavelength antenna integrated into the frame, which couples strongly to the dominant dipole-like mode running along the PCB length. However, because a single antenna is used it is more difficult to enforce the modal boundary, and the modal current distribution of the dominant dipole-like mode (see ***Figure 3***) exhibits some distortion on the opposite side of the PCB.

Due to the distortions, this mode is automatically assigned mode number 7. Looking at the modal weighting coefficients, it is noted that mode 7 is dominant throughout most (but not all) of the required bandwidth and that several other modes are also excited. The changes in the modal weighting coefficients with frequency implies that the total radiated pattern will differ at different frequencies within the band.

Design 2: Half-Wavelength Resonator – Iteration 1 – A similar approach to Design 1 is applied, however a half-wavelength antenna is now used (the advantage being that this design can easily be extended to dual-band GSM900 and DCS1800 operation). Because the half-wavelength resonator is longer, the modal boundary is not enforced well and mode 4 is excited more than the desired dipole-like mode (see ***Figure 4***). The modal weighting coefficients also show several modes come into and out of resonance, which is likely to result in sub-optimum bandwidth performance.

Iteration 2 – The first step to improve this design is to remove the anti-resonance (around 1.75 GHz in Figure 4) in the dipole-like mode to improve the radiation pattern and bandwidth performance. This is achieved by introducing grounding pins connecting the frame to the PCB opposite the antenna feed and at the lower PCB edge.

The pin opposite the antenna feed facilitates the current flowing down the long frame edge, while the pin at the lower edge introduces a passive resonator, both of which improve the excitation of the dipole-like mode. From the modal weighting coeffi-

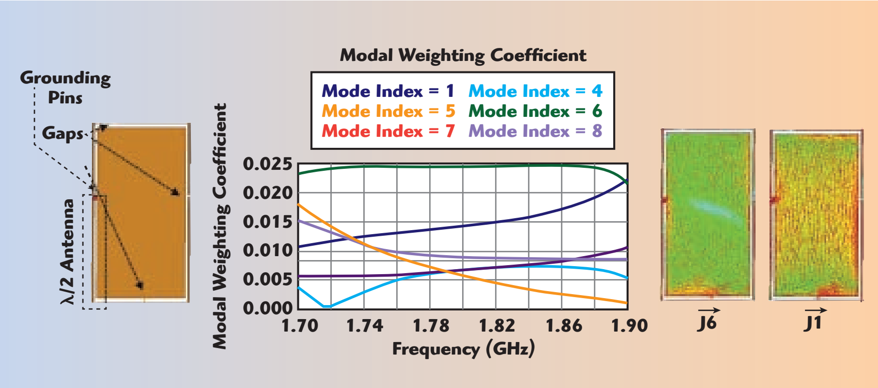

▲ *Fig. 6 Half-wavelength design iteration 3 – gaps are used to suppress the frame resonance.*

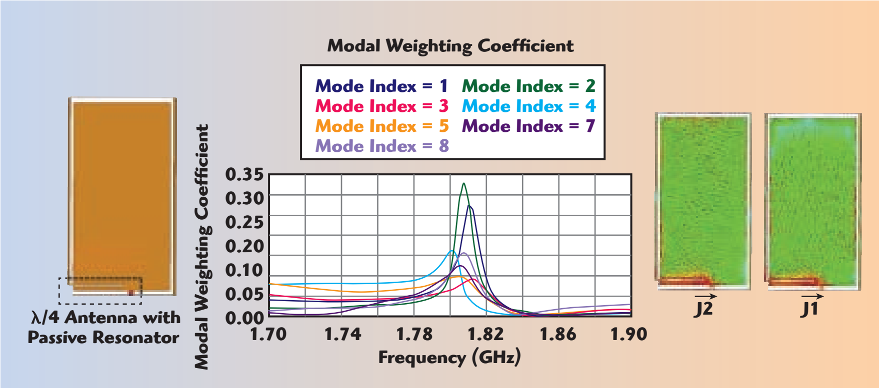

▲ *Fig. 7 Narrow band design with passive resonator.*

cients (see ***Figure 5***); we can now see that modes 4 and 1 are dominant with good bandwidth performance and that the anti-resonance has been removed.

Iteration 3 – It is noted that the presence of dominant mode 4 in iterations 1 and 2 could be caused by a resonance in the outer frame (seen in the mode 4 current distribution in Figure 5). The next step to improve the design is to suppress mode 4, which is achieved by introducing gaps in the frame to break the resonant current path. From the modal weighting coefficients (see ***Figure 6***), we now see that mode 4 has indeed been suppressed, the dipole-like mode 1 remains and mode 6 is now excited. The modal weighting coefficients of the dominant modes are relatively constant across the band, resulting in good overall bandwidth performance.

Design 3: Narrowband Design – This design uses a quarter wavelength antenna, as in Design 1, but oriented along the short edge of the PCB. A resonant slot and grounding pins are also used. In this case, both orientations of the dipole-like modes are excited (see ***Figure 7***) leading to very good performance. However, the solution is band limited and only covers a small frequency range at the center of the band.

The next section shows how the modal weighting coefficients relate to the actual bandwidth, which is a very useful concept. Bandwidth performance can be estimated before impedance matching, which can be considered in a later stage, either through rigorous optimization or including a matching circuit.

Comparing the Designs – As a means of comparison, matching circuits were generated for each design using Optenni Lab[5] and the S-parameter and radiation pattern perfor-

TABLE 1

MATCHING CIRCUIT MINIMUM EFFICIENCY

	Minimum Matching Network Efficiency (dB)
Design 1	-0.1
Design 2 - Iteration 1	-1
Design 2 - Iteration 2	-0.4
Design 2 - Iteration 3	-0.3
Design 3	-0.8 (Band Limited)

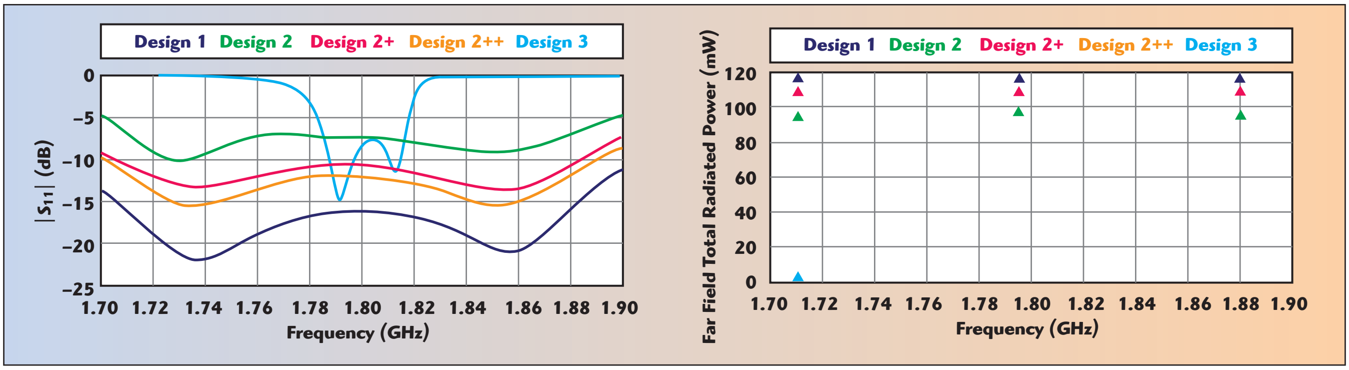

▲ *Fig. 8 The $|S_{11}|$ and total radiated power for the different designs.*

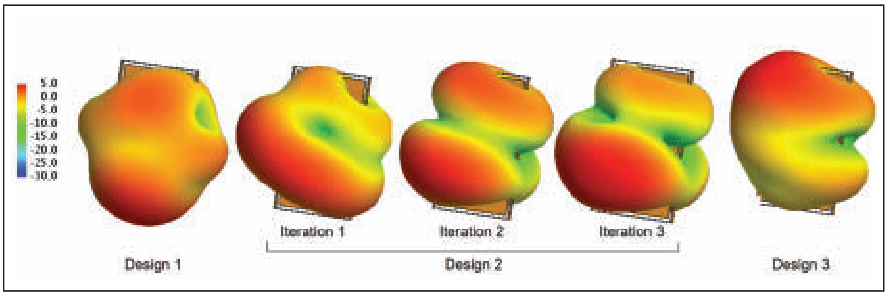

▲ *Fig. 9 The total radiation pattern for each design at 1.8 GHz.*

mance was simulated for each design. Due to the bandwidth constraints of Design 3, a band limited (1.785 to 1.815 GHz) matching circuit is designed to enable a meaningful comparison at the center frequency. The other designs are all matched across the full band. ***Table 1*** shows a comparison of the efficiency of the matching networks designed with Optenni Lab, while ***Figures 8*** and ***9*** show the $|S_{11}|$, total radiated power and radiation patterns for the different designs.

While Design 1 offers the best performance for this application, it was also demonstrated how CMA was applied to improve Design 2 performance. Furthermore, Design 3 illustrates how a CMA solution with good modal performance over a narrow frequency range will result in a narrowband design. Finally, the total radiation patterns in Figure 9 can also be calculated by superposition of the weighted modal patterns.

CONCLUSION

CMA offers a novel approach to address design challenges: insight into the inherent resonant behavior of the structure facilitates innovative design approaches. This article briefly introduced concepts and parameters that form part of a CMA analysis. A typical workflow was broken down in three main steps, which were then illustrated in more detail by means of a design example. Different design scenarios were illustrated to highlight the advantages of applying CMA as a design tool.■

References

1. D. Ludick et al., "Characteristic Mode Analysis of Electromagnetic Structures," *EuMW 2015*.
2. Altair Engineering Inc., "FEKO Suite 14.0," Troy, MI, www.altairhyperworks.com/product/FEKO.
3. P. Futter et al., "Simulation Approach for MIMO Antenna Diversity Strategies," *EDICON China 2015*.
4. R. Martens, et al., "Inductive and Capacitive Excitation of the Characteristic Modes of Small Terminals," *Loughborough Antennas & Propagation Conference 2011*.
5. Optenni Lab version 3.3, Optenni Ltd., Espoo, Finland, www.optenni.com

Measuring Phase Noise with Baluns

Gary Giust
JitterLabs, Milpitas, Calif.
Doug Jorgesen
Marki Microwave, Morgan Hill, Calif.

Differential clock and timing devices are commonly characterized for phase noise using baluns. While deceptively simple to use, baluns perform a fairly complicated process that can unknowingly introduce artifacts into measured results. This article describes such artifacts, discusses why they appear and how to eliminate them. Recommendations are provided for selecting a balun and using it to accurately characterize devices for phase noise.

Differential clock signals are widely used for a broad range of applications spanning data communications, wireless, instrumentation and medical. Differential signaling uses a pair of conductors; ideally, each carries a signal of the same magnitude but opposite phase. Examples include LVPECL, LVDS and CML. Compared with single-ended signals, differential signals have lower voltage swings on each conductor, which enables them to operate at higher frequencies. A composite (differential) swing, however, can be larger than a single-ended swing with the same power supply, which increases its signal-to-noise ratio.

Differential signals also perform better in noisy environments by rejecting common-mode noise. In addition, they provide more precise timing, since the crossover location for a differential signal is easier to control than for a single-ended signal (which depends on a voltage crossing an absolute reference level).[1]

Phase noise quantifies the short-term phase fluctuations in a signal[2] and is arguably the most important parameter for evaluating clock and timing devices used in critical timing applications. Phase noise (along with amplitude noise) can be measured using a spectrum analyzer or a dedicated phase noise analyzer. These instruments, however, analyze only single-ended signals. To convert a device's differential signal into a single-ended signal, an active probe, differential-to-single-ended amplifier or passive balun is required. For low noise measurements, baluns are preferred, since they do not add amplifier noise to the measurement. Broadband baluns are particularly attractive because a single device can support measurements over a wide range of frequencies.

This article explores how to use baluns for characterizing phase noise in differential clock signals. It begins by discussing artifacts that a balun can introduce into the measurement data. Example test results are shown to illustrate and are not intended to represent typical or worst-case scenarios. In practice, whether or not a balun impairs phase noise data, and by how much, is difficult to predict. This article analyzes the factors involved, such as the choice of balun, the device being measured and the cabling and components connecting the device to the balun. Experimental techniques are presented to determine if the balun is impacting phase noise measurements. Finally, recommendations are presented for how to select a balun and use it to accurately characterize devices for phase noise. To the authors' knowledge, this is the first published article studying the impact of baluns on phase noise measurements.

BALUN PRIMER

Figure 1 illustrates the role of a balun in converting a balanced impedance (or differential signal) to an unbalanced impedance (or single-ended signal). The balun itself is deceptively easy to use, requiring only three connections (two inputs and one output) and no power. Being a reciprocal device, a balun can be driven in either direction. A balun that converts a signal from single-ended to differential is called a splitter. When operated in reverse, it is called a combiner. In normal operation, the differential


AWS-0102
1515
531P

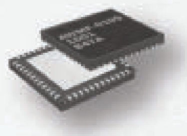

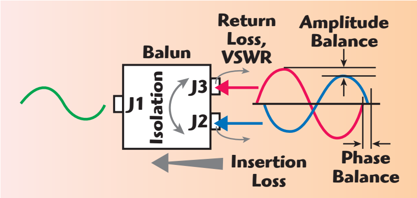

Fig. 1 Balun signal flow and performance characteristics.

ports J2 and J3 ideally provide equal and opposite signals. The unbalanced port J1 is matched to the transmission line impedance, typically 50 Ω.

A balun's performance can be summarized with a few key metrics.[3] Amplitude balance (in dB) is the differential insertion loss from the unbalanced port to one differential port versus the other. Phase balance (in degrees) is the differential phase shift on the differential ports. Insertion loss (in dB) is the additional loss in signal power — beyond the nominal loss caused by splitting the signal — introduced by inserting the balun in the signal path. Isolation (dB) is the ratio of signal power entering one differential port (e.g., J2) that appears at the other differential port (e.g., J3). Return loss (in dB) or voltage standing wave ratio (VSWR) represents how well the device is matched to a specific load and source impedance, typically 50 Ω.

Finally, common mode rejection ratio (CMRR) (in dB) is the ratio of common-mode to differential-mode gains, and reflects how well the balun attenuates common-mode signals passing from balanced to unbalanced ports. CMRR can be calculated from the amplitude and phase balance, based on vector cancellation.

TEST SETUP

Test data is measured using one of four basic setups as shown in ***Figures 2a*** through ***d***. Clock signals are analyzed for signal integrity using a high speed real-time oscilloscope, while phase noise is measured with a signal source analyzer.[4] While clock devices from many manufacturers were analyzed for this study, two devices under test (DUT) are presented here to illustrate key findings. Both DUTs are commercially available 5 mm × 7 mm surface-mount crystal oscillators (XO). The first DUT is a 156.25 MHz LVPECL XO based on analog multiplication. The second DUT is an LVDS XO whose output frequency can be changed by modifying an internal phase-locked loop (PPL) feedback divider to provide 78.125 MHz or 312.5 MHz. The termination for each DUT is shown in ***Figures 2e*** and ***f***, which is appropriate to drive 50 Ω test equipment. Unless otherwise noted, Figure 2 setups use 0.1 µF AC coupling capacitors, and 0 Ω series termination resistors.

Some setups use connectorized baluns with or without fixed coaxial attenuators (i.e., padding). While baluns from several manufacturers were analyzed for this study, two broadband baluns are presented here to illustrate key findings. Both baluns are from the Marki Microwave test and measurement product line,[5] namely BAL0006 (200 kHz to 6 GHz) and BAL0036 (300 kHz to 36 GHz).

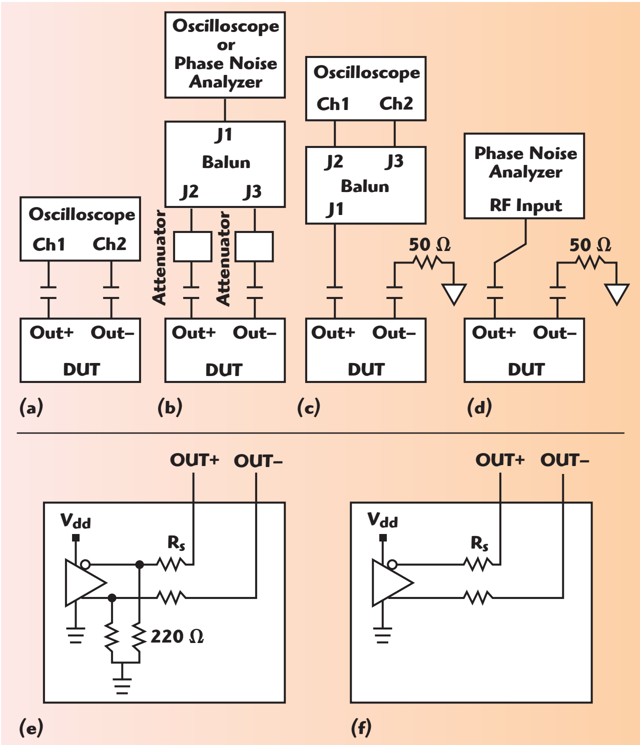

Fig. 2 Measurement setups for oscilloscope (a) combiner balun (b) splitter balun (c) and single-ended phase noise (d) with the DUT termination used for LVPECL (e) and LVDS (f) outputs.

Planar Monolithics Industries, Inc.

Monopulse Comparators

- Amplifiers – Solid State
- Attenuators – Variable/ Programmable
- Couplers (Quadrature, 180° & Directional)
- Detectors – RF/Microwave
- DLVAs, ERDLVAs & SDLVAs
- DTOs, VCOs, PLO, DROs, & Frequency Synthesizers
- Filters & Switched Filter Banks
- Form, Fit, Functional Products & Services
- Frequency Discriminators & IFMs
- Integrated MIC/MMIC Assemblies (IMAs)
- IQ Vector Modulators
- Limiters – RF/Microwave
- Log Amplifiers
- Millimeter Wave Components (Up to 50 GHz)
- Miscellaneous Products
- Multifunction Integrated Assemblies (MIAs)
- Monopulse Comparators
- Phase Shifters & Bi-Phase Modulators
- Power Dividers/Combiners (Passive & Active)
- Pulse Modulators (SPST)
- Rack & Chassis Mount Products
- Receiver Front Ends & Transceivers
- SDLVAs, ERDLVAs & DLVAs
- Single Side Band Modulators
- SMT & QFN Products
- Switch Matrices
- Switched Filter Banks
- Switches – Solid State
- Systems – Fly Eye Radars
- Threshold Detectors
- USB Products

PMI designs and manufactures a variety of coaxial monopulse compartors for beamforming antenna applications up to 26.5 GHz. Form, fit and functional designs can also be replicated to specific requirements. Standard models with various options are available at PMI's website (Link below)

http://pmi-rf.com/Products/monopulse_comparators/features.htm

Model: MPC-20R2G21R2G-CD-LNF
8 Input Monopulse Compartor with Gain

Frequency	20.2 - 21.2 GHz
Gain	0 dB, 5 dB Nom. (Selectable)
Noise Temperature /Figure	100 K / 1.3 dB Noise Figure
Phase Balance	±3° Maximum
DC Supply	+12 VDC @ 700 mA, -12 VDC @ 100 mA
Temperature	-55 °C to +85 °C

Package Size:
6.25" x Ø4.80" x 2.00"
Connectors: SMA (F)

Model: PMC-3G3D5G-6D8-SFF
4 Input Monopulse Comparator

Frequency	3.0 to 3.5 GHz
Insertion Loss	0.8 dB Max. - Measured 0.4 dB
VSWR	1.25:1 Max. - Measured 1.25:1
Isolation	23 dB Min. - Measured 25.052 dB
Amplitude Balance	±0.4 dB Max. - Measured ±0.2681 dB
Phase Balance	±5° Maximum - Measured ±3.2°
RF Input Power	Average: 11 Watt Max. Peak: 0.1 kW Max.
Temperature	-55 °C to +85 °C

Package Size:
3.23" x 3.23" x 0.43"
Connectors: SMA (F)

Model: PD-CD-001-1, 4 Way Phase Shift Power Divider with 0°, 90°, 180°, 270° Outputs

Frequency	9.3 - 9.9 GHz
Insertion Loss	8.0 dB Max. - Measured 6.97 dB Max
VSWR	2.0:1 Max. - Measured 1.60:1 Max.
Amplitude Balance	±0.5 dB Max. - Measured ±0.2 dB Max.
Phase Balance	±7.0° Max. - Measured ±4° Max.
RF Input Power	28 W CW, 750 W Peak
Temperature	-32 ºC to +77 ºC Operating

Package Size:
2.35" x 1.7" x 0.5"
Connectors: SMA (F)

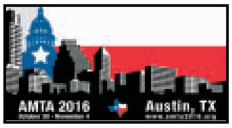

Austin, Texas
October 30 – November 4, 2016
amta2016.org
Booth: L01

MILCOM2016

Baltimore, MD
November 1-3, 2016
www.milcom.org
Booth: 3004

West Coast Operation:
4921 Robert J. Mathews Pkwy, Suite 1
El Dorado Hills, CA 95762 USA
Tel: 916-542-1401
Fax: 916-265-2597

East Coast Operation:
7311-F Grove Road
Frederick, MD 21704 USA
Tel: 301-662-5019
Fax: 301-662-1731

sales@pmi-rf.com • www.pmi-rf.com

ISO9001-2008 REGISTERED

They were selected for their different levels of isolation. For the DUT frequencies analyzed, BAL0006 has a standard isolation of 6 dB; BAL0036 has an improved isolation of 10 dB, much more at higher frequencies. For clarity, this article refers to BAL0036 and BAL0006 as the baluns "with" and "without" (added) isolation, respectively.

Since a phase noise analyzer's RF input port can only accept AC signals, a DC block must be inserted somewhere in the signal path between the DUT and the instrument. In general, DC can be blocked at either side of the balun. However, if the balun has its ports DC shorted to ground (refer to its datasheet), then DC blocks must be placed at the balun's input ports when it is used as a combiner. For this reason, it's probably best to develop a habit of placing DC blocks at the balun's input (differential) ports, as shown in Figure 2.

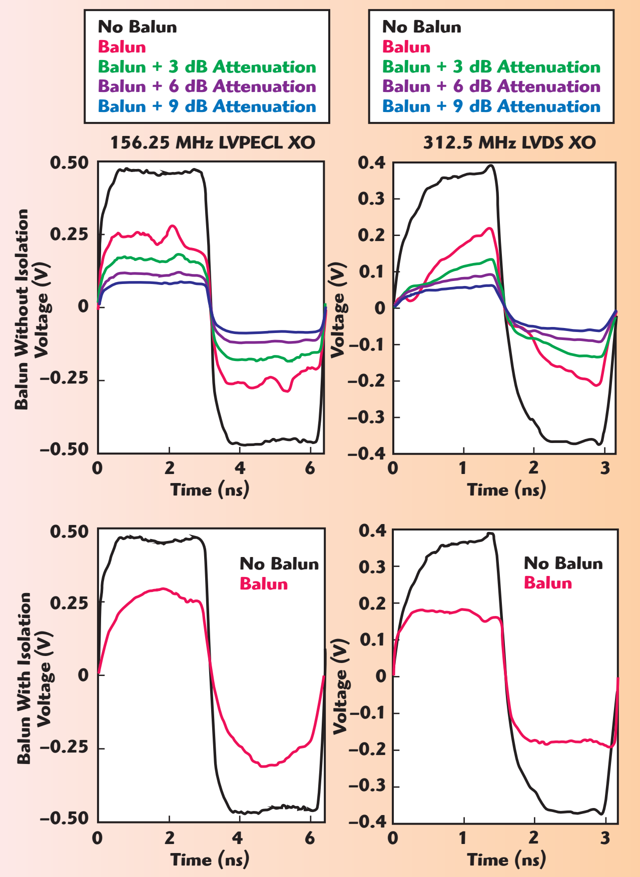

▲ *Fig. 3 156.25 MHz LVPECL (left) and 312.5 MHz LVDS (right) crystal oscillator waveforms using baluns with (bottom) and without (top) isolation.*

SIGNAL INTEGRITY

Oscilloscopes typically have more than one input, so a balun is not required to perform measurements. Nevertheless, viewing a balun's output signal in the time domain can provide insight into its operation. Figure 3 shows waveforms for two different XOs and two different baluns. The left and right sides of ***Figure 3*** correspond to LVPECL 156.25 MHz and LVDS 312.5 MHz waveforms, respectively. The bottom and top correspond to baluns with and without (added) isolation, respectively. The balun without isolation provides a noisier waveform, which external attenuation tends to clean up. For reference, each plot contains a "no balun" curve, which was measured using two oscilloscope channels (shown in Figure 2a), where one channel's data was subtracted from the other's to compute the differential signal.

The balun's insertion loss is apparent as all signals obtained with baluns swing less than the "no balun" reference waveform. The balun without isolation is observed to degrade both the LVPECL and LVDS waveforms' signal integrity. The bumps in the logic levels of the waveforms are indicative of signal distortion caused by feedback from the balun differential ports back to the DUT. By comparison, the balun with isolation provides significantly cleaner waveforms. Inserting external attenuators at the balun's differential ports (shown in Figure 2b) improves the signal integrity of the waveform in proportion to the level of attenuation. In this example, 9 dB of external attenuation is required at the balun without isolation's inputs to recover the "no balun" waveform shape (that is, normalizing each curve by their peak amplitude produces overlapping curves).

Interestingly, ***Figure 4*** shows that operating a balun as a splitter provides much cleaner waveforms compared to operating it as a combiner. The signals shown in Figure 4 were measured as

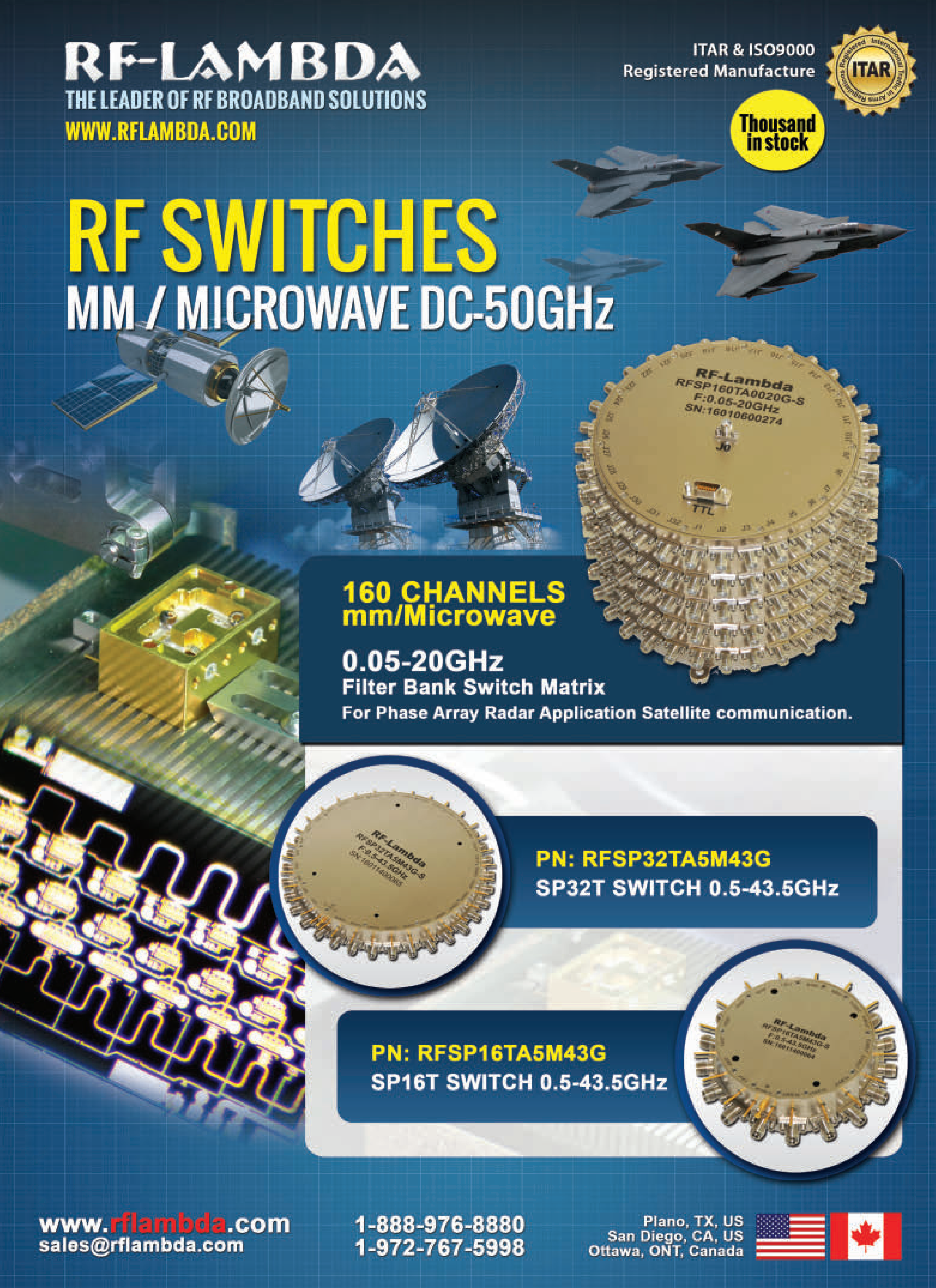
RF-LAMBDA
THE LEADER OF RF BROADBAND SOLUTIONS
WWW.RFLAMBDA.COM
ITAR & ISO9000
Registered Manufacture
ITAR
Thousand in stock
RF SWITCHES
MM / MICROWAVE DC-50GHz
RF-Lambda
RFSP160TA0020G-S
F:0.05-20GHz
SN:16010600274
J0
TTL
160 CHANNELS
mm/Microwave
0.05-20GHz
Filter Bank Switch Matrix
For Phase Array Radar Application Satellite communication.
PN: RFSP32TA5M43G
SP32T SWITCH 0.5-43.5GHz
PN: RFSP16TA5M43G
SP16T SWITCH 0.5-43.5GHz
www.rflambda.com
sales@rflambda.com
1-888-976-8880
1-972-767-5998
Plano, TX, US
San Diego, CA, US
Ottawa, ONT, Canada

ApplicationNote

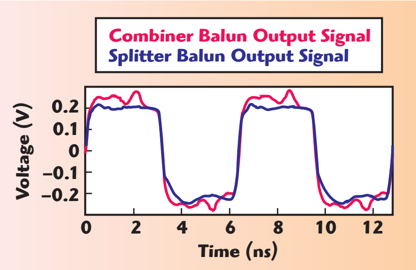

▲ *Fig. 4 Operating a balun as a splitter results in a cleaner differential signal than operating it as a combiner.*

shown in Figures 2a and c using the balun without isolation, the LVPECL XO and no external attenuation.

The above signal integrity impairments can largely be attributed to limited isolation in the balun. ***Figure 5a*** illustrates that a balun without isolation has appreciable signal leakage between its differential ports. The leakage signal from one differential port interferes with the forward signal at the other differential port. The leakage signal also appears at the DUT output drivers, which, depending on the driver architecture, can affect its operation.

The balun-with-isolation waveforms shown in Figure 3 have better signal integrity because the additional isolation inside the balun attenuates this leakage current (shown in ***Figure 5b***). Adding external attenuation to the balun without isolation, as shown in ***Figure 5c***, doesn't prevent leakage between differential ports, but the signal that does leak is attenuated compared to when no external attenuation is used. Additionally, external attenuation reduces the leakage signal appearing at the DUT output driver. This leakage signal is actually attenuated twice (once for each attenuator) as it travels from one output driver through the balun to the other output driver. Judging by the balun-without-isolation curves for "balun" and "balun + 9 dB attenuation" in Figure 3, whose shapes match well (after normalizing them by their peak amplitude), the effect of the leakage signal appearing at the DUT output driver circuitry is a major source of noise in the balun's output signal.

Finally, a balun operated as a splitter as shown in ***Figures*** 4 and ***5d*** provides cleaner waveforms than when used as a combiner, because the DUT output driver does not observe a leakage signal from the balun.

RANDOM PHASE NOISE

Phase noise is measured using the combiner balun setup in Figure 2b. Phase noise is a measure of phase variation in the frequency domain. The phase noise data can be integrated to obtain a phase jitter value in seconds RMS. The region of the phase noise curve that dominates this integral is located by lowering a -10 dB/decade line to where it first intersects the curve.[6]

Figure 6a shows how external attenuation can dramatically change the measured phase noise for the LVPECL XO. With no attenuation, the balun without isolation phase noise measurement provides overly optimistic and pessimistic results below and above, respectively, about 600 kHz offset frequency. Adding 3 dB of attenuation significantly reduces balun artifacts in the measured phase noise. As more attenuation is added, the

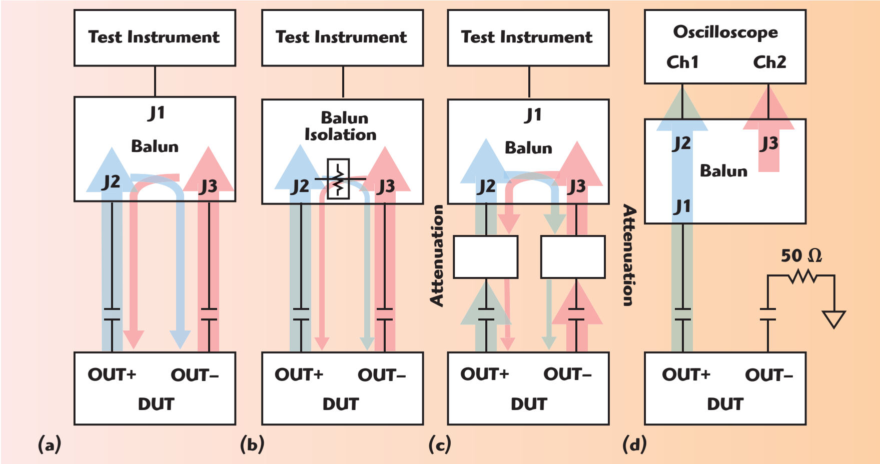

▲ *Fig. 5 A balun with poor isolation (a) allows signal leakage inside the balun, which can be reduced by increasing the isolation (b) or adding external attenuation (c). Baluns operating as splitters (d) don't have a leakage signal, resulting in a cleaner output waveform.*

level of improvement eventually diminishes. Phase noise measured with 6 dB of attenuation (not shown) overlaps the 9 dB attenuation curve.

The balun with isolation phase noise shown in ***Figure 6b*** is independent of the level of external attenuation, indicating the added isolation inside the balun eliminates a significant source of balun-induced artifacts in the measurement. Therefore, adding external attenuation to the balun without isolation provides a similar benefit as isolation in the balun with isolation.

One disadvantage of adding external attenuation to remove balun artifacts from phase noise data is that it reduces the signal power entering the phase noise analyzer, which can lead to less accurate data. The Keysight phase noise analyzer used for these measurements has diode-based phase detectors inside its PLLs, which must be biased with current. An input signal power of 0 to 5 dBm is recommended for this reason. Adding external attenuation essentially pushes the signal further into the noise floor of the instrument. Enabling cross correlation in the measurement can help recover the signal; however, cross correlation increases test time and, depending on how deep the signal lies below the instrument's noise floor, may not always help. The influence of the instrument's noise floor on the measured phase noise data can be seen in Figure 6, in which the 9 dB external attenuation curves have more noise at the lowest phase noise levels (i.e., above 2 MHz offset frequencies) compared to curves with less external attenuation.

It is therefore important to use baluns with high isolation between differential ports. If external attenuation is required, use the least amount required to stabilize the data. The optimum attenuation can be determined by increasing attenuation by small increments until the phase noise data no longer changes. Then, select the smallest amount of attenuation that produces this data. In Figure 6a, the optimum attenuation is 6 dB (not shown). In Figure 6b, no external attenuation is needed.

In addition to signal impairments caused by poor port-to-port isolation in the balun, reflections can also occur at interfaces that are not terminated at the characteristic impedance of the transmission line (typically 50 Ω). These reflections are synchronous with the forward wave, which can combine to form a standing wave. Here, the level of voltage (and current) at both DUT and balun ends of the cable is a function of cable length, which can affect the operation of the DUT and/or balun. The VSWR met-

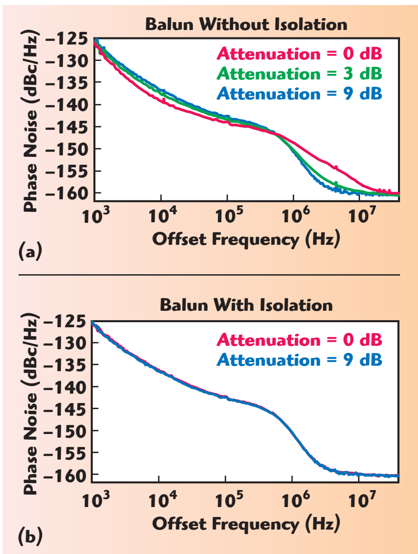

▲ *Fig. 6 LVPECL 156.25 MHz XO phase noise measured using baluns without (a) and with (b) added isolation, showing the effect of external attenuation.*

ric measures the ratio of maximum standing wave amplitude to minimum standing wave amplitude. A perfectly terminated component would have a VSWR of 1, indicating the voltage (and current) at any location in the cable remains constant. In practice, components have a VSWR greater than one. The impedance a DUT driver observes looking towards the balun is therefore a function of the cable length connecting the DUT to the balun. ***Figure 7*** shows how changing this cable length can affect signal integrity and phase noise characteristics.

In theory, the transmission line effects discussed become more noticeable at longer cable lengths. In short cables, where the delay from DUT to balun is less than the signal's transition time, the reflections settle before they are noticed. In the frequency domain, longer cables result in more of a phase variation as the frequency changes. In the time domain, longer cables result in a longer delay between when reflections occur, and more reflections contribute to standing waves and interference effects. These effects can be minimized by using baluns with excellent return loss (preventing the initial reflection) and when measuring a device with good return loss (preventing subsequent reflections).

SPURIOUS PHASE NOISE

Although a phase noise analyzer measures raw phase noise in dBc/Hz, it can post process this data to detect spurious phase noise in dBc. Phase noise data in dBc/Hz may be plotted along with the spurious data in dBc, where the spurious data is plotted using a different color to distinguish its change in units (since both share the y-axis scale). ***Figures 8a*** and ***b*** illustrate this process for two spurs in the 312.5 MHz LVDS XO.

Figures 8c and ***d*** quantify the spur magnitudes using horizontal lines for the single-ended signals, as measured for the configuration of Figure 2d. Single-ended spur magnitudes are shown using horizontal lines and differential spur magnitudes are shown using bars as a function of attenuation. The lines correspond to OUT+ and OUT–. For this DUT, the spurious levels between outputs are different. The bars in Figures 8c and d indicate the spurious magnitudes measured using the balun without isolation as shown in Figure 2b. Here, increasing the level of external attenuation reduces the spurious magnitude to roughly the mean dBc value of the single-ended (i.e., OUT+ and OUT–) spur magnitudes.

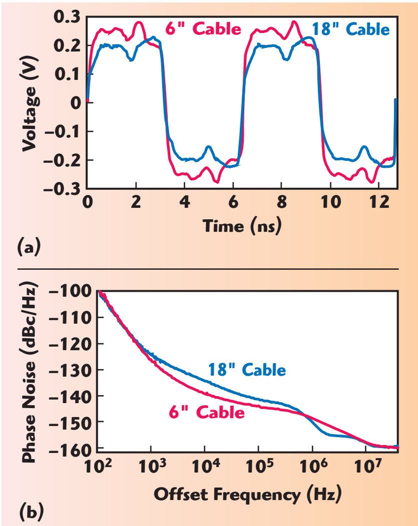

▲ *Fig. 7 LVPECL 156.25 MHz XO waveform and phase noise, measured using the balun without isolation and 6" (a) and 18" (b) coaxial cables.*

Rosenberger

www.rosenberger.com

Test, Measurement & Calibration

RF and microwave components from Rosenberger play a key role in a variety of test, measurement and calibration applications. RF high precision connectors, adaptors & devices, PCB connections – solderless, modular system or even spring loaded products – calibration kits, microwave test cables, VNA test port cables or automated test equipment products – renowned companies trust the precision and quality of Rosenberger test & measurement products.

Fields of Application

- Microwave measurements & VNA calibrations
- Lab testing
- Factory testing
- PCB connections
- Semiconductor test applications & high-speed digital testing
- Network testing
- Test & measurement equipment
- Service and support

Rosenberger | Hochfrequenztechnik GmbH & Co. KG
Hauptstraße 1 | 83413 Fridolfing | Germany | Phone +49 (0)8684 18-0 | info@rosenberger.de

SERIES TERMINATION

To further analyze the effect that component reflections and balun isolation have on measured phase noise data, the DUT outputs are matched to their transmission lines using a series termination and re-characterized with the balun without isolation. Specifically, the LVPECL XO output impedance measured 35 Ω at 156 MHz, so a value of 15 Ω is used for Rs in Figure 2e. Likewise, the LVDS XO output impedance measured 3 and 13 Ω at 78 and 312 MHz, respectively, so 47 and 37 Ω are used, respectively, for Rs in Figure 2f. In each case, the resulting phase noise data is more accurate using a series termination.

Figure 9 summarizes the test results for two cases. The red curve is the original phase noise data, measured using the balun without isolation with no series termination and no external attenuation. The green curve uses a similar setup as the red curve, but includes a series termination. The blue curve uses a similar setup as the green curve, but adds more external attenuation than needed to stabilize the phase noise curve (e.g., 3 dB less attenuation produces the same blue curve data

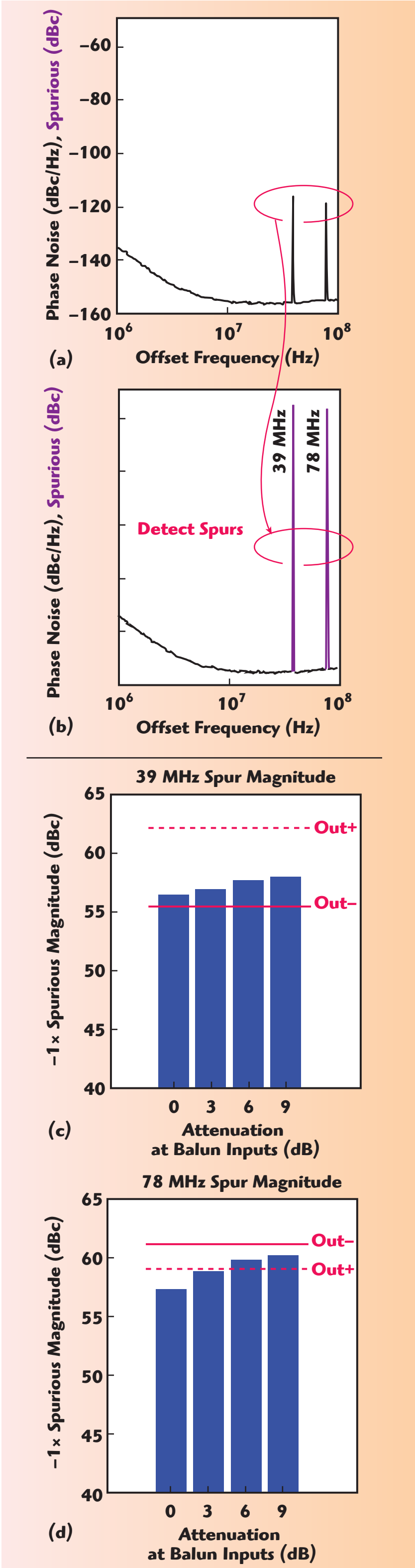

▲ *Fig. 8 Phase noise for an LVDS 312.5 MHz XO (a), from which spurs are detected at 39 and 78 MHz (b) and their respective magnitudes measured (c) and (d).*

shown in Figure 9). The blue curve is also the same data as measured using the balun with isolation, and therefore represents the most accurate phase noise data for the device. A series termination (green curve) improves the phase noise measurement.

Since neither the balun, the cables, nor the DUT output circuit are perfectly matched to 50 Ω or to each other, reflections occur that can lead to standing waves and resonances. These reflections, together with any leakage signal resulting from poor balun isolation, form a reverse signal that travels from balun to DUT. If the DUT has poor isolation between its output buffer and its internal VCO, oscillator circuitry or other components, the phase noise output by the DUT can be affected. Matching the DUT to the transmission line impedance using a series termination absorbs the reverse signal, preventing it from traveling back and forth between DUT and balun. A series termination is observed to have a similar effect on phase noise as adding external attenuation (compare Figure 9a with Figure 6a). Introducing attenuation between the DUT and balun effectively improves the load return loss by twice the attenuation value.

Although a differential clock output buffer is designed to drive a 50 Ω load, it doesn't typically have a 50 Ω output impedance. This isn't a problem when connecting devices to test equipment terminated with 50 Ω, but becomes an issue when components are used with non-ideal loads. While it may not be practical to series terminate devices for the purpose of routinely measuring phase noise, reflections can be minimized by selecting components with higher return loss (lower VSWR) values. In addition, the impact of standing waves from reflections or poor isolation can be reduced by using the shortest possible cables (between the DUT and balun to prevent resonances).

CONCLUSION

A reverse leakage signal can travel from balun to device caused by poor balun isolation and reflections from components having non-ideal loads. Since the device's output impedance itself is not matched to the transmission line, this reverse signal again reflects at the device output buffer and travels

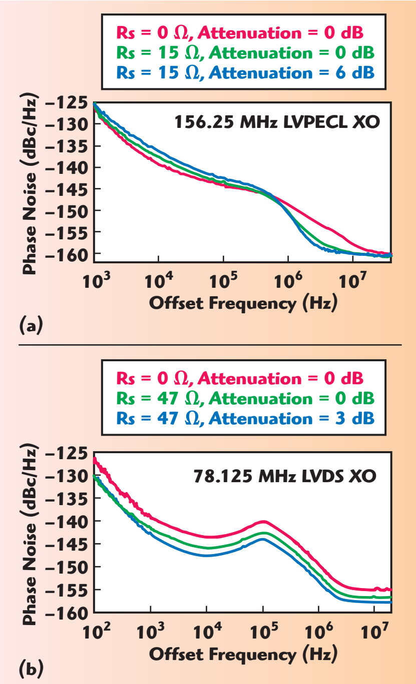

▲ *Fig. 9 DUT phase noise vs. output driver resistance and attenuation for a 156.25 MHz LVPECL XO (a) and 78.125 MHz LVDS XO (b) using a balun without isolation.*

WIN SEMICONDUCTORS

Leading Global Communications

PP10-10/-11 0.1µm Power pHEMT

- 0.1µm high performance power / low noise process
- 50µm and 100µm thickness are standard
- Useable gain to 110GHz
- 4V operation - Psat > 800mW/mm, > 50% PAE, and 13dB Gain at 29GHz

PP10 Transfer Curve

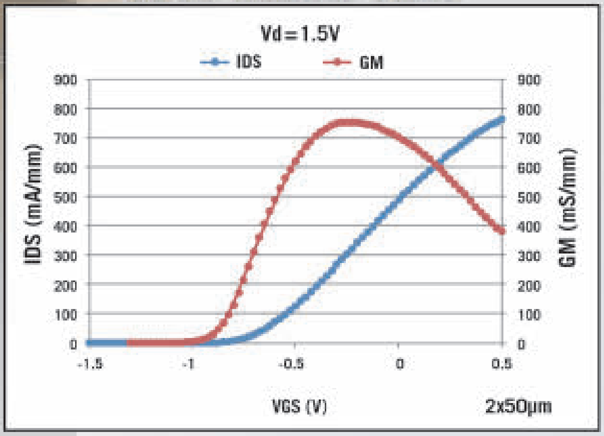

PP10 I-V Curves

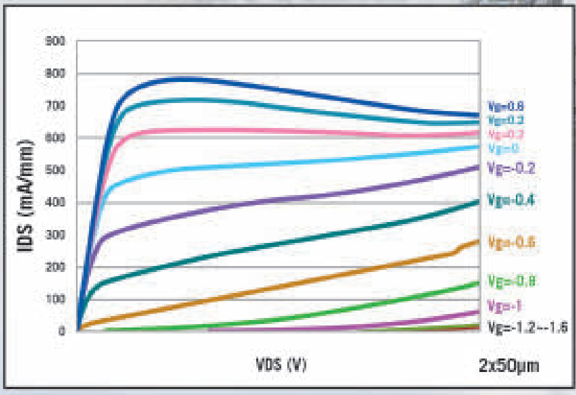

PP10 Load Pull Data

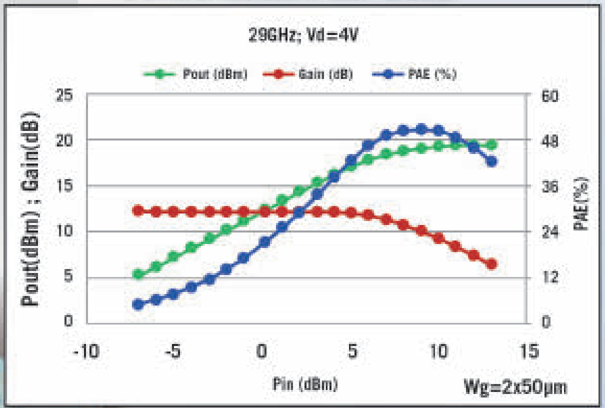

PP10 Max Gain

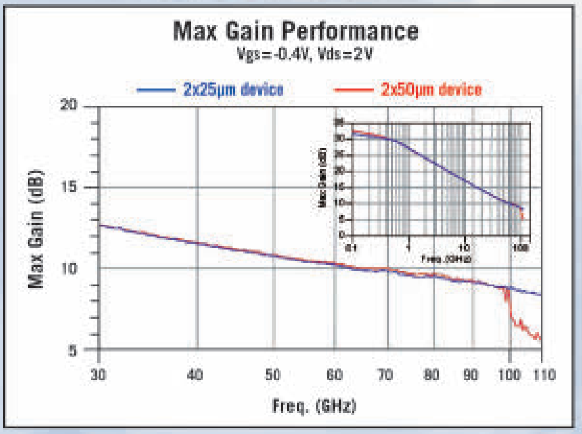

WIN SEMICONDUCTORS CORP. Tel:+886-3-397-5999 Fax:+886-3-397-5069 http://www.winfoundry.com

back and forth between device and balun. This results in a standing wave that can resonate and potentially affect device operation. If the device has poor isolation between its output buffer and internal VCO, oscillator, and/or other components, then the phase noise generated by the device may also change.

The effect that a given balun will have on measuring phase noise for a particular device is difficult to predict. Balun impairments may be observed rarely or often, depending on many complex factors. These impairments can cause the phase noise data to appear better or worse than observed by an actual system. The following is a prioritized list of recommendations to minimize measurement artifacts:

1. Select a balun primarily for high isolation (balanced port to balanced port) and high return loss. The balun should also have high common-mode rejection and good amplitude and phase balance. Everything else being equal, select a balun with low insertion loss.

2. Use short, phase-matched cables between the device and balun.

3. Use the smallest amount of external attenuation between device and balun necessary for the measured phase noise data to remain unchanged compared to measurements with larger attenuation.

4. Place DC blocks at the balun's differential ports if the balun's ports are DC shorted to ground.

From a phase noise measurement perspective, the balun market may be divided into generic and high performance products. Generic baluns generally have ±1 dB amplitude balance, ±10° phase balance, 6 dB isolation, 10 dB return loss and 20 dB CMRR — or worse. High performance baluns generally have ±0.5 dB amplitude balance, ±5° phase balance, 15 dB isolation, 15 dB return loss and 25 dB CMRR — or better. While a few high performance baluns include isolation, the term "180° hybrid combiner/divider" is often used to describe a balun with high isolation. Regardless of the terminology, baluns used to measure phase noise should target the high performance specifications above, especially isolation and return loss. Phase noise measurements will also benefit from low insertion loss baluns, which can vary from 3.5 to 6.5 dB, depending on architecture.

ACKNOWLEDGMENT

The authors wish to acknowledge useful discussions with Dr. Bob Temple, formerly with Agilent Technologies; Tony Wade, with Keysight Technologies; Dan Nehring, with CTS Corp.; Stuart Rumley, with Valon Technology; and Pierre Guebels and Boris Drakhlis, with Microchip Technology. ■

References

1. D. Brooks, "Differential Signals: Rules to Live By," Printed Circuit Design, CMP Media Inc., October 2001, https://www.ieee.li/pdf/essay/differential_signals.pdf.
2. T. H. Lee and A. Hajimiri, "Oscillator Phase Noise: A Tutorial," *IEEE Journal of Solid-State Circuits*, Vol. 35, No. 3, March 2000, pp. 326–336.
3. D. Jorgesen and C. Marki, "A Tutorial on Baluns, Balun Transformers, Magic-Ts, and 180° Hybrids," Marki Microwave, Application Note, 2014, https://www.markimicrowave.com/Assets/appnotes/balun_basics_primer.pdf.
4. "E5052B Signal Source Analyzer," Keysight Technologies, Product Brochure 5989-6389EN, 2009.
5. "Product Catalog for Broadband Test and Measurement Baluns," Marki Microwave, www.markimicrowave.com/3595/Baluns_/_Inverters.aspx?ShowTab=32.
6. G. Giust, "Determine the Dominant Source of Phase Noise By Inspection," JitterLabs, NOTE-4, Technical Note, 2016, www.jitterlabs.com/support/publications.

INVITED PAPER

The Methods and Problems of Capacitor ESR Measurement

Knowles Capacitors
Norwich, U.K.

There are many different types of capacitors with many different parameters; each is suited to a range of applications. As operational frequency requirements increase, electronic systems downsize and power usage becomes more critical, the most important parameters are quality factor (Q) and equivalent series resistance (ESR). Measurement and characterization of multi-layer ceramic capacitors (MLCC) for these parameters is demanding, and with limited standardization of test methods, comparison of ranges or competitors is difficult.

In this article, Knowles addresses the measurement of ESR in high Q MLCCs, probably the most requested parameter, describing the test methods in use and how Knowles measures the data published in the company's datasheets.

Q, ESR, POWER

Q is the quality factor, the reciprocal of the dissipation factor (DF), and represents the losses of the capacitor.

$$Q = \frac{1}{DF} \quad (1)$$

The higher the Q, the lower the DF and the lower the loss. ESR is the equivalent series resistance (RS), representing the effective resistance to RF current. ESR encompasses the loss properties of both the dielectric and electrode.

$$X_C = \frac{1}{2\pi fc} \quad (2)$$

where f is frequency (Hz), C the capacitance (F) and X_C the capacitive reactance (Ω). Then,

$$R_S = DF \times X_C \quad (3)$$

The power dissipated in the capacitor (W) is given by

$$P = I^2 R_S \quad (4)$$

where I is the RMS current flowing in the capacitor (A).

Knowing the value of ESR is important because it determines the suitability of the component for use in RF power applications. If the ESR value is too high, the self-heating due to I^2 R losses will be too great, and the part will overheat and fail. The ESR also enables the maximum current rating for the component to be calculated.

As an example, consider a cellular phone base station operating in the GSM900 band at 940 MHz. A high Q, 47 pF capacitor, with an ESR of approximately 0.088 Ω at 940 MHz, is

used as the coupling capacitor in this 50 Ω system. The RF power incident on the capacitor is 40 W. Using $P= I^2 R$, where R = Z + ESR, to find the circuit current gives 0.89 A. To find the power dissipated in the capacitor, we put this value of current back into $P= I^2 R$, where R = ESR, which gives 70 mW. The power dissipated in the capacitor is simply derived from the ratio of the ESR to the total circuit impedance multiplied by the system power:

$$\frac{ESR}{(Z+ESR)}P \quad (5)$$

For values of ESR significantly lower than the Z value, there is a negligible change to the overall circuit impedance; it can be ignored, leaving

$$\frac{ESR}{Z}P \quad (6)$$

Using the same calculations for a 47 pF, ultra-low ESR capacitor, with ESR = 0.07 Ω at 940 MHz, the power dissipated in the capacitor is 56 mW, a 20 percent reduction. This capacitor allows the system to either run cooler or at higher power.

Different dielectric and electrode combinations will exhibit different levels of Q and ESR. At lower frequencies, the dielectric material is the dominant factor; metal losses become more important at higher frequencies. X7R materials are used at low frequencies and typically have a DF of around 1 to 2 percent, measured at 1 kHz, which corresponds to a Q of 50 to 100. C0G/NP0 materials have Qs between 600 to 1000, measured at 1 MHz.

Under laboratory conditions, measurement of Q at 1 MHz can show higher Q values, 10,000 or greater. However, for practical purposes, the limit for 100 percent testing on high speed machines is ~2000. 100 percent measurement of Q is not practical above 1 MHz. Capacitance bridges and LCR meters are not accurate enough and, when combined with leads and contacts, rapid high frequency measurement is not possible. It is necessary, though, to assess the Q and ESR near the operating frequency. However, this risks test variance and accuracy issues which can cause problems interpreting the data.

ESR MEASUREMENT

Two measurement methods are commonly used to determine Q and ESR: a coaxial resonant tube, a swept impedance analyzer or a combination of the two. Each will be discussed.

Coaxial Resonant Tube Measurement

The most accurate method of determining Q and ESR at "high" frequencies, i.e., from approximately 100 MHz to 1.2 GHz, is with a resonant line coaxial jig. The industry standard tube for doing this was developed many years ago as the Boonton model 34A, manufactured by the Boonton Electronics Corp., and designed to be used with an RF millivolt meter and a signal generator (see ***Figures 1*** and ***2***).

Using this historic setup, the

$$\frac{\lambda}{4}, \frac{3\lambda}{4}, \frac{5\lambda}{4} \text{ and } \frac{7\lambda}{4}$$

resonant frequencies are measured by adjusting the signal generator until the peak reading is recorded on the millivolt meter. For each resonant frequency, the 3 dB bandwidth is determined by adjusting the frequency until the meter reading drops to 50 percent of the resonant value. The tube is characterized by measuring the

$$\frac{\lambda}{4} \text{ and } \frac{3\lambda}{4}$$

frequencies and bandwidths with both open and short circuits. Then the capacitor chip is inserted between the two conductors and held by the shorting plunger. From a full set of measurements, the ESR and Q can be calculated at the resonant frequencies. With data at three, four or five frequencies, ESR vs. frequency is plotted and a "best fit" line is drawn between them. The response curve between resonances is assumed to be relatively linear.

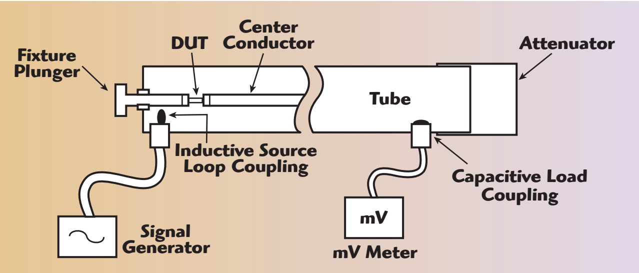

Fig. 1 Resonant tube.

The Boonton resonant tube system was developed before the advent of VNAs. Today, it is common to replace the signal generator and millivolt meter with a VNA (see ***Figure 3***). With the resonances visible as graphical peaks, the frequency and bandwidth can easily be read. Modern VNA equipment allows the data to be directly exported to the calculation program.

The resonant tube method remains the only relatively accurate way of measuring ESR and Q of small MLCCs. This was recognized when the international standard for ESR measurement, EIA-RS-483, was written, as it specifies using this equipment. However, there are limitations to this measurement method. The operating frequency range of the tube is limited by physical length to a frequency range from approximately 100 MHz to 1.25 GHz. EIA-RS-483 reflects this, as it only covers ESR measurements in that range. It can also be seen in the data published by some MLCC manufacturers that provide data between 1 and 1.5 GHz. To use a resonant tube to measure at frequencies outside this standard range, a new tube must be manufactured and characterized. Boonton made the only commercially available tube in the 34A; any other tube will be "homemade," and the build quality and characterization may not be as good as the

Fig. 2 Boonton 34A with traditional setup.

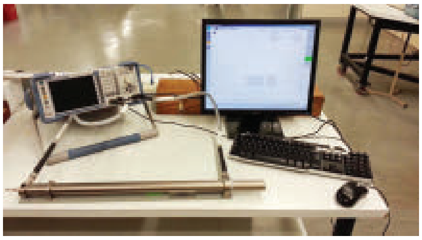

Fig. 3 Boonton 34A with VNA setup.

Boonton.

Resonances within the capacitor may cause problems and must be considered. The ESR response of an MLCC is not linear, peaking at the parallel resonant frequencies (PRF), where the capacitor response is erratic. If the resonances of the tube are close to a MLCC PRF peak, then the measurements need to be ignored. As the tube does not show the PRF of the MLCC, it takes an experienced operator to identify which measurements must be eliminated from the curve. As an example, consider a 47 pF MLCC measured using two resonant tubes: 1) measurements to 1.2 GHz using a Boonton 34A and 2) measurements from 700 MHz to 5 GHz using a homemade 10 cm resonant tube (see ***Figure 4***). Notice the severe change in response between the two tubes and the elevated readings in the GHz region. This MLCC had a PRF around 2.6 GHz and a second-level resonance around 5 GHz, rendering the measurements from the smaller tube irrelevant much beyond the 1.3 GHz data obtained with the Boonton 34A.

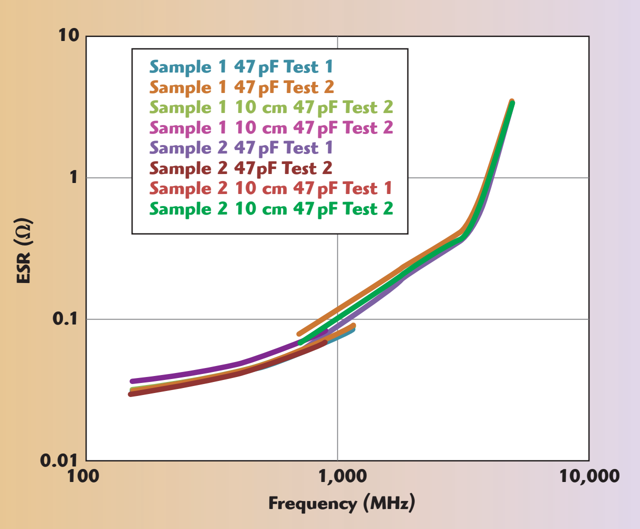

▲ *Fig. 4 47 pF capacitor measurements using Boonton 34A and 10 cm tube.*

Swept Impedance Analyzer Measurement

Given the limitations of the coaxial resonant tube measurement, it's desired to have an alternative to measure ESR. A swept frequency method takes more measurements across frequency and gives a better understanding of the performance of the component.

It is possible to take reasonably accurate readings by soldering parts to boards, measuring the response using a VNA to generate S-parameters, then reverse modeling to determine the ESR. While this is not as accurate as the resonant tube — it is vital to carefully compensate out the test board — it does have the advantage of producing a swept response highlighting any resonances in the system. (The problem with the accuracy of swept measurements used in isolation will be discussed later.)

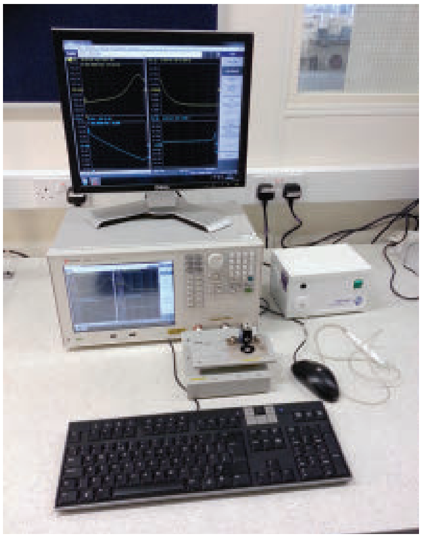

▲ *Fig. 5 Keysight E4991B with jig.*

For ease of testing, it is preferable to use test equipment that allows the device under test (DUT) to be placed directly into a test fixture of known characteristics and measured directly. One example of such equipment is the Keysight E4991 impedance analyzer (see ***Figure 5***), which is essentially a VNA with a modified front-end interface that allows direct measurement of the ESR, Q, Z and C of an MLCC. It performs a swept measurement up to a maximum of 3 GHz. This is now becoming recognized as the standard method for characterizing MLCCs, increasingly being adopted by the manufacturers and users of these capacitors. Various jigs are available to measue different chip sizes.

However, this method has a limit that is important to recognize. Analyz-

ing the accuracy of the measurement, as shown in Keysight's documentation, it becomes clear that measurement of the very small ESR of MLCCs is difficult. The errors and uncertainties are best shown with an example of the accuracy when measuring a 51 pF MLCC at 500 MHz, where Z_x = 6.153 Ω, Rs = 0.026 Ω, DF = 0.00423 and Q ≈ 250. Applying the accuracy calculation from Keysight's datasheet for the E4991A yields:

$$Z_S = 13 + 0.5f(\text{MHz}) = 263\ \text{m}\Omega \qquad (7)$$
$$Y_O = 5 + 0.1f(\text{MHz}) = 55\ \mu\text{S}$$
$$E_a = 0.8\%$$
$$E_b = \left(\frac{Z_S}{|Z_X|} + Y_O|Z_X|\right) \times 100 = 4.27\%$$
$$C_S = (E_a + E_b)\sqrt{1 + DF^2} = 5.07\%$$
$$R_S = (E_a + E_b)\sqrt{1 + Q^2} = 1200\%$$

Thus, the uncertainty is R_S= 0.026 ± 0.312 Ω.

Note that this calculation does not include the accuracy and uncertainty of the test fixture. Assuming the MLCCs are tested using Keysight's 16197A test fixture, the calculated accuracy is

$$Z_e = A + \left(\frac{Z_S}{Z_X} + Y_O Z_X\right) \times 100 = 2\%$$

where (8)

$$A = 1.2f(\text{GHz}) = 0.3\%$$
$$Z_S = 30 + 150f(\text{GHz}) = 105\ \text{m}\Omega$$
$$Y_O = 2 + 30f(\text{GHz}) = 17\ \mu\text{S}$$
$$R_{eS} = \frac{Z_e}{DF} = 473\%$$

Here, the uncertainty is R_{eS}=0.026 ±0.123 Ω. The combined accuracy and uncertainty is given from:

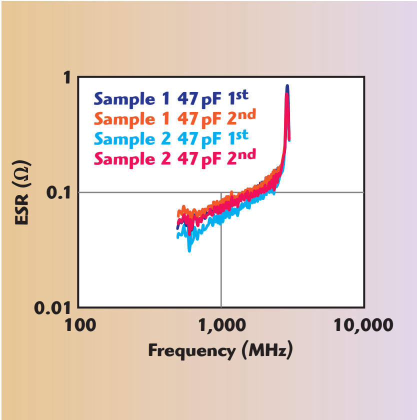

▲ *Fig. 6 47 pF capacitor measurements using Keysight E4991.*

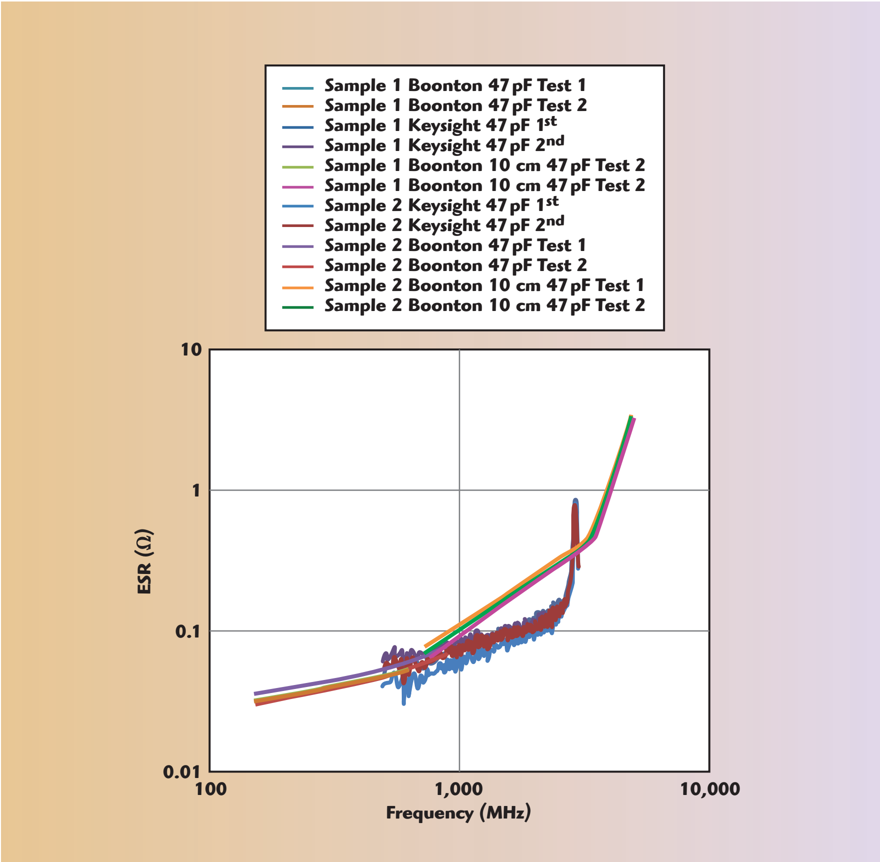

▲ *Fig. 7 Comparison of Boonton and Keysight measurements.*

$$\sqrt{0.312^2 + 0.123^2} = 0.335 \quad (9)$$

or $R_S = 0.026 \pm 0.335\ \Omega$.

The accuracy of this test method is not very suitable in isolation. The curves it produces, however, do include the PRF resonances and are much more useful in determining the actual performance of the component. ***Figure 6*** shows the E4991 measured data of the 47 pF MLCC previously measured with the resonant tube. Overlaying the two sets of data (see ***Figure 7***), we can see exactly how the resonant tube measurements are being affected by the PRF resonances and how inaccurate a resonant tube measurement and a swept measurement can be in isolation.

Combining the Boonton and Swept Measurements

Comparing the Boonton and swept measurement methods, both produce results that have accepted inaccuracies. Neither test method can be used in isolation; however, combining them enables cross checking the results and confirming that the readings taken are reasonably accurate. As such, the procedure adopted by Knowles is to:

- Measure the component using the Boonton 34A, generally following EIA-RS-483 and with a maximum frequency of 1.2 GHz
- Use the results of the Boonton test to verify the setup of the Keysight E4991, to demonstrate that the calibration is as accurate as possible
- Perform swept measurements on the Keysight E4991
- Combine both sets of readings.

Using this method, plots are generated for ESR, Q and Z (see ***Figure 8***).

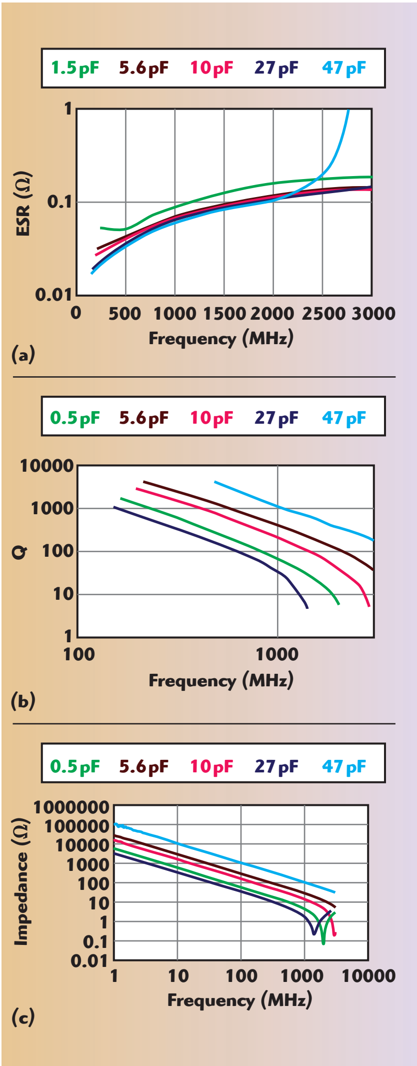

▲ *Fig. 8 ESR (a) Q (b) and impedance (c) measurements, combining the Boonton 34A and Keysight E4991B analyzer with 16197A test fixture.*

TEST JIG VARIATION

In defining the Knowles test regime, all data on MLCC chip sizes 0603 to 1206 is measured using the Keysight 16197 surface-mount fixture. An alternative fixture, the Keysight 16196, may also be used for testing. It has a range of jigs tailored to specific MLCC sizes, from 0603 and smaller. The major difference between the 16196 and 16197 jigs is the connection to the MLCC: the 16196 only contacts the end of the chip, while 16197 contacts the bottom pad of the termination. Neither connection is truly representative of an MLCC soldered on a board, but they do allow comparison testing of different MLCCs. It is not unusual to achieve different test results from the same component tested on the 16196 and 16197 jigs (see ***Figure 9***). So when making comparisons, the performance should be measured on the same type of fixture.

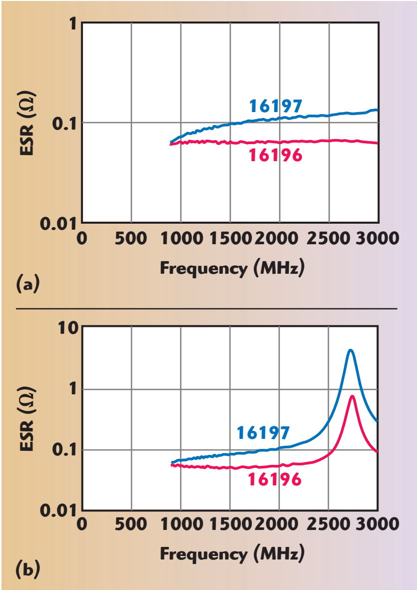

▲ *Fig. 9 Comparison of 18 pF (a) and 56 pF (b) capacitor ESR measurements using two test jigs.*

CONCLUSION

ESR and its associated data (i.e., Q and Z) are important considerations for circuit design, yet notoriously hard to measure. It's equally hard to compare data supplied from different companies or measure and verify supplier data. The difficulties and inaccuracy associated with these measurements mean that these parameters are always given as "typical" data. MLCCs are defined by the capacitance and working voltage. Good control of materials and design mean that the performance will be consistent, although actual measured data may vary.

ESR is best considered as a comparative measurement, meaning measuring components on the same system on the same day with the same compensation set will provide a good indication of relative performance. Comparison with data obtained from other sources or tested at other times may not give a true picture of how the parts will perform in the circuit. Even when considering comparison test data, remember that it is obtained from a component mounted in a test fixture and may not be totally representative of a component soldered into a circuit. Suitability of operation must always be confirmed by evaluation in the actual circuit. ESR, Q and Z plots are therefore supplied with the aim of giving an indication of the performance of an MLCC over a given frequency range of operation.■

Addressing Interference Problems Using Real-Time Spectrum Analysis

Keysight Technologies
Santa Rosa, Calif.

With the proliferation of wireless technologies now used in commercial, aerospace and defense (A&D) applications, interference problems are becoming more common and more severe. To mitigate these issues, many A&D systems — and some early 5G designs — are moving to higher frequencies, including the millimeter wave band. Related design enhancements include the use of narrow radar pulses and highly encrypted communication signals. While these techniques and technologies can fend off the effects of externally generated interference, they make field troubleshooting more difficult. As a result, new tools and measurement technologies are needed to effectively maintain deployed systems. One such tool is real-time spectrum analysis (RTSA), which is especially effective for interference hunting and signal monitoring. When these high speed, gap free measurements are added to a handheld spectrum analyzer or combination analyzer, field personnel can use a single instrument to detect, locate and fix interference problems.

To provide these capabilities up to Ka-Band, Keysight is now offering RTSA as an optional capability for many of its FieldFox handheld RF and microwave analyzers. These offer a maximum real-time bandwidth of 10 MHz at frequency ranges up to 50 GHz (N995xA and N996xA models).

THE MEANING OF REAL-TIME ANALYSIS

The phrase "real-time analysis" and the implied capabilities often mean different things to different people. Fortunately, a consistent core concept can be defined as follows: in a spectrum or signal analyzer with a digital intermediate frequency (IF) section, real-time operation is a state in which all signal samples are processed for some sort of measurement result without any gaps between time acquisitions (see ***Figure 1***). Achieving a wider real-time analysis bandwidth requires higher sampling and processing rates. Thus, for a given computational capability, there will be a maximum bandwidth above which the signal processing hardware cannot keep up with the sample stream. A closely related term is real-time bandwidth (RTBW), which is the widest measurement span at which the analyzer can maintain real-time operation.

As signal environments become more complex, it is increasingly important to represent a large amount of measurement data on a single screen. This is essential for RTSAs that generate thousands of spectra per second, many more than can be discerned by the human eye. As an example, FieldFox with RTSA can produce >120,000 spectra per second, yet the average human eye can detect only 30 per second. Therefore, to take advantage of real-time results, each display update needs to represent

about 4000 × 30 results in a useful way. The most informative displays are created by compiling statistics and displaying how often a particular measurement value occurs (e.g., a specific amplitude at a specific frequency). One example is the density display, which is a spectrum measurement enhanced to show frequency of occurrence and can be considered a backwards-looking version of probability. These displays are coded using color or trace intensity, and a persistence function can be added to focus attention on more recent events as older data fades away (see ***Figure 2***). Trace data such as the most recent single display update, or an average, can also be overlaid as a trace similar to a traditional spectrum measurement. This approach allows field personnel to see and focus on infrequent events or transients, then separate them from other behavior. By changing the persistence and color weighting, specific behaviors can be highlighted.

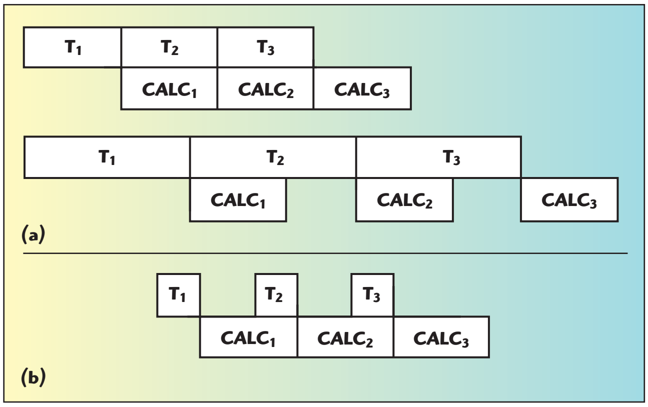

▲ *Fig. 1 Real-time operation occurs when the instrument's calculation speed is fast enough to ensure gap-free analysis of sampled data, including computation, averaging and display updates (a). If gaps occur between the time acquisitions (b), the operation is not real-time.*

RTSA also can reveal signals within signals. In a highly dynamic environment, it can be difficult to see small signals with low duty cycles when the frequency content overlaps with signals that are wider, larger or more frequent. Fortunately, adjusting the persistence time can enhance the small differences that reveal elusive signals. Any situation in which signals can be separated by frequency of occurrence is a candidate for this approach (see ***Figure 3***).

CARRYING PRECISION INTO THE FIELD

Keysight's FieldFox handheld analyzers deliver precise microwave and millimeter wave measurements and possess key attributes that support routine maintenance, in-depth troubleshooting, and virtually anything in between:

- Frequency coverage from 5 kHz to a maximum of 50 GHz
- Multiple capabilities, including cable and antenna tester (CAT), spectrum analyzer, RTSA, vector network analyzer (VNA), power meter, independent signal source, frequency counter and GPS receiver
- Rugged design meeting MIL PRF 28800 F class 2, type tested for IP 53 and MIL STD 810G 511.5 process 1 (explosive environment)
- Field ready at 7.1 lb (3.2 kg) and a battery life up to four hours.

A built-in interference analyzer includes the ability to record and playback captured signals. FieldFox can also perform pulse measurements using its spectrum-analyzer mode and a USB peak power sensor.

FieldFox key RTSA specifications are exceptional in field testing. For most over-the-air (OTA) applications, the maximum RTBW of 10 MHz is more than sufficient, because external interference typically occurs within a much narrower band. Another crucial spec is the probability of intercept (POI), which is the minimum duration for a signal of interest to be detected with 100 percent probability and measured with the same amplitude accuracy as when observing a CW signal. A FieldFox with RTSA has POI performance < 12.2 μs and can detect pulses as narrow as 22 ns.

When hunting for interference in the field, dynamic range and spurious performance are also important. Usable dynamic range is a function of front-end gain compression, preamplifier performance and the noise floor of the analyzer's receiver. Together, these factors determine the lowest detectable power levels. ***Figure 4*** shows the performance of the FieldFox analyzers with RTSA: the noise floor is at -93 dBm, no spurs are visible and the usable dynamic range is approximately 67 dB at a 2.45 GHz center frequency and 300 MHz span. In general, FieldFox can see signals down to -150 dBm with the preampli-

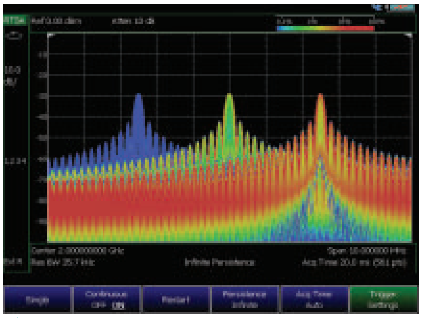

▲ *Fig. 2 Density display with user-selected persistence time helps to convey the behavior of multiple signals occupying the same frequency channel.*

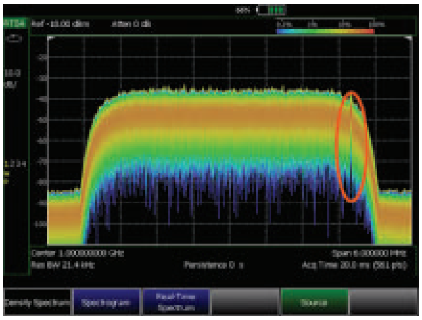

▲ *Fig. 3 A narrowband RF signal (red oval) "hiding" beneath a W-CDMA signal.*

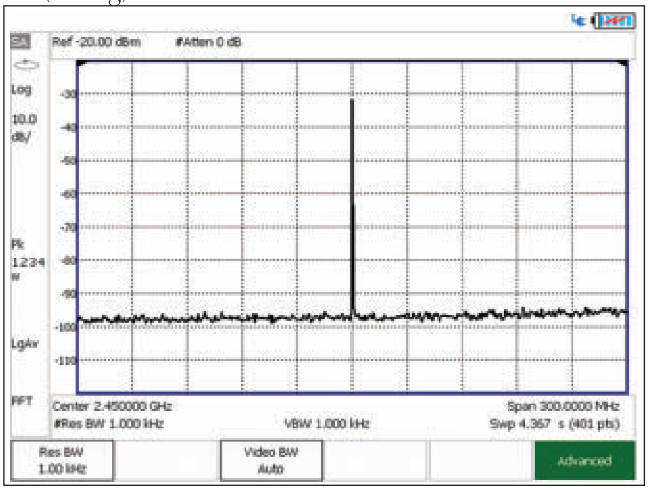

▲ *Fig. 4 Measuring a 2.45 GHz signal in RTSA mode shows the noise floor, absence of spurs and usable dynamic range.*


GREAT SERVICE ISN'T EXPENSIVE...
...IT'S PRICELESS.
EXCELLENT SERVICE
EXCELLENT DELIVERY
EXCELLENT QUALITY
RF COAXIAL RELAYS
SMA, N AND PCB LAUNCH
STANDARD AND CUSTOM DESIGNS
RELCOMM TECHNOLOGIES, INC.
• Mission Critical Communications:
- Security, Safety and Intelligence
- Commercial Telecom Infrastructure
- Military Defense Fixed, Mobile & Shipboard
• Instrumentation:
-Test and Measurement
RF Relay Store.com is the answer to your urgent small quantity needs.
RF Coaxial Relays available from Stock at www.rfrelaystore.com
sales@relcommtech.com • www.relcommtech.com • 410-749-4488
EXCELLENCE BY DESIGN

fier activated and at narrow resolution bandwidth (RBW) settings.

ENHANCING REAL WORLD MEASUREMENTS

FieldFox capabilities lend themselves to a variety of real world measurement situations. The characterization of radar signals in the field provides a good example. With a pulsed radar system, the analyzer must provide a variety of RBW and span settings that enable measurements of characteristics such as pulse repetition frequency (PRF), pulse width, duty cycle and peak power. For OTA testing, precise triggering functions are needed to capture specific pulses of interest. With a FieldFox running in RTSA mode, the user simply enters the center frequency, and the analyzer will immediately capture the pulsed signal. Pulse width and peak power can easily be measured, and the user can adjust the frequency span to zoom in or out. Measuring duty cycle or PRF requires a simple change to zero-span mode. The spectrogram display makes it possible to view an entire pulse train over a period of time, and an individual frequency spectrum (i.e., a single line in the spectrogram) can be selected for viewing in a separate trace (see ***Figure 5***). This type of measurement is not possible with a swept or "snapshot" spectrum analyzer.

With today's multiplicity of wireless technologies, advanced measurement tools are needed to effectively maintain deployed A&D and commercial systems. In a millimeter wave FieldFox handheld spectrum or combination analyzer, RTSA is especially effective for interference hunting

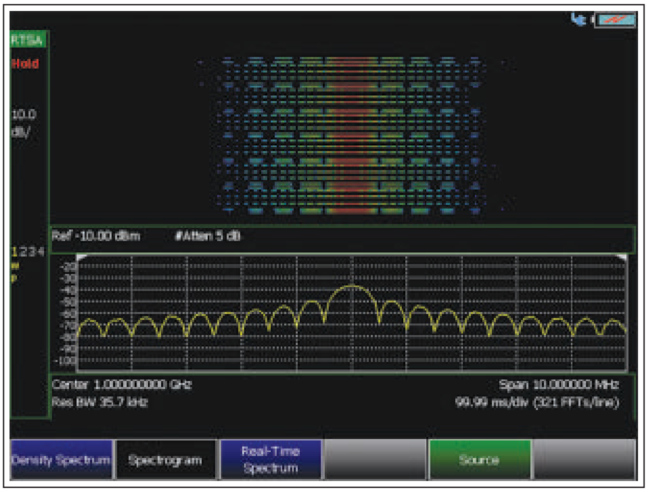

▲ *Fig. 5 The spectrogram (top) uses a color-coded overhead view of frequency spectra vs. time (y-axis) that reveals pulses with various widths. The individual spectrum display (bottom) shows a specific instant.*

and signal monitoring. Field personnel can use this single instrument to detect, locate and fix interference problems in scenarios that range from radar testing and LTE analysis to signal monitoring and IED jamming.

VENDORVIEW

Keysight Technologies
Santa Rosa, Calif.
www.keysight.com/find/fieldfox

HIGH POWER
100 MHz to 20 GHz

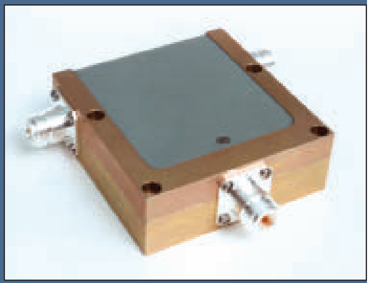

For Military/Radar Applications.

Isolators/Circulators

As one of the leading suppliers of ferrite components in the industry, UTE Microwave has pioneered innovative designs, quality craftsmanship and exceptionally high quality products. Custom designs, standards...many of them off-the-shelf, are the result of over 35 years of experience in the industry. UTE Microwave continues this tradition with new products for ever changing applications. Our broad line of HIGH POWER, low loss circulators and isolators spans the spectrum from below 100 MHz in coax/stripline units to waveguide devices at 18 GHz for both peak and average powers.

325 MHz NEW HIGH POWER Circulator for Radar & UHF Frequencies

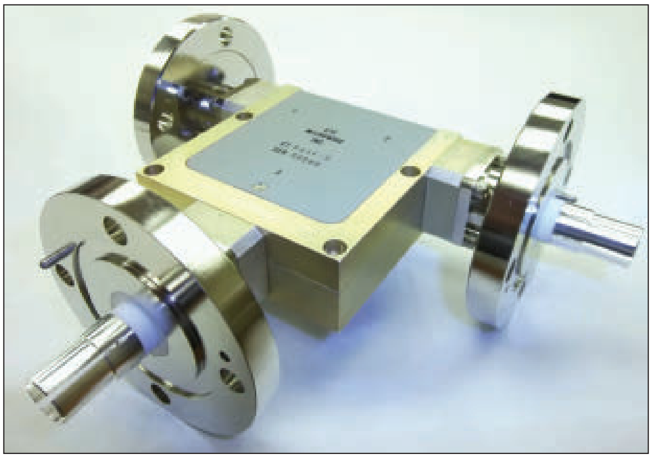

Model CT-1864-S is rated at 60kW peak and 600W average power at 325 MHz. The unit provides 20 dB minimum isolation, 0.2 dB insertion loss and 1.20:1 maximum VSWR. Its extremely compact design has flange to flange insertion length of only 6-3/4" and a height of 5-1/4". For use in radar applications, it has 1-5/8" EIA connectors. It is also available at other UHF frequencies and connector types.

HIGH POWER Drop-in Series

A broad line of low loss HIGH POWER Drop-in circulators are available from VHF to Ku band including Kilowatt average power levels at VHF thru S band. L and S band radar are a specialty. A few of these are shown here.

A) 2.7–3.1 GHZ 1 kW pk, 100 W av

B) 1.2–1.4 GHZ 3 kW pk, 300 W av

C) UHF TV Band 5 kW pk, 500 W av

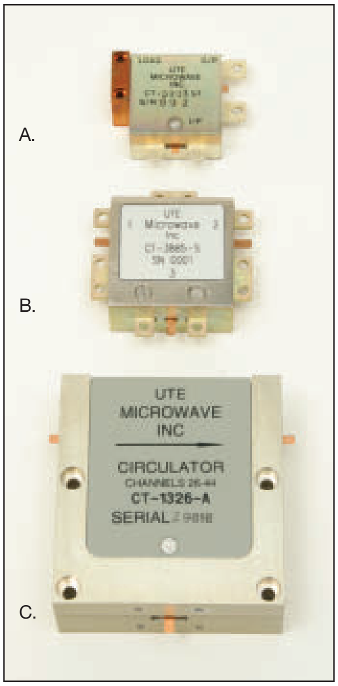

Our "POWER-LINE" serves the COMMUNICATIONS, TELECOM, MEDICAL, SCIENTIFIC, TV, PCS and INDUSTRIAL markets.

The following models are examples of our High Power units

Model No.	Power	Connectors	Freq. Range
CT-1542-D	10 Kw Pk 1 Kw Av	DIN 7/16	420–470 MHz
CT-2608-S	3 Kw Pk 300 W Av	"Drop-in"	1.2–1.4 GHz
CT-3877-S	2.5 Kw Pk 250 W Av	"Drop-in"	2.7–3.1 GHz
CT-3838-N	5 Kw Pk 500 W Av	N Conn.	2.7–3.1 GHz
CT-1645-N	250 W Satcom	N Conn.	240–320 MHz
CT-1739-D	20 Kw Pk 1 Kw Av	DIN 7/16	128 MHz Medical

FEATURES:

- **Power levels to 5 KW CW, 75 KW Pk.**
- **Low Intermod Units**
- **Low Loss Options**
- **Extended Octave Bandwidths**
- **Power Monitors and DC Blocks**
- **Iso Filter-Monitor Assemblies**

Broadband Units • Common Band Devices • High Isolation Units • Multiport Devices • Drop-In Devices • Wireless/PCN Devices • High-Power Industrial/Medical Iso Adaptors Waveguide Junctions • High-Power TV Units • VHF and UHF Devices

sales@utemicrowave.com

UTE MICROWAVE INC.

3500 Sunset Ave., Asbury Park, NJ 07712
Tel: 732-922-1009 Fax: 732-922-1848
E-mail: info@utemicrowave.com

Contact us for more information on our extensive product line and current catalog. We accept Visa, MC, Amex

Up To 100 W Out and 60 dB Gain From Compact, SMA, GaN Amplifiers

Pasternack
Irvine, Calif.

Expanding their selection of in-stock amplifiers available for same-day shipment, Pasternack has introduced a family of solid-state power amplifiers (SSPA) using GaN technology to achieve high power and power-added efficiency (PAE).

The SMA-connectorized portfolio comprises 12 models (see ***Table 1***) that offer 10 to 100 W of saturated output power, PAE to 35 percent, gain from 43 to 60 dB and gain flatness as low as ±1.25 dB. The high output load impedance of GaN eases impedance matching, allowing lower loss matching components. The amplifiers are unconditionally stable, matched to 50 Ω at the input and output, with at most a 2:1 input VSWR. Harmonics are typically -15 or -20 dBc, spurious at -70 dBc—even with the broadband high frequency amplifiers—providing a predictable and stable response. Other features include DC on/off control using a TTL logic signal, and some models have voltage regulation, bias sequencing, current monitoring and temperature shutdown up to +90°C, for added reliability.

Amplifier operating temperature range is from -40° to 85°C. Many of the power amplifiers (PA) come in hermetically sealed packages for rugged environments. The PE15A5032F and PE15A5033F models have integrated heat sinks and cooling fans to ensure performance in high temperature applications. Aside from the technical performance, the GaN amplifier series offers a wide variety of monitoring features, for ease of use and optimum power handling.

TABLE 1
GaN POWER AMPLIFIER FAMILY

Model	Frequency Range	Gain	Saturated Power		PAE	DC Power
	(MHz)	(dB)	(W)	(dBm)	(%)	(V/A)
PE15A5011	30-2500	43	10	40	35	28/1.2
PE15A5017	700-6000	43	10	40	20	32/2
PE15A5016	6400-7100	58	20	43	35	33/2.3
PE15A5019	7200-7500	58	15	42	35	33/2.3
PE15A5024	2000-6000	50	25	44	30	28/3
PE15A5025	2000-6000	50	50	47	30	28/6
PE15A5026	1000-3000	50	50	47	25	28/7
PE15A5027	100-6000	60	10	40	20	28/2.2
PE15A5032	500-3000	48	50	47	25	36/8.3
PE15A5032F	500-3000	48	50	47	25	36/8.3
PE15A5033	700-2700	45	100	50	30	30/16.7
PE15A5033F	700-2700	45	100	50	30	30/16.7

TABLE 2

GaN AMPLIFIER FAMILY FEATURES

	Model # (PE15A50_ _)											
Features	**11**	**16**	**17**	**19**	**24**	**25**	**26**	**27**	**32**	**32F**	**33**	**33F**
TTL Control	✓	✓	✓	✓	✓	✓	✓	✓	✓	✓	✓	✓
Internal Voltage Regulation	✓	✓		✓	✓	✓	✓	✓	✓	✓	✓	✓
Bias Sequencing	✓	✓		✓	✓	✓	✓	✓				
Over/Under Voltage Protection		✓		✓								
Reverse Bias Protection	✓	✓		✓								
Over Temperature Shutdown		✓		✓	✓	✓	✓	✓	✓	✓		
Linear COFDM Power Output		✓		✓								
Load VSWR Protection		✓		✓								
Current Monitoring					✓	✓	✓	✓	✓	✓		
Hermetically Sealed					✓	✓	✓	✓				
CW Operation					✓	✓	✓		✓	✓		
Mismatch Handling					✓	✓	✓	✓				
RF Input Signal format CW/AM/FM/PM/ Pulse									✓	✓	✓	✓

BIAS SEQUENCING

GaN high electron mobility transistor (HEMT) technology is a very attractive option for the amplifier industry due its many advantages, including high power density, reliability, heat dissipation and the capability to amplify signals in the millimeter wave band. Still, the biasing and bias circuitry of high power RF devices require detailed analysis and design to prevent instabilities that can affect linearity or cause thermal runaway. The risk of instability can intensify with high current, continuous wave (CW) applications. To ensure best performance, Pasternack offers bias sequencing for most of these GaN amplifier models.

CURRENT AND TEMPERATURE MONITORING

Some models in Pasternack's GaN PA series offer current monitoring to minimize potential instability and noise, as the current in GaN HEMT amplifiers can increase with temperature. An over temperature shutdown at +85° to +90°C provides thermal protection to maintain the safe working operation of the device.

OVER VOLTAGE PROTECTION AND VOLTAGE REGULATION

Pasternack's GaN amplifiers have under- and over-voltage shutdown, where the unit will shut down if the bias is below or above specified voltages. When the load at the output of the amplifier varies, the output voltage can change due to the change in current from the power supply, making internal voltage regulation a useful feature in a high power amplifier. Internal voltage regulation is also used to control temperature variation that can cause erratic operation of the sensitive internal semiconductor circuitry.

LOAD VSWR AND REVERSE BIAS PROTECTION

Ideally, an RF amplifier with a 50 Ω output impedance will be connected to a perfectly matched load, i.e., with an impedance of 50 Ω, where all the power from the amplifier transmitted to the load without any reflected. However, in real applications, the load impedance can vary greatly from the output impedance of the amplifier, reflecting an excessive amount of power back and potentially damaging the amplifier. Some of the models in Pasternack's GaN SSPA family will withstand a 5:1 mismatch, with internal circuitry to protect the amplifier. Pasternack's GaN amplifier lineup also offers infinite load VSWR protection at all amplitude and phase angles, as well as reverse bias protection, where the unit will not enable or draw current if the $+V_{DC}$ bias and ground are switched.

MORE FEATURES

For digital communications applications, some of Pasternack's GaN PAs offer linear coded orthogonal frequency division multiplexing (COFDM) power output for multi-path propagation. CW operation is also available in some models, as well as RF input signal formats of CW, amplitude modulation (AM), phase modulation (PM) and pulsed. Hermetically sealed amplifiers are available for applications that are exposed to the elements.

Most systems impose many challenging requirements on a high power amplifier, considering the type of signal, mismatch effects, operating temperature, current and voltage control and other environmental factors. Pasternack's SSPA family offers multiple monitoring and protection systems to ensure the robustness of the amplifier design for long-term use and reliability (see ***Table 2***).

APPLICATIONS

The frequency coverage and high output power of Pasternack's family of GaN SSPAs make them ideal for military and other radar systems, military and commercial communications, air traffic control, weather and earth observation satellite and medical applications. Amplifiers with linear COFDM power output ability are excellent for unmanned aerial vehicle and unmanned ground vehicle (UAV/UGV) data links as well as COFDM video applications. Pasternack's GaN amplifier series can be used as high gain driver amplifiers and high gain, high output PAs.

VENDORVIEW

Pasternack
Irvine, Calif.
www.pasternack.com

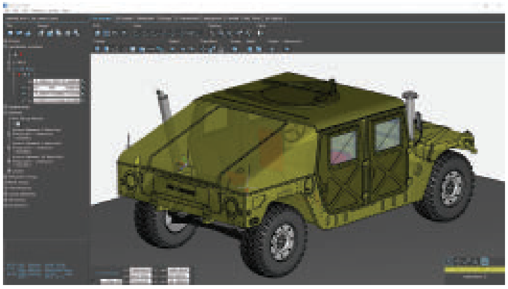

EMPIRE XPU 7.5: 3D EM Design Suite

IMST GmbH
Kamp-Lintfort, Germany

EMPIRE XPU is a 3D EM design suite for antennas, microwave circuits and components, EM chip design, medical applications and more. Since its original introduction to the market, it has been recognized as a key tool for the EM design of complex structures. The new release 7.5 follows that tradition with enhancements now able to handle structures up to hundreds of wavelengths in size.

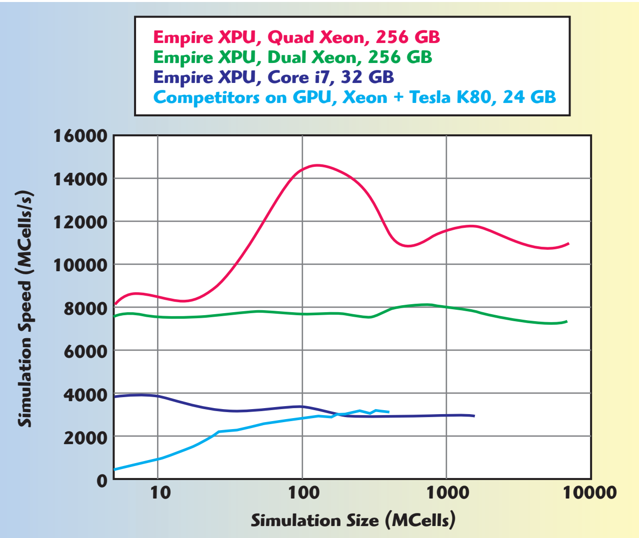

▲ *Fig. 1 FDTD simulation speed vs. simulation size for different processors (CPU and GPU).*

Aiming to be faster on CPUs than others on GPUs the EMPIRE XPU offers fast and accurate 3D EM and thermal simulations of complex RF build-ups and modules using off-the-shelf PC equipment. With this tool the time-to-market can be reduced to a bare minimum. Because of the high accuracy of the simulation results, prototype cycles are considerably shortened and hence development costs are reduced.

EMPIRE uses XPU technology, which is an IMST proprietary software acceleration technique specifically developed for running FDTD simulation on modern CPUs. A multiple time stepping algorithm enables the calculation of multiple FDTD time steps in the cache memory of the CPU. Just In Time (JIT) compilation ensures the best fitting code for both the hardware used and simulation model.

This combination increases the simulation speed drastically as it is no longer limited by the main memory interface. The whole RAM memory of the PC is now 'high-speed' accessible for the EM simulation. With this highly optimized kernel 3D EM simulations have seen processing rates of over 14 GCells/s on Intel Xeon workstations. ***Figure 1*** compares the simulation performance of the EMPIRE XPU on different workstations vs. GPU computing.

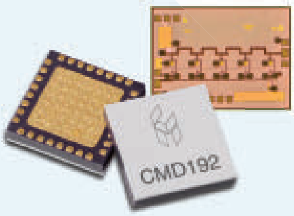
CMD192

INTUITIVE MODELING

One main feature of the EMPIRE XPU 7.5 release is a new 3D design modus with an enhanced modeling kernel and direct import and export options for all major 3D CAD formats. The 3D design mode allows intuitive modeling and supports unlimited local coordinate systems. It complements the 2D design mode with superior editing functionalities for planar multilayer designs. As data exchange between different software tools becomes more and more important, EMPIRE supports the import of EM simulation vendor projects.

To be as flexible as possible when it comes to the hardware for EM simulations, EMPIRE XPU 7.5 supports cloud computing. The Amazon Elastic Compute Cloud (EC2) can be easily directly accessed via an encrypted connection from the EMPIRE simulation control. Floating licenses can be used to perform simulations on every PC. The Amazon EC2 provides a large selection of instance types worldwide, fitting all simulation needs from small single core PCs up to large 64 core workstations with 2TB main memory.

To help customers support U.S. government compliance requirements, including the International Traffic in Arms Regulations (ITAR) and Federal Risk and Authorization Management Program (FedRAMP), Amazon offers an isolated AWS region designed to host sensitive data and regulated workloads in the cloud (AWS GovCloud US).

EMPIRE XPU 7.5 is well suited to designing highly integrated RF front ends at microwave frequencies. Front ends are a key component for K/Ka-Band satellite communications on-the-move, multimedia entertainment systems and 5G base stations as well as 60 GHz broadband home access equipment and backbone networks. Designing such complex modules were a real challenge in the past but not anymore with EMPIRE XPU.

As an example, the DBF Ka-Band/5G front end module (digital beamforming), which is shown in ***Figure 2*** is designed using EMPIRE XPU. Each front end consists of a low temperature co-fired ceramic (LTCC) module with an 8 × 8 patch antenna array on the underside (see ***Figure 3***), integrated active RF electronics and cooling system.

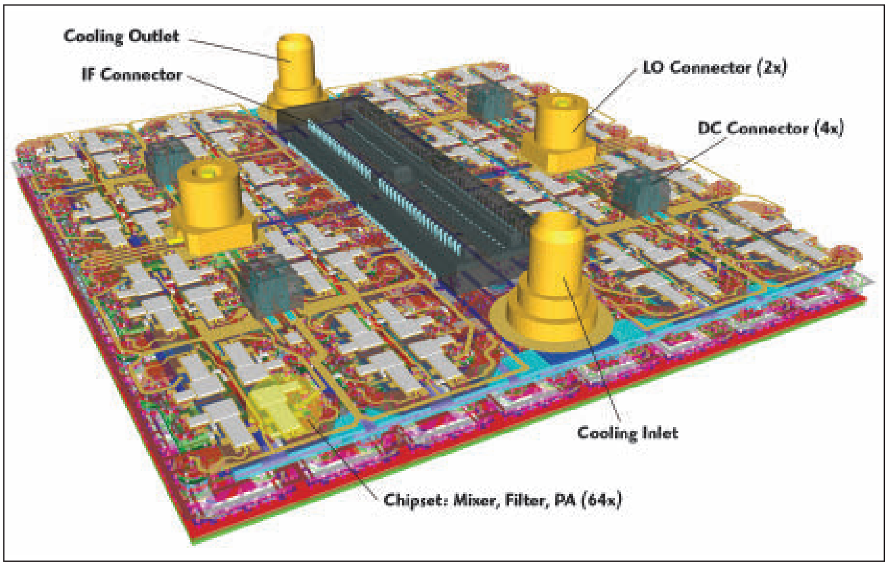

▲ *Fig. 2 RF circuit and interface side of Ka-Band 5G front-end module.*

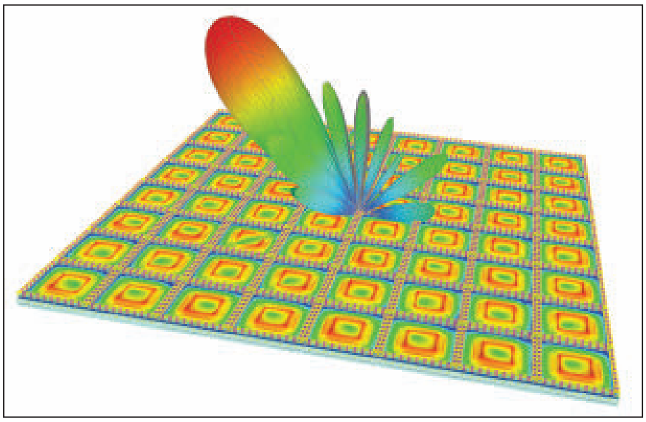

▲ *Fig. 3 Antenna side of Ka-Band 5G front-end module, showing electric near field and 3D far field.*

MODULAR APPROACH

A modular design approach is used to combine several modules for a larger array in order to fulfill the requirements dictated by the specific application. This modular approach requires a design where all RF and DC electronics including cooling must fit behind the antenna area. The antenna area for each patch element is limited by the antenna element spacing, which is half a wavelength. A larger distance between the antenna elements would degrade the antenna performance with respect to the sidelobe level, grating lobe level and scan range.

The antenna element area for this Ka-Band antenna design is 5 mm × 5 mm. This is a small space especially for a DBF antenna as each patch element needs its own chipset consisting of mixer, filter and PA with IF and DC connections to allow for amplitude and phase control at baseband level.

The design flow for this LTCC module started with the design of the patch antenna, the 90° hybrid circuit and the calibration network. Next, the RF chipsets were integrated together with the connectors on the top surface of the LTCC. The design of the LO network and the IF network was done afterwards. Finally, the antenna and the RF parts were integrated into one LTCC module.

It is important to simulate the complete module with a full wave 3D EM simulation tool to include all parasitic couplings between the different elements. Retuning of the LO network and some antenna paths were necessary to compensate for these parasitics. In addition to the RF characterization, the complete module simulation allows for layout errors such as shorts or open circuits to be checked. This simulation technique ensures a short turnover from design to manufacturing, even for such a complex design with more than 40,000 objects. The simulation of the complete LTCC module needs about 16 GB memory and a simulation time below two hours on a modern Intel Xeon workstation.

IMST GmbH
Kamp-Lintfort, Germany
www.empire.de

Rugged, Conduction-Cooled, COTS Digital Transceiver

Innovative Integration released the latest model in their family of digital transceivers, turnkey and commercial off-the-shelf solutions that integrate data logging, digital down-conversion (DDC), digital up-conversion (DUC) and spectrum analysis (FFT) in a compact system. The K706 digital transceiver has two antenna inputs and four independent channels of DDC, two channels of DUC and one spectrum analyzer embedded in a Xilinx Kintex-7 FPGA. It supports monitoring and recording of wideband or narrowband spectra or channelized IF band data. The system runs on a 64-bit Linux or Windows application. A touch screen is available, which is useful for custom wireless surveillance or SDR receiver instrumentation.

The analog front-end is modularized via an FMC site which, fitted with an FMC-1000, employs dual, 1 GHz, 14-bit ADCs and DACs. The product supports contiguous recording at 160 MBps to internal 1.8" SATA drives. Each DDC has its own programmable tuner, programmable lowpass filtering, gain control and decimation settings that support output bandwidth to 100 MHz. Data is packetized in the VITA-49 format, with accurate timestamps synchronous to an external PPS signal. Each DDC channel can be enabled and disabled on the fly, to conserve host computer storage and bandwidth. An embedded power meter monitors the input power to the ADCs, which allows analog gain control using optional, user supplied and external front-end devices.

The spectrum analyzer, which supports windowing, calculates the wideband spectrum of raw ADC data or the narrowband spectrum of the DDC output data at a programmable update rate. A programmable peak hold feature may be enabled to latch transient activity in the spectrum. The programmable threshold monitoring spectrum feature tracks spectral activities to 512 bins.

Innovative Integration
Camarillo, Calif.
www.innovative-dsp.com

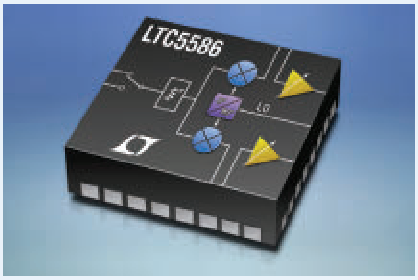

Wideband Zero-IF I/Q Demodulator Improves Receiver Performance

Linear Technology has developed a high linearity, I/Q demodulator with more than 1 GHz bandwidth and an operating frequency range from 300 MHz to 6 GHz. The LTC5586 is a true zero-IF design that demodulates wideband RF signals directly to baseband DC or low IF. It provides superior performance, with a calibrated OIP2 of 70 dBm and 70 dBc image rejection at 3.5 GHz. The LTC5586 was designed for wireless infrastructure equipment, such as base stations, microwave backhaul, software-defined radios (SDR) and other broadband receivers.

With a single network, the LTC5586's RF input is matched to 50 Ω from 500 MHz to 6 GHz, covering all the LTE bands and the emerging 4.5G and 5G bands at 3.6 and 5 GHz. An additional capacitor extends the match from 300 to 500 MHz. The demodulator includes an RF switch at the front end that directs one of two inputs to a programmable attenuator, controlled via the on-chip serial bus. The attenuator has a gain control range of 31 dB in 1 dB steps, allowing the receiver to accommodate a wide range of signal inputs. The demodulator consists of I and Q mixers, with their respective LO ports driven by a wideband quadrature phase shifter. After demodulation, two programmable amplifiers route the I/Q signals to external A/D converters. A maximum gain of 7.7 dB in 1 dB steps can be set by the serial port, enabling the output level to be optimized for the A/D converters. The LTC5586 also has built-in SPI tunability, allowing the demodulator to set its LO input to any frequency band from 300 MHz to 6 GHz with no external matching components.

VENDORVIEW

Linear Technology Corp.
Milpitas, Calif.
www.linear.com/product/LTC5586

CatalogUpdate

Real-Time Spectrum Analyzers

VENDORVIEW

Aaronia AG released a new eight-page, real-time spectrum analyzer short form catalog. The catalog features Aaronia's full lines of real-time spectrum analyzers (1 Hz to 20 GHz with 350 MHz real-time bandwidth), EMC and direction finding antennas (1 Hz to 40 GHz), RF drone detection systems (counter-UAV) and portable signal generators up to 6 GHz. Aaronia products are known worldwide for their affordability and high quality, and are made in Germany. Visit Aaronia's website for a free download and more information.

Aaronia AG
www.aaronia.de

New Product Catalog

VENDORVIEW

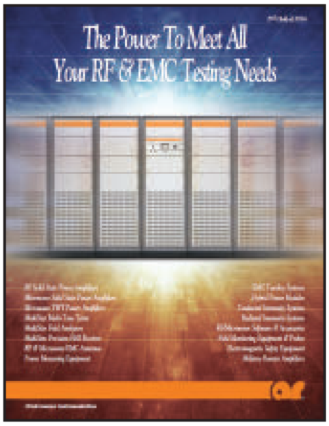

AR's comprehensive new catalog includes virtually everything necessary for RF and EMC testing. You'll find important information on RF/microwave amplifiers, antennas, probes, analyzers, accessories and integrated test systems that make testing quicker, easier and more accurate. Exciting new products include high power solid-state pulsed amplifiers and USB peak power sensors. Read about the company's new RF solid-state water cooled amplifiers with respective chillers, see photos of the expanded microelectronics lab and learn about AR Europe's new partnership with CETC41. Visit www.arworld.us/html/catalogRequest.asp to request a free download.

AR RF/Microwave Instrumentation
www.arworld.us

Small Cell DAS Solutions

VENDORVIEW

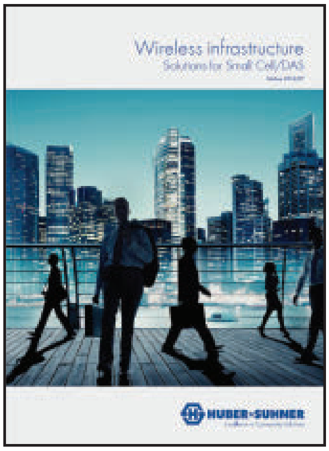

HUBER+SUHNER has published a Small Cell DAS Solutions Catalogue for the first time. Its broad knowledge in different technologies makes the Swiss Company the leading provider of interconnectivity solutions in the field of indoor and outdoor small cells and distributed antenna systems (DAS). The broad RF portfolio includes recently developed antennas and connections. The fiber optic part comprehends dedicated cable systems and transport solutions which allow operators and network providers a fast, easy and modular installation of small cell and DAS infrastructures.

HUBER+SUHNER
http://wirelessinfrastructure.hubersuhner.com

Filtering Solutions

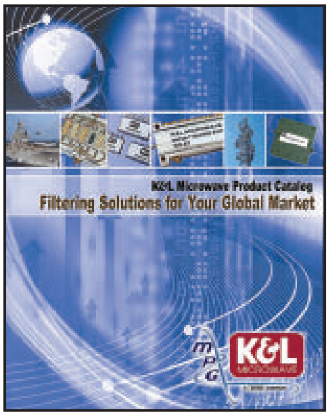

K&L designs and manufactures a full line of RF and microwave filters, duplexers and subassemblies, including ceramic, lumped element, cavity, waveguide and tunable filters. The catalog shows filter responses, loss calculations and standard packages for all products. K&L supplies many of today's most significant military and homeland security electronics programs. Applications include space flight, radar, communications, guidance systems and mobile radio base stations, as well as air traffic communication and control. Visit www.klmicrowave.com to download the complete catalog.

K&L Microwave
www.klmicrowave.com

Real-Time Spectrum Analysis

VENDORVIEW

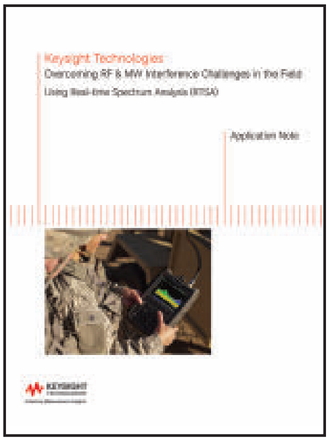

This application note covers practical strategies to overcome RF and microwave interference challenges in the field using real-time spectrum analysis (RTSA). Read about the different types of interference encountered in both commercial and aerospace defense (A/D) wireless communication networks. Uncover the drawbacks associated with traditional interference analysis and get an in-depth introduction to RTSA. Plus, see why this type of analysis is required to troubleshoot interference in today's networks with bursty and elusive signals.

Keysight Technologies Inc.
www.keysight.com/find/fieldfox

RF Power Selector Guide

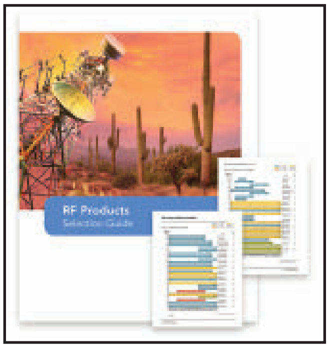

NXP's latest RF Power Selector Guide is now available at www.nxp.com/RFSelectorGuide. One fascinating new feature is the "RF Power Map" of products—to help customers find RF power solutions more easily. You can now choose the output power and frequency range from NXP's RF power products that meet design requirements for your applications. NXP offers RF power transistors for communication and industrial applications serving these markets: wireless infrastructure, industrial, scientific, medical (ISM) and broadcast, 2-way radio, aerospace and defense, cooking and low power.

NXP Semiconductors
www.nxp.com/RFSelectorGuide

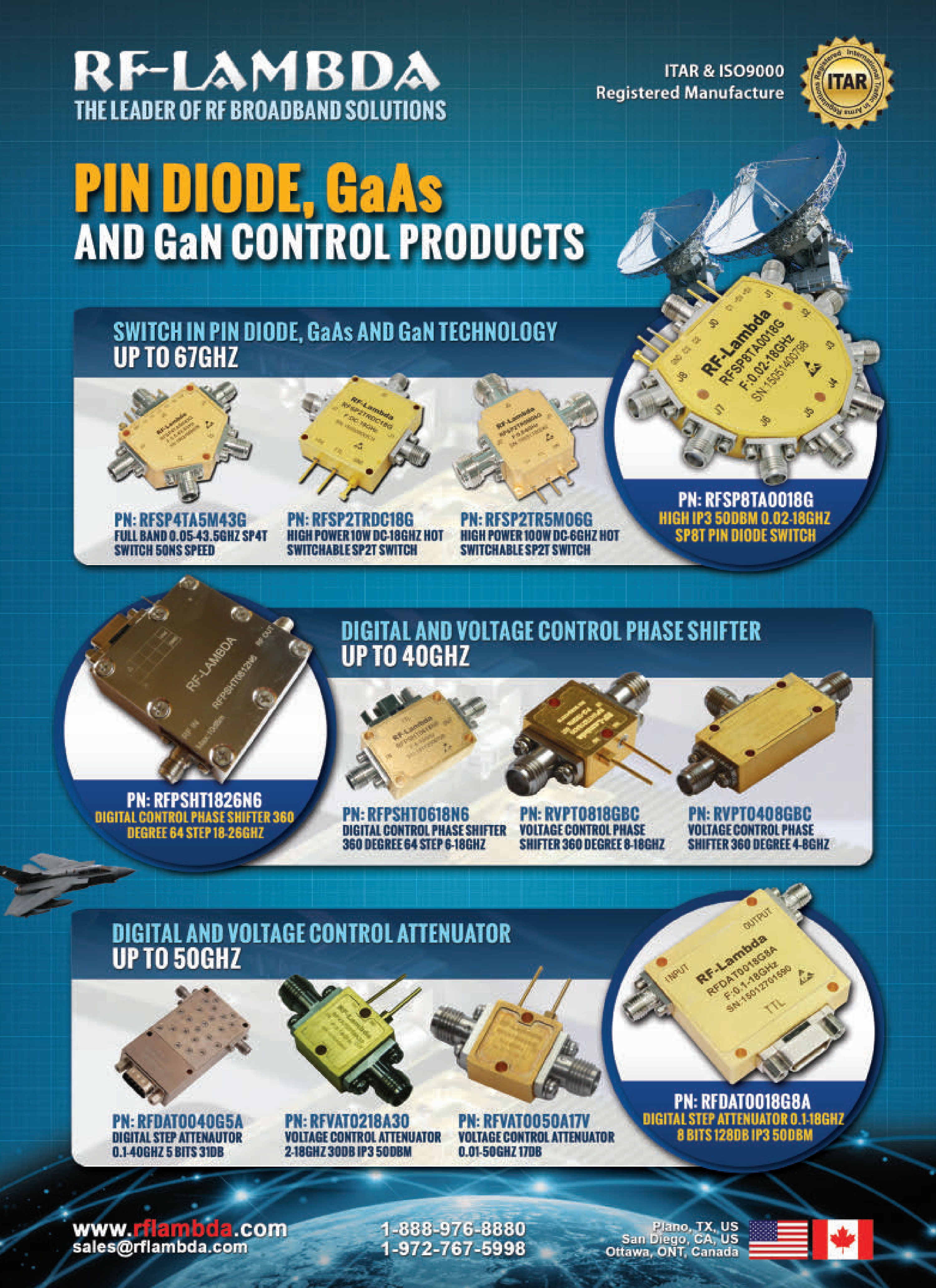
RF-LAMBDA
THE LEADER OF RF BROADBAND SOLUTIONS
ITAR & ISO9000
Registered Manufacture
ITAR
PIN DIODE, GaAs
AND GaN CONTROL PRODUCTS
SWITCH IN PIN DIODE, GaAs AND GaN TECHNOLOGY
UP TO 67GHZ
PN: RFSP4TA5M43G
FULL BAND 0.05-43.5GHZ SP4T SWITCH 50NS SPEED
PN: RFSP2TRDC18G
HIGH POWER 10W DC-18GHZ HOT SWITCHABLE SP2T SWITCH
PN: RFSP2TR5M06G
HIGH POWER 100W DC-6GHZ HOT SWITCHABLE SP2T SWITCH
RF-Lambda
RFSP8TA0018G
F:0.02-18GHz
PN: RFSP8TA0018G
HIGH IP3 50DBM 0.02-18GHZ
SP8T PIN DIODE SWITCH
DIGITAL AND VOLTAGE CONTROL PHASE SHIFTER
UP TO 40GHZ
RF-LAMBDA
PN: RFPSHT1826N6
DIGITAL CONTROL PHASE SHIFTER 360 DEGREE 64 STEP 18-26GHZ
PN: RFPSHT0618N6
DIGITAL CONTROL PHASE SHIFTER 360 DEGREE 64 STEP 6-18GHZ
PN: RVPT0818GBC
VOLTAGE CONTROL PHASE SHIFTER 360 DEGREE 8-18GHZ
PN: RVPT0408GBC
VOLTAGE CONTROL PHASE SHIFTER 360 DEGREE 4-8GHZ
DIGITAL AND VOLTAGE CONTROL ATTENUATOR
UP TO 50GHZ
PN: RFDAT0040G5A
DIGITAL STEP ATTENAUTOR 0.1-40GHZ 5 BITS 31DB
PN: RFVAT0218A30
VOLTAGE CONTROL ATTENUATOR 2-18GHZ 30DB IP3 50DBM
PN: RFVAT0050A17V
VOLTAGE CONTROL ATTENUATOR 0.01-50GHZ 17DB
RF-Lambda
RFDAT0018G8A
F:0.1-18GHz
PN: RFDAT0018G8A
DIGITAL STEP ATTENUATOR 0.1-18GHZ
8 BITS 128DB IP3 50DBM
www.rflambda.com
sales@rflambda.com
1-888-976-8880
1-972-767-5998
Plano, TX, US
San Diego, CA, US
Ottawa, ONT, Canada

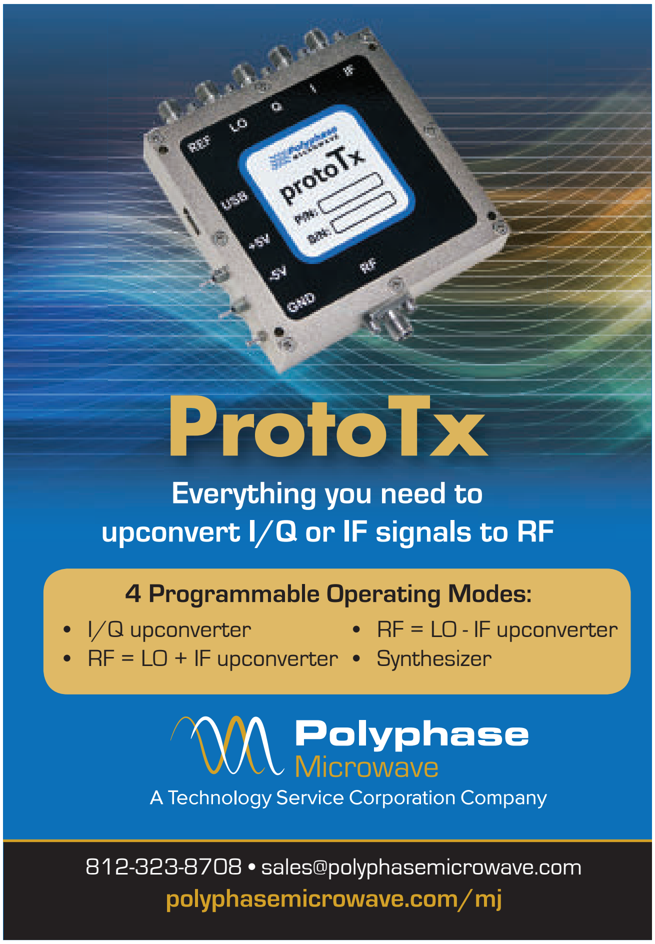

CatalogUpdate

Test & Measurement Catalog

VENDORVIEW

The 2016 Rohde & Schwarz Test & Measurement Catalog features more than 200 pages of information about instruments, systems and software. It includes a short description and photos of each product, the most important specifications and ordering information. You can download this catalog as a PDF from the Rohde & Schwarz website or order from customer support (order number: PD 5213.7590.42, version 06.00) Rohde & Schwarz offers a broad spectrum of solutions for the newest wireless technologies as well as for RF/microwave applications up to 500 GHz.

Rohde & Schwarz GmbH & Co. KG
www.rohde-schwarz.com

Phase Adjuster Handbook

Spectrum's precision phase adjusters, also called phase shifters, allow the adjustment of the electrical separation between components. A precision mechanical movement provides for smooth and accurate adjustment over the entire frequency range. A secure locking mechanism is furnished with every unit. A wide selection of components is available, offering different mechanical configurations, frequency ranges, electrical lengths and many different connector configurations. Frequency ranges are DC to 2 GHz, DC to 12.4 GHz, DC to 18 GHz, DC to 26.5 GHz, DC to 40 GHz, DC to 50 GHz and DC to 63 GHz.

Spectrum Elektrotechnik GmbH
www.spectrum-et.org

4.3-10 The Future is Now

VENDORVIEW

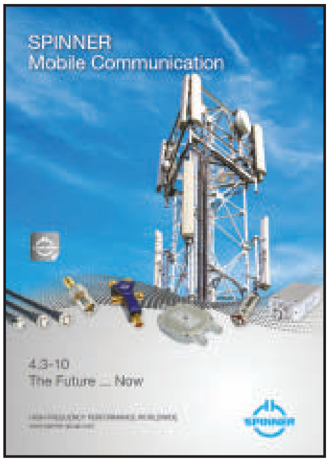

There can be no doubt that the 4.3-10 connector system belongs to the future of mobile communication. The first 4.3-10-based equipment has already been rolled out, and SPINNER has been supplying related components for on-site installation and in-building projects since early 2015. And now the third edition of their 4.3-10 product catalog is available and ready for downloading. Get it and check out their latest 4.3-10 portfolio as well as ways to customize your products with 4.3-10 and other interfaces.

SPINNER GmbH
www.spinner-group.com

NEW PRODUCTS

FOR MORE NEW PRODUCTS, VISIT WWW.MWJOURNAL.COM/BUYERSGUIDE
FEATURING VENDORVIEW STOREFRONTS

COMPONENTS

High Performance S-Band Cavity Filter

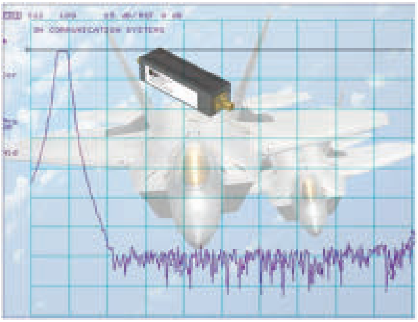

3H's new S-Band Cavity bandpass filter offers low in-band insertion loss of <0.5 dB over a 95 MHz bandwidth while rejecting frequencies with >90 dB attenuation out to 9 GHz. The filter size is 3.58" × 1" × 1". Meets Mil-Std-202 conditions. For more information contact: sales@3hcomm.com or call 949-529-1583.
3H Communication Systems
www.3Hcommunicationsystems.com

Space Qualified Items

Experience and heritage are of great importance when providing products for space programs. Dow-Key Microwave, with nearly 150 designs found on over 100 space vehicles is a manufacturing leader in space qualified items. Dow-Key supplies waveguide products focusing on compact, lightweight and cost effective designs with superior RF performance and power handling capability. Now, nearly all of their waveguide switches can be supplied in either "C" or "R" configurations for use in complex switching systems.
Dow-Key Microwave
www.dowkey.com

Digital Step Attenuator

DS Instruments introduced the DAT64H, a compact but full featured RF step attenuator that covers 100 MHz to 12 GHz. The minimum step size is 0.5 dB. Attenuation can be manually via front panel controls, or remotely programed from a PC over the range of 0 to 31.5 dB with USB SCPI commands. Typical insertion loss at 10 GHz is 10 dB. Maximum input power is +23 dBm. The DAT64H has a complete front panel user interface displaying current attenuation value and confirming device settings.
DS Instruments
www.dsinstruments.com

RF Power Combiners

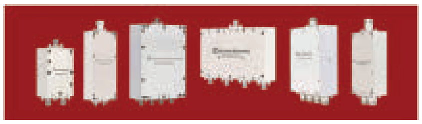

Fairview Microwave, a provider of RF, microwave and millimeter wave products, introduced high power RF power combiners with functionality up to 6 GHz and a low VSWR of up to 1.3:1. These combiners are excellent for amplifier systems and amplifier power combining by offering a low insertion loss that minimizes power dissipation through the combiner for a more ideal combined signal at the output.
Fairview Microwave
www.fairviewmicrowave.com

Surface Mount Highpass Filters

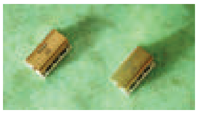

The new surface mount highpass filters with 3 dB cutoffs range from 6 to 18 GHz. These high performance parts produce extremely wide bandwidths in a surface mount package with an excellent match over the entire passband. The parts share common sizes and land patterns making them interchangeable on a patterned PCB.
Knowles DLI
www.knowlescapacitors.com

Bias Tees

VENDORVIEW

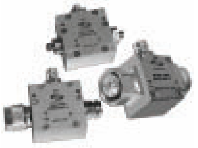

High power (7 amp), bias tees that cover VHF to S-Bands also lower power models covering UHF to E-Band. Available in 2.92 mm, SMA, 7/16 DIN, N, BNC & TNC configurations plus custom solutions. Weatherproof IP 65/67 available. Made in the U.S. with 36-month warranty.
MECA Electronics Inc.
www.e-MECA.com

YIG-Tuned Filters

Micro Lambda Wireless Inc. announced the production release of YIG-tuned filters with field replaceable RF connectors covering the frequency range up to 26.5 GHz. First models released are the MLFRC- 42026 and the MLFRC-46026. However, this technique can be applied to other model series packages including the 1", 1.4", 1.7" and 2" size packages. The standard models operates over the 0° to +65°C temperature range, but Military versions covering -40° to +85° C are available on special order.
Micro Lambda Wireless Inc.
www.microlambdawireless.com

Voltage Variable Attenuators

VENDORVIEW

Pasternack, a provider of RF, microwave and millimeter wave products, introduced an all new line of voltage variable attenuators offering up to 60 dB of attenuation across broad frequencies from 400 MHz to 18 GHz. This line of voltage variable attenuators is most commonly deployed in applications such as electronic warfare, instrumentation, point-to-point and point-to-multipoint radios, fiber optic and broadband telecom, microwave radio and VSAT, military radios, radar, ECM, SATCOM and sensors, and R&D.
Pasternack
www.pasternack.com

Pin Diode Attenuator

VENDORVIEW

PMI Model PDVAN-6012-60-8 is an 8-bit programmable 60 dB pin diode attenuator with

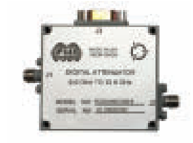

step resolution as low as 0.25 dB over the frequency range of 6 to 12 GHz. Features include SMA female connectors, 15 Pin Subminiature D (Male) with supplied mating connector and 8-Bit TTL compatible. Unit size is 2" × 1.8" × 0.5".

Planar Monolithics Industries Inc.
www.pmi-rf.com

High Performance SPDT Switch with SC Connectors

RelComm Technologies introduced high performance SPDT switch configured with 'SC' type connectors with excellent RF performance up to 6 GHz. Power rating is 1250 W CW to 1 GHz and 500 W CW to 6 GHz. The relay measures 3.5" in width with a depth of 1" and is less than 2.4" tall. It is fitted with standard eyelet terminals for ease of wire up. This switch is fully RoHS compliant and available in either failsafe or latching configurations.
RelComm Technologies Inc.
www.relcommtech.com

New**Products**

Coaxial SP2T Switch

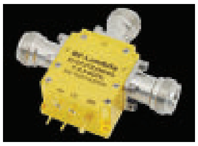

Features include wide band operation 0.5 to 6 GHz, an included TTL compatible driver, fast switching speed 50 ns, low insertion loss and high isolation and temperature range -45° to +85°C . Customization is available upon request. Hermetically sealed packages up to 60,000 ft are also available upon request.

RF-Lambda USA
www.rflambda.com

High Power Cavity Filters

RLC Electronics is currently manufacturing high power cavity filters for military and commercial applications. Filters can accommodate any high power connector desired, including but not limited to N, SC, HN or 7/16. The benefits of this type of filter include sharp attenuation, low loss and consistent performance from unit-to-unit. The unit pictured above is a 1280 MHz bandpass filter with 65 dB rejection at 1000 and 1800 MHz. The filter is rated for 400 W avg and 2000 W CW (20% duty cycle) and exhibits low loss (0.3 dB).

RLC Electronics Inc.
www.rlcelectronics.com

E-Band Third Harmonic Mixer

VENDOR**VIEW**

Model SFH-7039030318-12KFSF-S1 is an E-Band third harmonic mixer. The mixer is designed with high performance GaAs Schottky diodes to provide mixing at 3× LO frequency to cover the RF frequency range from 70 to 90 GHz. The low LO frequency makes this mixer well suited for low cost E-Band system solutions with an LO frequency range of 23.33 to 30 GHz. The mixer provides 17 dB conversion loss and 30 dB LO to IF isolation.

SAGE Millimeter
www.sagemillimeter.com

CCT-49K Family

The CCT-49K is an internally terminated broadband 40 GHz, latching multi-throw, electromechanical coaxial switch designed to switch a microwave signal from a common input to any of 3 to 6 outputs. The characteristic impedance is 50 Ω and incorporates 2.92 mm high performance connectors. Internal terminations provide an impedance match for the unselected ports. The new CCT-49K series expands Teledyne's switching line card to frequencies as high as 40 GHz.

Teledyne Relays
www.teledynerelays.com

CABLES & CONNECTORS

Corrosion Resistant RF Connectors

The Pisces waterproof connector range is now manufactured in nickel aluminum bronze, a high strength alloy with superior corrosion resistance that does not require plating for environmental protection. This material has a highly-durable non-reflective surface, provides a high level of corrosion resistance, is inherently resistant to erosion in desert type environments and provides high resistance to sand and dust. Typical applications include video and communications systems, industrial control (SCADA) systems, military radar systems, nuclear and chemical systems, marine and naval systems.

Intelliconnect
www.intelliconnect.co.uk

110 GHz Cable Assemblies

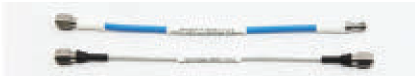

MegaPhase offers its Mega110 products with 1 mm connectors in both semi-rigid and flexible cable assemblies. Their lightweight 110

NewProducts

GHz cable assemblies are specifically designed for the demands of high-bandwidth applications such as automotive radar, probe stations and mobile backhaul.
MegaPhase
www.megaphase.com/rf/110

One-Step Connectors

SGMC Microwave's new one-step connectors have "captivated" center contacts offering excellent performance up to 65 GHz (usable up to 67 GHz). Assembly is as simple as trimming the cable and then inserting it into the body for soldering. Features include: DC to 65 GHz, VSWR: 1.25:1 max. per connector; 24" flexible cable assembly produced 1.34:1 max VSWR to 65 GHz; 8" semi-rigid cable assembly produced 1.21:1 max VSWR to 65 GHz; captivated center contact (beryllium copper, gold plated) and body components (corrosion resistant type 303 stainless steel, passivated).
SGMC Microwave
www.sgmcmicrowave.com

Coaxial Cable Assemblies and Connectors

SV Microwave offers a variety of mmWave coaxial cable assemblies and connectors for 5G mobile communication development and production. Their high frequency (26 GHz and beyond) push-on and threaded RF connectors offer industry leading signal fidelity in the 5G frequency spectrum and unique packaging designs for high density requirements including in house tape and reel. Let SV Microwave be your partner in 5G product development enabling the Internet of Things (IoT) revolution.
SV Microwave
www.svmicrowave.com

AMPLIFIERS

Remote Gain Control Amplifier

This product covers a frequency range of 0.1 to 27 GHz, 40 dB of gain, +20 dBm output with remote gain adjust of 15.5 dB (.5 dB LSB). It comes with IU rack mount as well. Needs Ethernet/LAN access. 90 to 250 VAC input.
Advanced Microwave Inc.
www.advmic.com

TWT Amplifier

The Model 176 TWT amplifier has been designed specifically to operate pulsed traveling wave tubes in the 1 to 2 kW peak power range at frequencies up to 18 GHz. Particular emphasis has been placed on the generation of the output RF pulse shape without the use of RF switches. Pulse width control is with an external pulse. Internal power supplies are DC to DC converter designs with fast loop response times so that output level variations are minimal for any PRF including a non-periodic or burst type PRF.
Applied Systems Engineering Inc.
www.applsys.com

Solid-State Pulsed Amplifiers

VENDORVIEW

There is now a very attractive alternative to Traveling Wave Tube Amplifiers (TWTA) for automotive and military EMC radiated immunity susceptibility testing, as well as radar and communication applications. AR's new offerings include the following frequency ranges: 1.2 to 1.4

New**Products**

GHz, 2.7 to 3.1 GHz, 1 to 2 GHz and 2 to 4 GHz. Output levels range from 1 to 150 kW. Designs can also be tailored to suit your specific application. Numerous applications include, but are not limited to automotive, MIL STD 464, DO-160 and military radar.

AR RF/Microwave Instrumentation
www.arworld.us/pulsedamps/

Solid-State RF PA Module

VENDOR**VIEW**

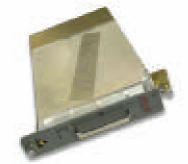

High efficiency, high power and compact with proven GaN technology. Can be easily combined to create high power C-Band radar transmitters. CPI BMD's solid-state power amplifiers are reliable, highly efficient and easy to maintain. The VSC3644 solid-state power amplifiers are designed for use in maritime surveillance and weather radar transmitters and cover 5.2 to 5.9 GHz. GaN transistors are combined into a 1.1 kW output and are air cooled.

Communications & Power Industries
Beverly Microwave Division
www.cpii.com/BMD

X-Band Solid-State PA Module

COMTECH PST introduced another new gallium nitride (GaN) amplifier for X-Band applications. This class AB linear design operates over the full 9 to 10 GHz frequency range and is ideal for use in phase array radar applications, as a TWT replacement or for a microwave communication link. The amplifier features phase and amplitude control, internal DC to DC converters and DC filtering, PA self-test and LED fault indications, unique waveguide coupling circuits, an internal isolator and digital control via a magic tee.

COMTECH PST
www.comtechpst.com

Solid-State RF Amplifier Module

VENDOR**VIEW**

Exodus introduced the AMP1071 - a solid-state RF amplifier module covering the entire ultra-wide 2 to 20 GHz frequency range instantaneously at 20 W CW minimum. Using state-of-the-art GaN devices, the AMP1071 operates from a 32 VDC source at less than 10A consumption. This module is suitable for use with all single channel modulation standards and applications requiring high power and ultra-wide band coverage. It has built-in protection circuits, high reliability and ruggedness. Typical applications include high power testing, EMI/RFI, EW and communications and jamming.

Exodus Advanced Communications
www.exoduscomm.com

Low Noise Amplifier

VENDOR**VIEW**

Mini-Circuits' ZX60-83LN+ is a wideband low noise connectorized amplifier providing a

unique combination of low noise figure, high IP3 and flat gain over a very wide frequency range, supporting a wide range of sensitive, high-dynamic range receiver applications and many systems where high performance over wideband is needed. This design operates on a single 5 or 6 V supply and comes in a rugged, compact unibody case (0.74" × 0.75" × 0.46") with SMA connectors, making it an excellent candidate for tough operating conditions and crowded system layouts.

Mini-Circuits
www.minicircuits.com

50 W GaN Amplifier

VENDOR**VIEW**

Richardson RFPD Inc. announced the availability and full design support capabilities for a new 2.8 to 3.2 GHz 50 W GaN amplifier from Qorvo. The QPA1000 is a high-power, S-Band amplifier fabricated on Qorvo's QGaN25 0.25 µm GaN on SiC production process. Covering 2.8 to 3.2 GHz, the QPA1000 provides greater than +47 dBm of saturated output power and greater than 24 dB of large-signal gain, while achieving more than 58 percent power added efficiency.

Richardson RFPD
www.richardsonrfpd.com

SOURCES

Surface-Mount Frequency Synthesizer

The THOR-7500-XA is a 6 to 7.5 GHz frequency synthesizer designed for an Airborne

RF Jammer that operates under extreme vibration and shock conditions. The design also features low phase noise (<- 95 dBc/Hz at 100 KHz) and fast switching capability (<300 µSec. band-edge to band-edge) critical for signals intelligence applications. The THOR-7500-XA also locks to a ±5 ppm stability and contains a channel step size of 500 KHz, +15 dBm output power, -60 dBc spurs and -25 dBc harmonics.

EM Research Inc.
www.emresearch.com

Internally Phase Locked Oscillator

VENDOR**VIEW**

New EDPLO-3030 series Internally Phase Locked Oscillator series covers single

frequencies of 30 MHz to 50 GHz with an output power up to +25 dBm, manufactured in a 2.25" × 2.25" × 0.65" low profile housing. The units are single biased with +12 VDC generating frequency

eLEARNING center

Presented by: Microwave Journal

Scan page using layar app

October Short Course Webinars

Keysight in Aerospace/Defense
Real-Time Recordings and Post-Processing of Wide-Bandwidth EW Signals
Live webcast: 10/11/16

Technical Education Training
VCO Fundamentals
Sponsored by: Mini-Circuits
Live webcast: 10/12/16

Technical Education Training
Innovative Passives and Substrates Enable RF Power Amplifier Designs for Cooking Applications
Sponsored by: Rogers Corp.
Live webcast: 10/13/16

Technical Education Training
Preparing for the Autonomous Car: Developing a 5G Network and Integrating Sensors
Sponsored by: IDT
Live webcast: 10/19/16

Technical Education Training
Millimeter Wave PA
Sponsored by: National Instruments/AWR
Live webcast: 10/25/16

Register to attend at mwjournal.com/webinars

Past Webinars On Demand

Technical Education Training Series

- On the Road to 5G, Advances in Enabling Technology: A Materials Perspective
- Vector Network Analyzers as a Tool for Signal Integrity in High Speed Digital Systems
- SiGe and RF SOI for Sub-6 GHz LNA Applications
- The Promise and Perils of mmWave
- Specifying Flexible Building Blocks for Automated Production Test Systems
- Improving Base Station Design – RF Innovations
- The Power of Testing IoT Devices in All Phases of the Product Lifecycle
- Radar Signal Generation with up to 2 GHz Bandwidth for Single-Channel and Multichannel Receiver Testing
- Faster Analysis of Complex RF Signals
- 802.11ax – High Efficiency Wireless Improving User Throughput in Dense User Environments
- Practical Antenna Design for Advanced Wireless Products
- Expanding the Possibilities of Cellular Wireless Infrastructure with GaN
- Designing Next-Gen Cellular and Wi-Fi Switches Using RF SOI Technology
- Improving Reliability and Efficiency with Solid State Spatial Combining Technology
- Effect of Conductor Profile Structure on Propagation in Transmission Lines

RF/Microwave Training Series

Presented by: Besser Associates

- Introduction to Radar
- Mixers and Frequency Conversion

Innovations in EDA

Presented by: Keysight Technologies

- How to Design Phased Arrays for 5G, Radar and Satellite
- Advances in High Power RF Design

Keysight Technologies Webcast

- LTE in the Unlicensed Spectrum

Keysight RF and Microwave Basics Education Series

- Simulating, Generating and Analyzing Custom-Modulated Satellite Signals

Keysight FieldFox Series

- Wireless Site Survey, Spectrum Monitoring and Interference Analysis

New**Products**

stability of ±0.8 ppm over -40° to +70°C with 1 minute warm-up time and only 100 mA surge current over the steady state. Typical phase noise for 18.5 GHz is -105 dBc/Hz at 1 KHz and -115 dBc/Hz at 100 KHz offset.

Exodus Dynamics
www.exodusdynamics.com

Full Octave VCO

VENDORVIEW

RFMW Ltd. announced design and sales support for Qorvo's RFVC6405 voltage controlled oscillator. The RFVC6405 covers the full 2 to 4 GHz (S-Band) in a single device with exceptional performance. Output phase noise is -90 dBc@10K offset (typ.) with second harmonic suppression of -15 dBc. With an output power of 0 dBm, the RFVC6405 draws 25 mA from a 5 V supply. Tuning voltage is 0 to 16 VDC. This Qorvo VCO is housed in a 0.5"×0.5" castellated package and operates over a temperature range of -40° to +85°C.

RFMW Ltd.
www.rfmw.com

Phase Locked Ultra-Low Noise Signal Sources

Synergy Microwave Corp. introduced a series of ultra-low phase noise, fixed-frequency, phase-locked DRO oscillators (PLDRO). The KS-FLOD1280-12-1280 is a 12.8 GHz fixed frequency source which, when locked to a low noise reference at 1200 MHz, will deliver exceptional phase noise of -96 dBc/Hz at 100 Hz offset and -158 dBc/Hz at 10 MHz offset. This source is packaged in a 2.25" × 2.25" module housing and includes lock alarm. Options are available to 15 GHz and extendable to 30 GHz.

Synergy Microwave Corp.
www.synergymwave.com

MATERIALS/PACKAGING

Mini-JLT GPSDO

Jackson Labs Technologies Inc. has upgraded its Mini-JLT GPSDO 10 MHz reference and several other products with an 8th-generation GNSS timing receiver that today allows receiving Galileo signals as well as concurrent GPS, GLONASS, and BeiDou signals. Galileo will provide higher performance, and concurrent GNSS reception will allow operation in urban canyons, under foliage and indoors. Various low phase-noise 10 MHz and 1 PPS signals as well as position/velocity information are generated by these GNSDOs.

Jackson Labs Technologies Inc.
www.jackson-labs.com

TFLE

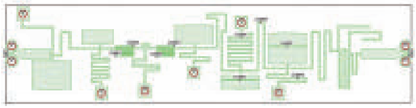

The Microwave Products Group has launched a new K&L Microwave® brand Thin Film Lumped Element (TFLE) product line utilizing sputtering deposition on Alumina to realize designs supporting fractional bandwidth beyond the range typically associated with quarter-wavelength edge-coupled lines. The figure shows a bandpass filter centered around 4 GHz with 60% relative bandwidth. The main coupling line has inductors and capacitors, making the skirts nearly linear. A clean-up lowpass reduces spurious up to 23 GHz. The PWB measures 0.85"L × 0.204"W × 0.02"H.

K&L Microwave
www.klmicrowave.com

Low Viscosity Epoxy

Ideal for encapsulation, bonding and sealing applications, Master Bond EP30Med offers excellent electrical insulation properties and exceptionally low shrinkage upon cure. It is a two component, room temperature curing biocompatible epoxy adhesive designed for high performance medical device applications. It features high bond strength, superior durability, outstanding resistance chemicals as well as cold sterilants, EtO and gamma radiation. It also meets FDA requirements for indirect food contact as per FDA CFR 175.105.

Master Bond
www.masterbond.com

Metalized Ceramic and Glass-to Metal Packaging

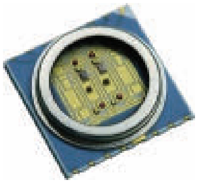

Remtec Inc. has merged its metalized ceramic packaging capabilities with the glass-to-metal packaging capabilities of parent company, LTI. The expanded product offerings for Remtec and LTI include sensors for industrial accelerometers, fluid analyzers, liquid and gaseous flow meters, thermal conductivity measurement, sensing flow and content of liquids in corrosive environments, printed biosensors, medical instrumentation, optical detectors for tissue properties, x-ray imaging sensors for dental instrumentation and wireless sensors.

Remtec Inc.
www.remtec.com

New**Products**

ANTENNAS

Ceramic Patch Antennas

VENDORVIEW

MCV GPS, GlobalStar, Glonass ceramic patch antennas offer precision and high gain along with a wide band PIFA chip antenna covering 698 to 960 MHz and 1700 to 2700 MHz for 3G/4G applications. MCV VHF/UHF and LTE MIMO DAS antennas are ideal for base station and indoor/outdoor repeater. Metamaterial antenna can effectively isolate Wi-Fi frequency from LTE bands.

MCV Microwave
www.mcv-microwave.com

ISM Band Panel Antenna

VENDORVIEW

Southwest Antennas announced the release of a new small form factor panel antenna designed specifically for IEEE 802.11g/n Wi-Fi or other ISM applications in the 2.4 to 2.5 frequency band. The antenna is designed to handle up to 10 W of RF input power, has a maximum gain of 7.8 dBi, and is vertically polarized. Measuring only half an inch thick, this antenna is ideal for use as a stand-alone solution for providing Wi-Fi/ISM band coverage within a building or other structure while remaining unobtrusive.

Southwest Antennas
www.southwestantennas.com

TEST EQUIPMENT

Dielectric Rod Tester

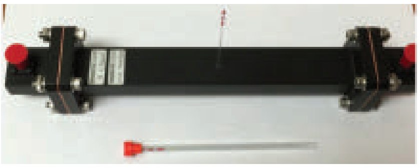

DI announces its ASTM compliant dielectric rod tester measurement systems. These systems allow one to measure dielectric constant and loss tangent properties of small diameter rods according to ASTM standard D2520 Parts B and C over the waveguide frequency bands from 1.7 to 40 GHz comes with one or more fixtures, test samples, carrying cases, user's guide, test data and instrument control/data processing software for common network analyzers.

Damaskos Inc.
www.damaskosinc.com

Built-In Spectrum Analyzer

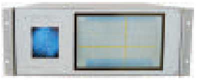

DEV Systemtechnik, a Quintech company, announces that its ARCHIMEDES L-Band matrix switch now comes with an Integrated Spectrum Analyzer (ISA) option, which offers cable head end operations managers even more key features and benefits. The ARCHIMEDES L-Band matrix switch with ISA gives operators the ability to easily and flexibly analyze their RF and satellite signals via a Graphical user interface over Ethernet, or the ARCHIMEDES' multi-touch display. This new option for the ARCHIMEDES distributing matrix can be integrated to meet customer requirements.

DEV Systemtechnik
www.dev-systemtechnik.com

RF Multiplexer Switch Module

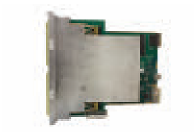

The GX6864 from Marvin Test Solutions is a 500 MHz, 75 Ω RF multiplexer switch module for high I/O count, video switching/test applications. Like other GENASYS switch cards, the GX6864 is compatible with the MAC Panel 6U SCOUT receiver and offers "cable-less" connection to the receiver connectors - eliminating the need for cable harnesses and the reliability issues that come with cabled solutions. The result is a design that is cost-effective, reliable and maintainable.

Marvin Test Solutions Inc.
www.marvintest.com

Radiation Measurement System

The RMS-0740 portable, compact radiation measurement system enables wireless developers to measure (antenna) radiation patterns and TRP of RF devices from 700 MHz to 4 GHz. It consists of a turntable and a measurement unit and is optimized for measuring devices without the need for an anechoic chamber. Devices can be measured stand-alone in constant carrier mode, and a separate generator output allows for full characterization and frequency sweep of custom antennas and prototypes.

MegiQ
www.megiq.com

N-type Calibration Kit

The Compact N-type calibration kit is specially designed for fine-tuning in production environments and quality testing facilities using 50 Ω N-type connectors from DC to 6 GHz. This kit meets all the required calibration standards (open, short, load) in one unit, which enables it to comfortably handle the calibration of VNAs, especially in the field. The standard kit includes an N-type (male) open-short-load. Features include a return loss: load < -38 dB and phase deviation (open, short) < 1.5°.

Withwave
www.with-wave.com

IEEE MTT-S

IMS
Connecting Minds. Exchanging Ideas.

2017 INTERNATIONAL MICROWAVE SYMPOSIUM

4 – 9 JUNE 2017 HONOLULU, HAWAI'I

CALL FOR PAPERS

COME JOIN US IN HONOLULU AND ENJOY THE FLAGSHIP MICROWAVE THEORY AND TECHNIQUES SOCIETY (MTT-S) CONFERENCE IN THE ALOHA STATE OF HAWAI'I

PHOTO BY NEAL MIYAKE

The IEEE Microwave Theory and Techniques Society's 2017 International Microwave Symposium (IMS2017) will be held 4 - 9 June 2017 at the Hawai'i Convention Center in Honolulu, Hawai'i as the centerpiece of Microwave Week 2017. IMS2017 offers technical sessions, interactive forums, plenary and panel sessions, workshops, short courses, industrial exhibits, application seminars, historical exhibits, and a wide variety of other technical and social activities including a guest program. As usual, the Microwave Week 2017 technical program also comprises the RFIC Symposium (**www.rfic-ieee.org**) and the ARFTG Conference (**www.arftg.org**).

With over 8000 participants and 500 industrial exhibits of state-of-the-art microwave products, Microwave Week is the world's largest gathering of radio-frequency (RF) and microwave professionals and the most important forum for the latest research advances and practices in the field. IMS2017 offers something for everyone:

- The first-ever IMS Hackathon and IMS 3-Minute Presentation Competitions
- A 5G Summit showcasing next-generation wireless technologies
- An Executive Forum to discuss the latest in 5G and Internet of Things (IoT)
- RF Boot Camp – a three-quarter day course on RF/microwave basics
- The first-ever IMS Exhibitor Workshops for exhibitors to present the technology behind their products
- Networking events for Young Professionals and Women in Microwaves
- Student Design, Student Paper, Best Industry Paper, and Best Advanced Practice Paper Competitions
- Project Connect for under-represented minority engineering students, and the PhD Student Initiative for new PhD students
- *Teaching that inspires...students that aspire* – an exciting STEM program exposing middle school and select high school students, as well as their teachers, to RF/microwave technology

IMS2017 will include a comprehensive portfolio of events featuring recent 5G developments, including a plenary session, focus session, workshops, panel session, and a technology-development pavilion.

Paper Submission: Authors are invited to submit technical papers describing original work and/or advanced practices on RF, microwave, millimeter-wave, and terahertz (THz) theory and techniques. The deadline for submission is 5 December 2016. A double-blind review process will be used to ensure anonymity for both authors and reviewers. Detailed instructions on submitting a double-blind compliant paper can be found at **www.ims2017.org**. Papers will be evaluated on the basis of originality, content, clarity, and relevance to IMS.

Emerging Technical Areas: IMS2017 enthusiastically invites submission of papers that report state-of-the-art progress in technical areas that are outside the scope of those specifically listed in this Call for Papers, or that may be new to IMS, but are of interest to our attendees.

Workshops, Short Courses, Focus and Special Sessions, Panel and Rump Sessions: Topics being considered for these areas include Next-Generation Wireless Systems (5G and beyond), Internet of Space, Latest Technologies for RF/Microwave Measurements, and Advances in RFIC Technology. Please consult **www.ims2017.org** for a more detailed list of topics and instructions on how to prepare a proposal. Proposals must be received by 6 September 2016.

MicroApps and Exhibitor Workshops: The Microwave Application Seminars (MicroApps) serve as a forum for IMS exhibitors to present technology behind their commercial products and special capabilities. New for IMS2017 are Exhibitor Workshops, which offer IMS exhibitors a chance to present in-depth technical topics, via two-hour sessions, in a meeting room off the exhibit floor. Both presentation formats are open to all conference and exhibit attendees – MicroApps are free of charge and Exhibitor Workshops require a nominal fee. Please visit **www.ims2017.org** for details on submitting MicroApps and Exhibitor Workshop presentation ideas.

HAWAI'I 5G Catch the Wave!

Symposium Chairs
W. Shiroma (General Chair), K. Miyashiro (Co-Chair), V. Lubecke (Vice Chair)

Technical Program
O. Boric-Lubecke (Co-Chair), R. Miyamoto (Co-Chair), T. Itoh (Senior Advisor), A. Crahan (Administrator)

Electronic Paper Management
J. Hacker, M. DeLisio, S. Owens

Workshops and Short Courses
C. Hang, Y.-C. Shih, K. Leong, B. Wu, C. Song, L. Dunleavy, K. Hall, S. Kumar

Panel, Rump, Focus, and Special Sessions
C. Jackson, R. Kagiwada, A. Oki, T. LaRocca, Y. Wang, C. Rodenbeck

Interactive Forum
D. Bibb, G. C. Huang, R. Perron

Plenary Session and 5G Summit
V. Lubecke, D. Choudhury, T. LaRocca, D. Zuckerman

Technical Program Competitions
R. Gough, E. Yavari, X. Gao, A. Rahman, P. Orel, S. Rosenau, J. Bandler, E. Kiley

TPC At Large
J. Lin, H. Okazaki

Publicity, Promotions, and Publications
M. Watanabe, K. Kogasaka, J. Roque, A. Scacchitti

Website and Program Book
C. Brough, D. Goshi, M. Moorefield

Social Media
K. Cho, J. Hofer, M. Visitacion, J. Warner

Microwave Magazine
I. Mostafanezhad, A. Singh

Local Arrangements / Operations
J. M. Akagi, A. Noveloso, Z. Bardai, M. Tamamoto, J. T. Akagi, B. Lei, G. Uyeda, A. Ohta, A. Combs

Finance and Registration
D. Goshi, K. Leong, T. Fujishige, R. Alongi, N. Jordan

Student Volunteer Coordination
A. Morishita, J. Dang, T. Chun

Focus Groups
R. Pang, R. Iwami, B. Lei

Young Professionals
A. Zamora, K. Lu, W. Tonaki, T. Sharma, K. Allen

Women in Microwaves
C. Kitamura, J. Nakatsu, A. Pham, S. Yamada

STEM and Project Connect
C. Ishii, K. Matthews, D. Ah Yo, R. Mukai, A. Noveloso, K. Lau, G. Zhang

MicroApps and Exhibitor Workshops
J. Guzman-Vazquez, G. Uekawa, J. Weiler, B. Wu

Historical and University Exhibits
A. Combs, J. Hausner, J. Navarro, K. Sarabia

Global Ambassadors
K. Wu, D. Zimmerman

Conference and Exhibition Management
E. Vega, L. Wood, S. Horn, D. Waldron

Senior Advisors
T. Weller, S. Kanamaluru

Reader Recommendations

We recently asked our social media community to submit technology or marketing books they would recommend to colleagues. This month, rather than reviewing a single book, BookEnd is passing along these suggestions.

Antonio Fernández Sánchez, from the Granada area of Spain, recommends "Semiconductors and the Information Revolution," by John Orton. Sánchez writes, "In my opinion, one of the best books that will make you love semiconductor electronics. All you haven't learned at a university is here, explained in detail. Dense and great." The book covers the development of electronics by tracing the semiconductor materials and physics that have enabled the 70-year solid-state revolution, launched with the invention of the transistor in 1947.

Rick Pierson, the technical marketing manager at Efficient Power Conversion (EPC), recommends the three volumes EPC has authored on GaN and its use in power conversion systems: "GaN Transistors for Efficient Power Conversion" and the two supplements "Wireless Power Handbook" and "DC-DC Converter Handbook." Rick writes, "These textbooks provide power system design engineers basic technical and application-focused information on how to design more efficient power conversion systems using GaN-based transistors." Alex Lidow, CEO of EPC, a GaN evangelist and a co-author of the first volume, endorses Rick's recommendation of "GaN Transistors for Efficient Power Conversion," saying it "is a basic textbook on GaN transistors that I like."

While power conversion is not "pure" RF/microwave, it is an adjacent, high speed application. Companies pursuing GaN on Si for RF applications will likely benefit from the production volumes and attendant process maturity that the power conversion market will drive.

Semiconductors and the Information Revolution
Publisher: Academic Press
ISBN-13: 978-0444532404 (print)
Also available in e-book format
350 pages

GaN Transistors for Efficient Power Conversion, 2nd Ed.
Publisher: Wiley
978-1118844762
Also available in e-book format
266 pages

Wireless Power Handbook
Publisher: Power Conversion Publications
978-0996649216
Paperback
205 pages

DC-DC Converter Handbook
Publisher: Efficient Power Publications
978-0996649209
Paperback
200 pages

Asia Pacific Microwave Conference

5th - 9th December, 2016, New Delhi, India

The 2016 Asia Pacific Microwave Conference (APMC2016) will be held in New Delhi, India, from the 5th to 9th of December 2016. APMC2016 is supported by the IEEE MTT Society. It is also technically supported by European Microwave Association (EuMA). This symposium has been held since 1984 with first APMC in New Delhi, India. This year APMC is will be collocated with IEEE International Microwave and RF Conference (IMaRC).

The conference will cover the entire scope of microwave engineering, including RF/microwave, antennas & propagation and EMC/EMI. Prospective authors are invited to submit original papers on their latest research results. All papers presented at the conference will be submitted to IEEE Xplore for publication. Proposals for special sessions, workshops and tutorials are also solicited. All submissions have been subjected to a rigorous review by an international panel of reviewers. All accepted and presented papers will be available in electronic format (USB memory stick) and will be submitted to IEEE Xplore. Outstanding papers presented at APMC2016 will be awarded the APMC2016 Prize and the Best Student Paper award.

Around 480 papers were submitted to APMC 2016 of which 270 were selected. These will be presented at 38 oral sessions and 3 poster sessions from Dec 6 - 8, 2016. There will also be workshops and the very popular SIGHT (Special Interest Group on Humanitarian Technology) program including Amateur Radio demonstrations on Dec 5, 2016. The inaugural session on Dec 5, 2016 afternoon will feature three keynote addresses by well-known Experts in different areas. Additionally, IMARC 2016 will feature a few more sessions on Dec 8 -9 , focusing on areas such as biological effects and nanotechnology, which are 'non-standard' for the field of microwaves.

2016 marks an important year for Indian and global Industry as the Indian Govt. has announced a number of initiatives for manufacturing Industry like "Make in India", " Startup India" etc. As a part of the conference, we will be organizing a showcase exhibition which will be held in conjunction with the technical symposia and offers an excellent opportunity for all segments of the microwave community to meet. It is the synergy of the Exhibition in conjunction with the Technical Symposia for everyone involved in technologies associated with RF, microwave, millimeter wave, and THz frequencies. Some companies including the sponsors of APMC 2015 will exhibit the latest microwave products and technologies at this exhibition. Also, some exhibition booths will be provided for university to present their latest research outcomes.

Online registration is now open. Onsite registration will be available from Dec 5-9 , 2016. The registration area will be located on the conference venue Hotel Pullman, (Aerocity) New Delhi, India.

The Exhibition

APMC 2016 will feature an exhibition with many companies, universities and other organizations (from India and many other countries) demonstrating their products and research activities. This will take place on 3 days , from Dec 6 – 8, 2016.
Conference venue: Pullman Hotel, Aerocity, New Delhi
Web-site: www.apmc2016.org

Shiban K Koul (General Chair)

Kamran Ghorbani, Ananjan Basu (TPC co-chairs)

Mahesh Abegaonkar (Finance and Operations)

Advertising**Index**

Advertisers in blue are enabled with the layar app

Sales Representatives

Microwave Journal
Frequency Matters.

Eastern and Central Time Zones
Chuck Boyd
Northeast Reg. Sales Mgr.
(New England, New York, Eastern Canada)
685 Canton Street
Norwood, MA 02062
Tel: (781) 619-1942
FAX: (781) 769-5037
cboyd@mwjournal.com

Michael Hallman
Eastern Reg. Sales Mgr.
(NJ, Mid-Atlantic, Southeast, Midwest, TX)
4 Valley View Court
Middletown, MD 21769
Tel: (301) 371-8830
FAX: (301) 371-8832
mhallman@mwjournal.com

Pacific and Mountain Time Zones
Brian Landy
Western Reg. Sales Mgr.
(CA, AZ, OR, WA, ID, NV, UT, NM, CO, WY, MT, ND, SD, NE & Western Canada)
144 Segre Place
Santa Cruz, CA 95060
Tel: (831) 426-4143
FAX: (831) 515-5444
blandy@mwjournal.com

International Sales
Richard Vaughan
International Sales Manager
16 Sussex Street
London SW1V 4RW, England
Tel: +44 207 596 8742
FAX: +44 207 596 8749
rvaughan@horizonhouse.co.uk

Germany, Austria, and Switzerland (German-speaking)
WMS.Werbe- und Media Service
Brigitte Beranek
Gerhart-Hauptmann-Street 33,
D-72574 Bad Urach
Germany
Tel: +49 7125 407 31 18
FAX: +49 7125 407 31 08
bberanek@horizonhouse.com

Korea
Young-Seoh Chinn
JES Media International
2nd Floor, ANA Bldg.
257-1, Myungil-Dong
Kangdong-Gu
Seoul, 134-070 Korea
Tel: +82 2 481-3411
FAX: +82 2 481-3414
yschinn@horizonhouse.com

China
Shenzhen
Michael Tsui
ACT International
Tel: 86-755-25988571
FAX: 86-10-58607751
michaelt@actintl.com.hk

Shanghai
Linda Li
ACT International
Tel: 86-21-62511200
lindal@actintl.com.hk

Beijing
Cecily Bian
Tel: +86 135 5262 1310
cecilyb@actintl.com.hk

Hong Kong, Taiwan, Singapore
Mark Mak
ACT International
Tel: 852-28386298
markm@actintl.com.hk

Japan
Katsuhiro Ishii
Ace Media Service Inc.
12-6, 4-Chome,
Nishiiko, Adachi-Ku
Tokyo 121-0824, Japan
Tel: +81 3 5691 3335
FAX: +81 3 5691 3336
amskatsu@dream.com

Ed Kiessling Traffic Manager/Inside Sales • 685 Canton Street Norwood, MA 02062 • Tel: (781) 619-1963 FAX: (781) 769-6178 • ekiessling@mwjournal.com

FABS and LABS

Performance Drives at Custom MMIC

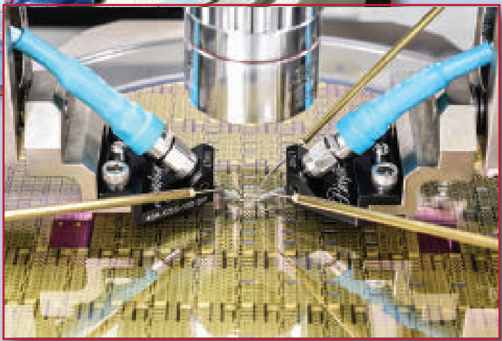

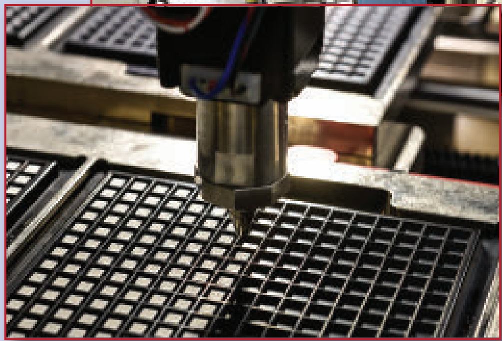

As a fabless MMIC house, Custom MMIC provides value by being flexible and nimble to meet customer demands. They provide diligence in the selection of the best fabrication facilities and processes for a given application to best leverage their design, simulation and testing expertise. Higher demand this year has led Custom MMIC to build a new 10,800 square foot facility in Chelmsford, Mass. that includes more automated equipment. This new facility is enabling Custom MMIC to address higher volume products and reduce lead times to better serve their customers.

Examples of the state-of-the-art equipment in the new facility include a Cascade 12000 autoprober with high and low temperature capability and an Exatron 903 autohandler for plastic and air cavity QFN packages. These acquisitions were required due to the transition to high volume production of its extensive standard product library.

Their engineering and production test equipment operates to 70 GHz including VNAs, sources, phase noise test station, temperature chambers, pulse power and more. The lab is modular and can be reconfigured as needed for the most complex setups. In-house derived test code is also in place to automate all engineering and production measurements. The lab also has the flexibility to test both die and packaged parts while de-embedding all surrounding losses and parasitics, to accurately characterize the products.

Custom MMIC is certified to ISO9001:2008 and has successfully transferred the certification to the new facility. They also have the capability to produce space qualified products to MIL-PRF-38534 Class K. The facility has laminar flow hoods used for wafer test, die pick and visual inspection in a clean environment.

They are celebrating their 10-year anniversary as the company evolved from humble beginnings in 2006 as a start-up founded by Paul Blount. In 2011, Custom MMIC was awarded the Army Innovation Achievement Award for improvements over an existing design with 8 dB more gain, 1 dB less noise figure and 8x reduction in power dissipation. Company investment in recent years has yielded an extensive standard product library, based upon addressing the needs of system engineers. Over 100 standard products incorporate key improvements over standard COTS parts, such as positive gain slope, low phase noise, and all positive bias (no sequencing).

Custom MMIC excels at high performance GaAs and GaN products, emerging as a key MMIC supplier focused on military and aerospace applications. Their design team has extensive experience developing MMICs at frequencies from DC to 100 GHz. They design single function MMICs to complex integrated transmit/receive MMIC signal chains including various types of amplifiers, switches, phase shifters, attenuators, mixers and multipliers.

www.custommmic.com

WERLATONE®

We Are High Power

Absorptive Filters

Werlatone Absorptive Filters are NON-Reflective!

Out-of-Band Signals are NOT reflected back to the source.

- Out-of-Band signals are **internally terminated.**
- Electrical Specifications are less susceptible to temperature change.
- Reduces the dependency of the system on the length of interconnecting cable between two non-perfect components.

Model AF9350

Werlatone Absorptive Filters Eliminate:

- Instability of power amplifiers at out-of-band frequencies.
- Excessive In-Band ripples due to out-of-band reflected energies.
- False trigger of power detector circuitry due to reflected harmonics.
- Potential damage to power amplifiers due to reflection of high power out-of-band energies.

Model AF10200

Low Pass Absorptive Filters

Model	Frequency (MHz) Pass Band	Frequency (MHz) Stop Band	Power (W CW) Pass Band	Power (W CW) Stop Band	Insertion Loss(dB) Pass Band	Rejection(dB) Stop Band	VSWR Pass Band	VSWR Stop Band	Size (Inches)
AF10200	0-2.5	4.5-30	500	150	0.5	45	1.30:1	1.60:1	12 x 5.6 x 3.25
AF10201	0-4.2	7.5-50	500	150	0.5	45	1.30:1	1.60:1	12 x 5.6 x 3.25
AF10202	0-7	12.6-100	500	150	0.5	45	1.30:1	1.60:1	12 x 5.6 x 3.25
AF10203	0-12	21-150	500	150	0.5	45	1.30:1	1.60:1	12 x 5.6 x 3.25
AF10204	0-19	34-200	500	150	0.5	45	1.30:1	1.60:1	12 x 5.6 x 3.25
AF10205	0-30	57-250	500	150	0.5	45	1.30:1	1.60:1	12 x 5.6 x 3.25
AF10502	0-2.5	4.5-25	1,500	400	0.5	45	1.30:1	1.60:1	15 x 6.1 x 3.5
AF10503	0.-4.1	7.4-41	1,500	400	0.5	45	1.30:1	1.60:1	15 x 6.1 x 3.5
AF10504	0-6.7	12.1-67	1,500	400	0.5	45	1.30:1	1.60:1	15 x 6.1 x 3.5
AF10505	0-11	19.8-110	1,500	400	0.5	45	1.30:1	1.60:1	15 x 6.1 x 3.5
AF10506	0-18	32-180	1,500	400	0.5	45	1.30:1	1.60:1	15 x 4.6 x 3.5
AF10507	0-30	54-300	1,500	400	0.5	45	1.30:1	1.60:1	15 x 4.6 x 3.5
AF9438	1-30	50-380	5,000	250	0.5	45	1.30:1	1.60:1	20 x 16.9 x 3.5
AF9349	10-150	270-1500	500	25	0.4	50	1.35:1	1.60:1	4.5 x 1.75 x 1.1
AF9187	10-490	850-3000	100	10	0.5	45	1.40:1	1.90:1	2.5 x 1.3 x 1
AF9350	10-500	750-3000	400	25	0.5	45	1.25:1	1.60:1	4.2 x 1.75 x 1.1
AF9960	10-500	750-3000	600	25	0.5	45	1.25:1	1.60:1	4.2 x 1.75 x 1.1
AF9680	10-520	1040-3000	160	10	0.6	60	1.25:1	1.60:1	4.2 x 1.75 x 1.1
AF9313	10-870	1700-4000	100	10	0.6	53	1.30:1	1.60:1	2.5 x 1.3 x 1

Werlatone, Inc. 17 Jon Barrett Road Patterson, NY 12563 (845) 278-2220 www.werlatone.com sales@werlatone.com